CEX-65.11

B-6

AEC Category: HEALTH AND SAFETY

CEX-65.11

OPERATION HENRE

ENERGY AND ANGULAR DISTRIBUTION OF NEUTRONS AND GAMMA RAYS— OPERATION HENRE

J. H. Thorngate, D. R. Johnson, and P. T. Perdue

Issuance Date: August 1969

CIVIL EFFECTS TEST OPERATIONS
U.S. ATOMIC ENERGY COMMISSION

LEGAL NOTICE

Printed in USA. Price ~~$3.00~~. Available from the Clearinghouse for Federal Scientific and Technical Information, National Bureau of Standards, U. S. Department of Commerce, Springfield, Virginia 22151.

USAEC Division of Technical Information Extension, Oak Ridge, Tennessee

ENERGY AND ANGULAR DISTRIBUTION OF NEUTRONS AND GAMMA RAYS – OPERATION HENRE

By

J. H. Thorngate
D. R. Johnson
P. T. Perdue

Approved by:

F. F. Haywood
Technical Director
Operation HENRE
Oak Ridge National Laboratory

L. J. Deal
Chief
Civil Effects Branch
U.S. Atomic Energy Commission

Health Physics Division
Oak Ridge National Laboratory
Oak Ridge, Tennessee
April 1969

NOTICE

This report is published in the interest of providing information which may prove of value to the reader in his study of effects data derived principally from nuclear weapons tests and from experiments designed to duplicate various characteristics of nuclear weapons.

This document is based on information available at the time of preparation which may have subsequently been expanded and re-evaluated. Also, in preparing this report for publication, some classified material may have been removed. Users are cautioned to avoid interpretations and conclusions based on unknown or incomplete data.

ABSTRACT

The HENRE experiment, conducted at the Nevada Test Site in the winter and summer of 1967, was an extension of the experimental programs related to the Ichiban program to determine the doses received by the survivors at Hiroshima and Nagasaki. This report presents the data obtained on the neutron and gamma-ray dose as a function of polar angle, the fast neutron spectrum as a function of distance, and the high energy gamma-ray spectrum as a function of polar angle. It was found that the neutron spectrum did not reach equilibrium within the distances at which measurements were made. This has an effect on the dose as a function of polar angle measured with different air densities. In addition, the measurements show the gamma-ray dose received from angles below the air-ground interface is affected by the diffuse source of gamma rays. Where possible, these data have been compared with data from previous field experiments. In every case, they were compared with calculations which approximated the experiment. Agreement in both cases is generally good, and this strengthens confidence in calculated results.

ACKNOWLEDGMENTS

Any program of this magnitude is the result of the efforts of a large number of people. To name all of those who contributed to the work described in this report would be difficult. We would like to acknowledge the general assistance of the Dosimetry Research Section and especially the efforts of W. H. Shinpaugh and M. L. Snow. A number of individuals temporarily assigned to the DOSAR staff during the preparation stages also offered considerable aid such as W. Croft, whose preliminary work in the design and setup of the pair spectrometer made an early success in the operation of this device possible. E. A. Straker of the Neutron Physics Division of the Oak Ridge National Laboratory generously made available all of the calculations with which the experimental data are compared.

CONTENTS

ILLUSTRATIONS

ILLUSTRATIONS (Continued)

ILLUSTRATIONS (Continued)

TABLES

CHAPTER 2 EQUIPMENT AND PROCEDURES

CHAPTER 3 RESULTS

Chapter 1

INTRODUCTION

The Ichiban program, established to determine the radiation doses received by the survivors at Hiroshima and Nagasaki, has required a number of field experiments.[1-4] These were a part of the weapons testing program until the test moratorium was established in 1958, after which other means were sought to obtain the required data. For example, experiments performed at the Nevada Test Site (NTS) in 1962 during Operation BREN (Bare Reactor Experiment Nevada) used the Health Physics Research Reactor (HPRR), an unshielded, Godiva-type reactor and a ^{60}Co source on a tower.[5-9] The BREN experiments provided data on the spatial, angular, and spectral distributions of the neutron and gamma radiation. The differences between the reactor radiation field and that from the "Japanese weapons" were great enough to make the results difficult to apply to the Ichiban program, and it was apparent that better spectral results were needed in order to get direct comparisons with calculations. Spectrum measurements were incomplete during BREN due to the low intensity radiation fields and relatively insensitive spectrometers.

Operation HENRE (High Energy Neutron Reactions Experiment) was designed to overcome some of the problems encountered during BREN.[10-12] By using an accelerator as the source, monoenergetic neutrons were obtained which simplified the input information for the calculational programs so that straightforward comparisons between experiment and calculations would be possible. Measurements were made of the angular, spatial, and spectral distributions of neutron and gamma radiations at relatively large distances from the source when it was mounted at various heights on the BREN tower.

This report describes the measurements made by Project 1.1: (1) the angular distribution of neutron and gamma-ray dose rates at 750 yds from the base of the tower; (2) the neutron energy distribution at 500 ft, 500 yds, and 750 yds from the base of the tower and inside an experimental civil defense shelter; and (3) the high energy gamma-ray energy distribution (at 500 yds) as a function of angle.

Some additional measurements were made during the course of the experiment to determine such factors as the relative shielding effectiveness of the collimators used in their weapons test and BREN configurations and in the modified HENRE configuration and measurements to define better effects of the air-ground interface on the dose as a function of polar angle.

While most measurements were made in a manner to make them specifically useful to the Ichiban program, some measurements, such as the gamma-ray spectrum as a function of angle, are useful in extending the understanding of the interactions of 14 Mev neutrons with air.

Operations were conducted in two sections: (1) during the winter of 1967 and (2) during the late summer of 1967. A break in data taking was required by a severe malfunction and subsequent repair of the accelerator.

REFERENCES

1. P. S. Harris, G. S. Hurst, H. H. Rossi, S. C. Sigoloff, and W. H. Langham, Project 39.7, Operation Teapot Report, ITR-1167, April, 1955. (Classified)

2. G. S. Hurst and R. H. Ritchie, Project 39.5, Operation Plumb Bob Report, WT-1504, September 19, 1958. (Classified)

3. R. H. Ritchie and G. S. Hurst, Penetration of Weapons Radiation: Application to the Hiroshima-Nagasaki Studies, *Health Phys. 1*: 390-404 (1959).

4. J. A. Auxier, J. S. Cheka, F. W. Sanders, Projects 39.1 and 39.2, Operation Hardtack (Phase II) Report, WT-1725, March 1961. (Classified)

5. J. S. Cheka, F. W. Sanders, T. D. Jones, and W. H. Shinpaugh, *Distribution of Weapons Radiation in Japanese Residential Structures*, USAEC Report CEX-62.11, August, 1965.

6. J. H. Thorngate, J. A. Auxier, F. F. Haywood, and S. Helf, *Energy and Angular Distributions of Neutrons and Gamma Rays - Operation BREN*, USAEC Report CEX-62.12, February, 1967.

7. J. H. Thorngate and E. T. Loy, Post Pulse Gamma-Radiation Spectrum - Operation BREN, USAEC Report CEX-62.13, June, 1966.

8. F. F. Haywood, J. A. Auxier, and E. T. Loy, *An Experimental Investigation of the Spatial Distribution of Dose in an Air-Over-Ground Geometry*, USAEC Report CEX-62.14, October, 1964.

9. F. F. Haywood, Spatial Dose Distribution in an Air-Over-Ground Geometry, *Health Phys. 11:* 185-192 (1965).

10. F. F. Haywood and J. A. Auxier, *Technical Concept - Operation HENRE*, USAEC Report CEX-62.02, March, 1965.

11. Technical Director's Staff, *Operations Plan - Operation HENRE*, USAEC Report CEX-65.03, September, 1965.

12. J. S. Cheka, *Distribution of Radiation from a 14 Mev Neutron Source in and Near Structures*, USAEC Report CEX-65.12 (to be published).

Chapter 2

EQUIPMENT AND PROCEDURES

2.1 SOURCE

2.1.1 Accelerator

Only a brief description of the Operation HENRE neutron source will be given here, since a more detailed description is available in CEX-65.02.[1] The $T(D,n)^4He$ reaction is widely used as an abundant source of fast neutrons of 14 to 15 Mev, because the reaction has a large cross section and is exoergic making low acceleration voltages adequate. There is a peak in the total cross section for the reaction near 100 kev deuteron energy, so the commonly used acceleration potential of 150 kev provides for energy loss as the deuterons enter the target material.[2] Yield is a function of both the target thickness and the number of deuterons bombarding the target, normally expressed as current in μa or ma. Use of a low deuteron energy results in a nearly isotropic distribution of the neutron output.

For Operation HENRE, an accelerator was built which used a 150 kv accelerating potential and a 500 ma deuteron current to produce a total neutron output of 10^{13} neutrons/sec. While accelerators which operate at this potential are widely used, innovations were required in the design of the HENRE accelerator due to the high current required. A duoplasmatron ion source was used to provide the required current of ionized deuterium, and a single accelerating gap was used with the high voltage supplied from a transformer-rectifier power supply. (See Fig. 2.1.) After the ion beam passed through the accelerator gap into the field-free drift region between the gap and the target, it was allowed to diverge due to mutual repulsion of the ions. Used in conjunction with a 14-in.-dia. target, the beam blowup decreased the power dissipated per unit area on the target and the subsequent heat transfer problems encountered with 75 kw of beam power.

Targets for this type of accelerator generally consist of tritium adsorbed on a material such as titanium, zirconium, or yttrium. Greater tritium adsorption with less release during target heating was obtained using erbium evaporated to a thickness of 4 mg/cm^2 on a copper plate. Tritium-to-erbium ratio was approximately 1.8.

After the accelerator was operated for 80 min, the contamination due to neutrons from the $D(D,n)^3He$ reaction reached a maximum of 10^{11} neutrons per sec which was 1% of the planned 14 Mev neutron output. The effects of the undesired 3 Mev neutrons upon measurements made at large distances from the tower were reduced by the anisotropy of the reaction.

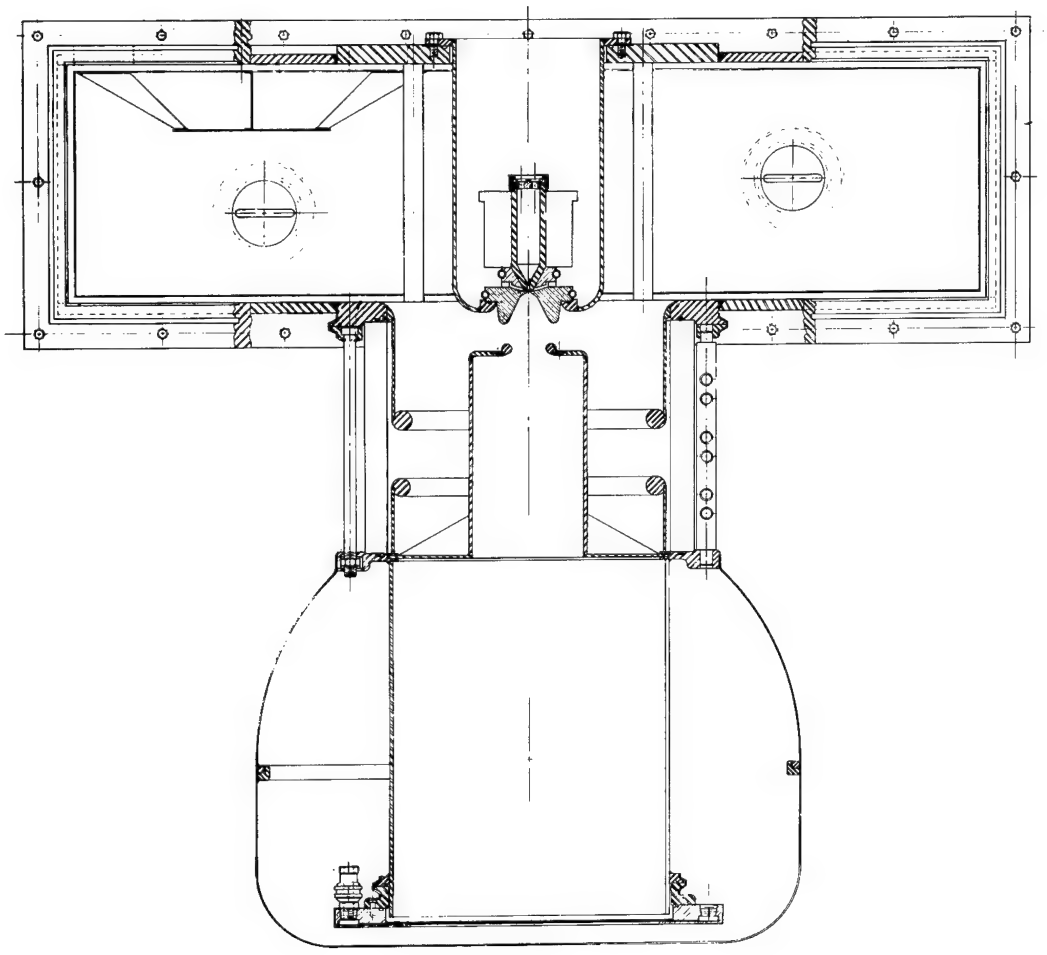

Fig. 2.1—Cross sectional diagram of HENRE accelerator.

2.1.2 Tower

The accelerator, vacuum system, and power supply were housed in a hoist car located on the face of a tower originally built in Area 4 of the Nevada Test Site for Operation BREN and later moved to Area 28 for this operation. (Figs. 2.2 and 2.3) This tower has a maximum height of 1527 ft and a triangular cross section with the three legs spaced 10 ft apart.[3] Six sets of six guy wires, attached at various heights, hold the top of the tower to a maximum sway of 2 in. for normal wind conditions. Control wires were installed on the tower so the accelerator could be operated from an underground bunker, and connector boxes were located at each tower height where exposures were made. Source heights used during the experiment were 300, 500, and 1125 ft.

2.2 COLLIMATORS

2.2.1 Description

Most measurements made by this project used modifications of collimators originally designed for weapons tests; a water-filled cylinder 54 in. in diameter and 54 in. long.[4] (A diagram is shown in Fig. 2.4.) A 45° conical opening on the front face terminated in a cylindrical opening at the center of the collimator that held a water-filled or lead insert, depending upon whether neutrons or gamma rays were to be measured. Modifications were made to the inserts to accommodate the detectors used. A cylindrical opening 5 in. in diameter along the axis and through the rear of the collimator provided both an access to the detector and a cable passageway. The angular openings in the front of the water or lead basic inserts were decreased to smaller angles using lead or water inserts which fit into the 45° opening and had 15, 20, or 30° openings. Major modifications to a basic lead insert were required to accept the gamma-ray spectrometer. In this case, a water insert was fitted in front of the lead insert to further reduce the effect of neutron-produced gamma rays. It is shown in Fig. 2.5. For the same reason, borated water was used in all collimators. Because the neutron energies encountered during this experiment were higher than the fission spectrum for which the collimators were originally designed, 5 inches of polyethylene sheets were placed around the collimators for additional neutron shielding. The resulting configuration is shown in Fig. 2.6.

The effectiveness of the collimators used for angular dose rate measurements were investigated by placing neutron and gamma-ray sources at a fixed distance in front of the turret and observing the relative dose rates as a function of collimator position. Relative response was obtained by taking ratios of the corresponding readings to those taken with the collimator aimed directly at the sources. For angles much greater than the collimator opening, these ratios could not be determined precisely because the measurements were little more than background. Figures 2.7 and 2.8 show the angular definition for the 30° neutron and gamma-ray collimators, respectively. Similar measurements were made for the pair spectrometer collimator using the 4.43 Mev $^{12}C^{*}$ de-excitation gamma rays produced by a PuBe neutron source. Response of the main detector crystal of the spectrometer was measured as a function of collimator angle in 5° increments, and the response relative to the zero direction was determined. These results are shown in Fig. 2.9.

A question arose about the effectiveness of the collimator in minimizing the production of gamma rays from neutrons and the ability of the collimator to shield against such gamma rays. To determine these factors in some detail, a standard collimator with a 30° lead insert was placed with the axis of the opening at 90° with respect to the horizon so that the polar angle with

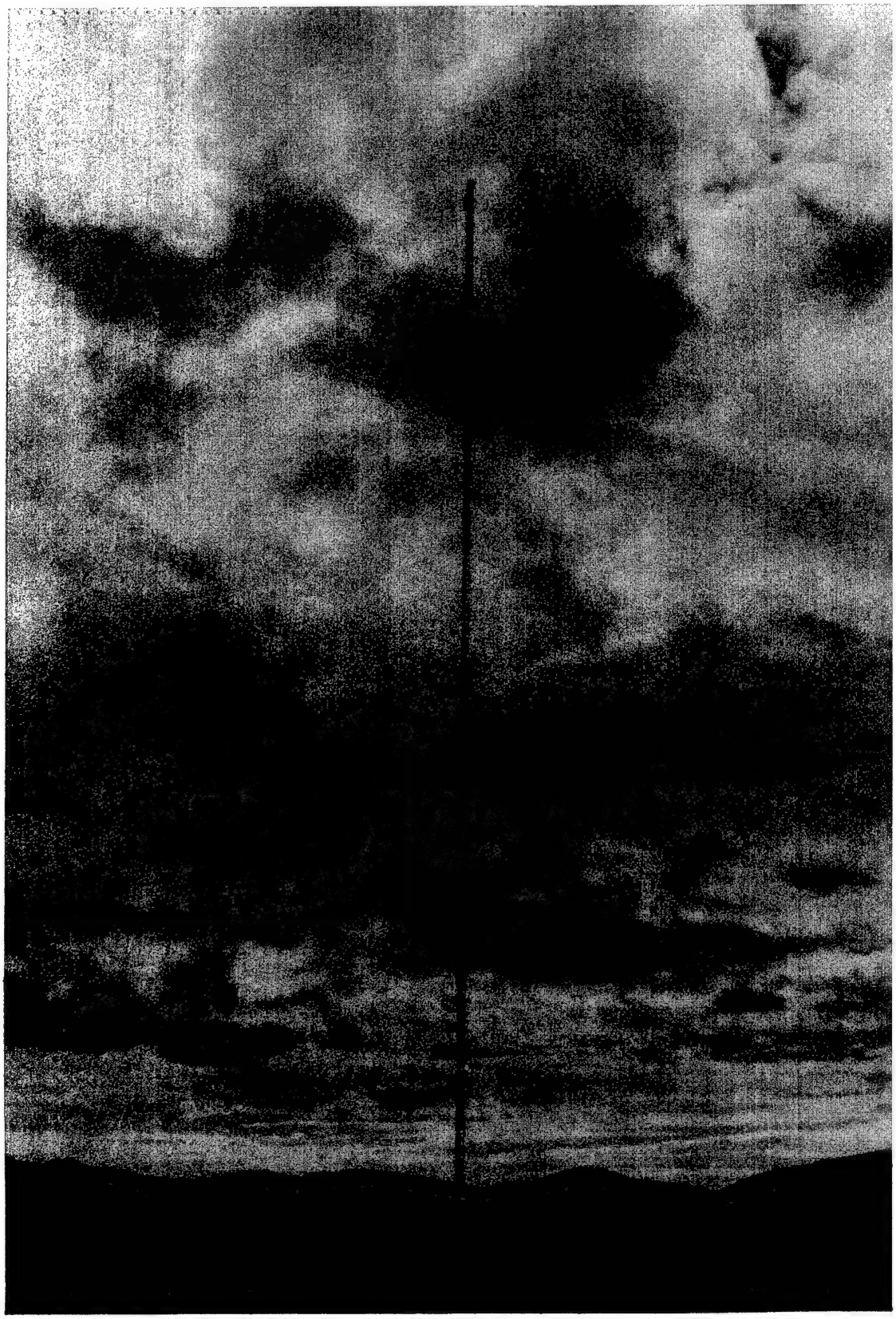

Fig. 2.2—BREN tower after relocation to NTS Area 28 for Operation HENRE.

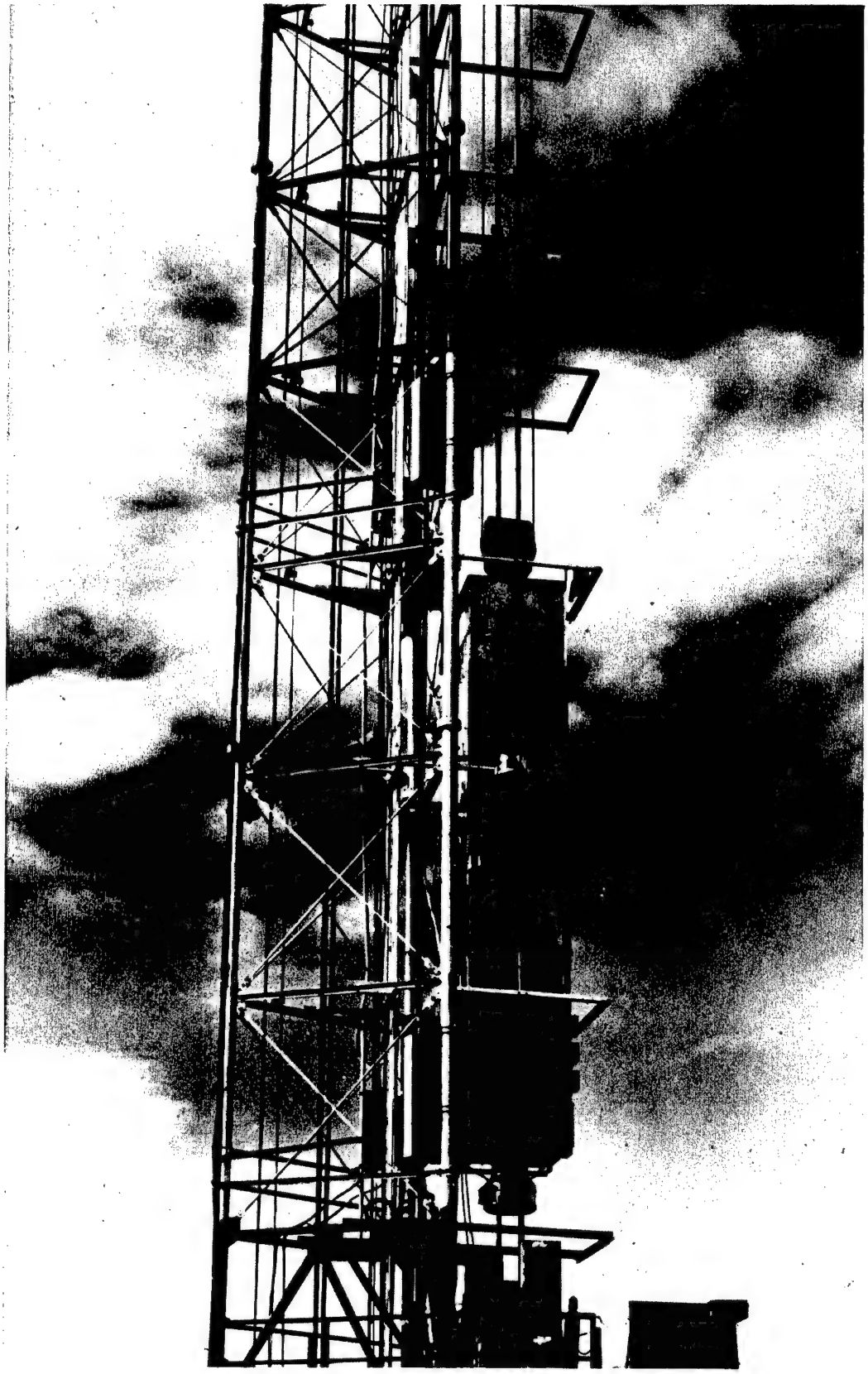

Fig. 2.3—HENRE accelerator installed in the source hoist car on the face of the tower showing power supply and the radiator fan for the target cooling system.

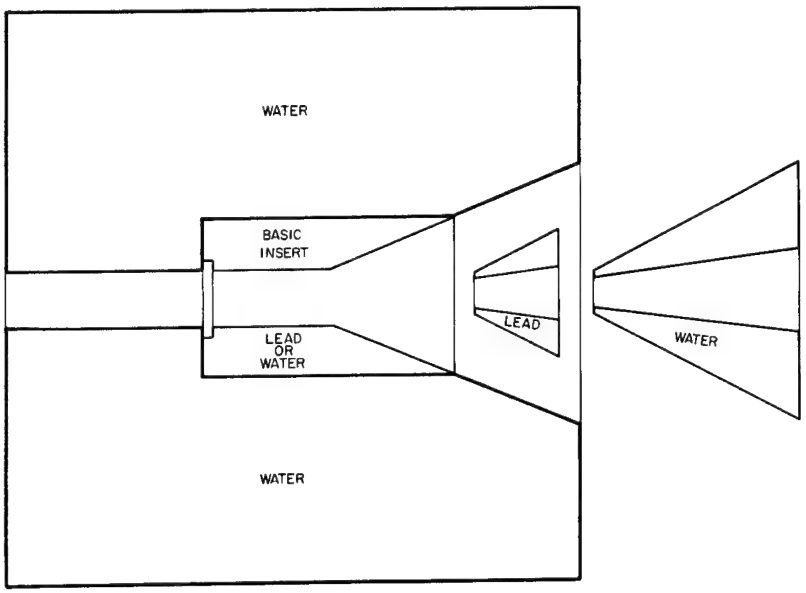

Fig. 2.4—Diagram showing the construction of the collimator as originally designed for weapons tests.

respect to the source-detector line was about 63 degrees. This experimental setup is shown in Fig. 2.10. Gamma dose measurements were made in this collimator when it was filled with plain water and when it was filled with borated water. Also measured was the gamma dose in the HENRE collimator that had both borated water and additional polyethylene shielding. The results of these measurements are given in Table 2.1. Although the statistics are consistently poor, an improvement is noted for each modification.

Table 2.1

NORMALIZED GAMMA-RAY DOSES

Comparing the Capabilities of Various Collimator Configurations

Standard Collimator without Boron	Standard Collimator with Boron	HENRE Collimator
0.033 ± 0.014 c/norm.	0.020 ± 0.012 c/norm.	0.018 ± 0.010 c/norm.

2.2.2 Supporting Turrets

Collimators of this size are hard to position. To simplify orientation, a turret was built that held two collimators. Lateral movement was achieved by rotating the collimator and turret on a horizontal bearing.[5] Vertical angles were set using a crank and a gear reduction system with a chain and sprocket drive to rotate the collimators in vertical planes. The two turrets used during HENRE were mounted on special concrete pads, one located 500 yds and the other 750 yds from the tower base. Because only

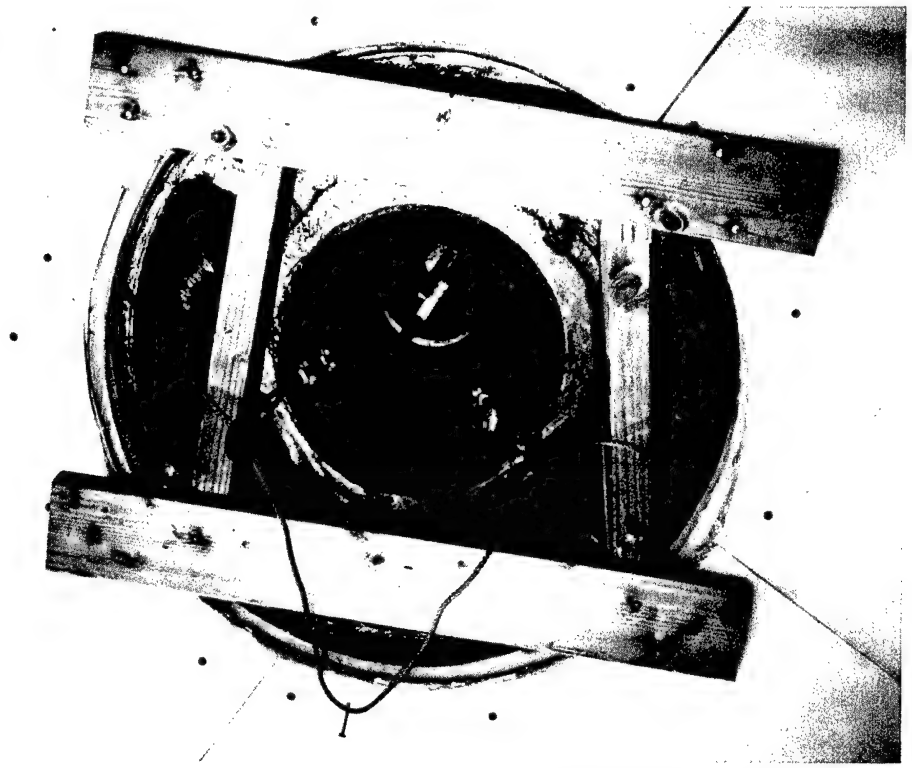

Fig. 2.5—Front of collimator used with pair spectrometer showing additional water insert in front of normal lead insert. Total angle of the conical opening is 30°.

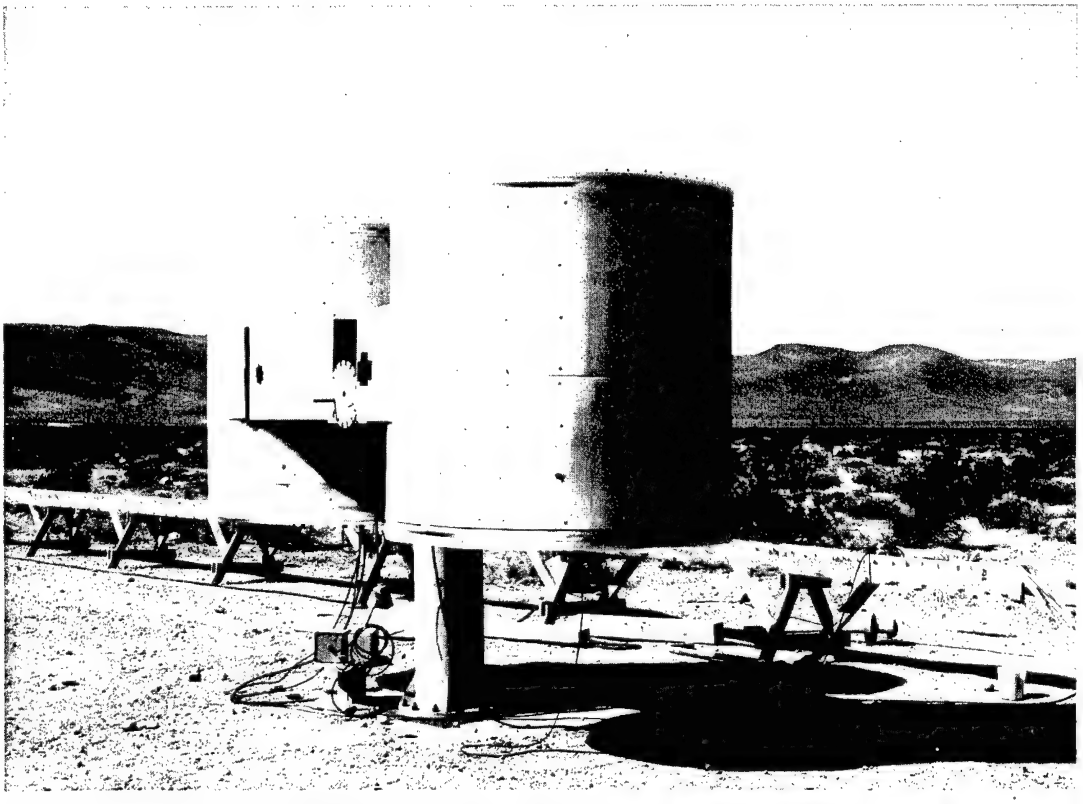

Fig. 2.6—Collimators for angular dose measurements showing polyethylene sheeting added for Operation HENRE. The collimators are pointing straight up.

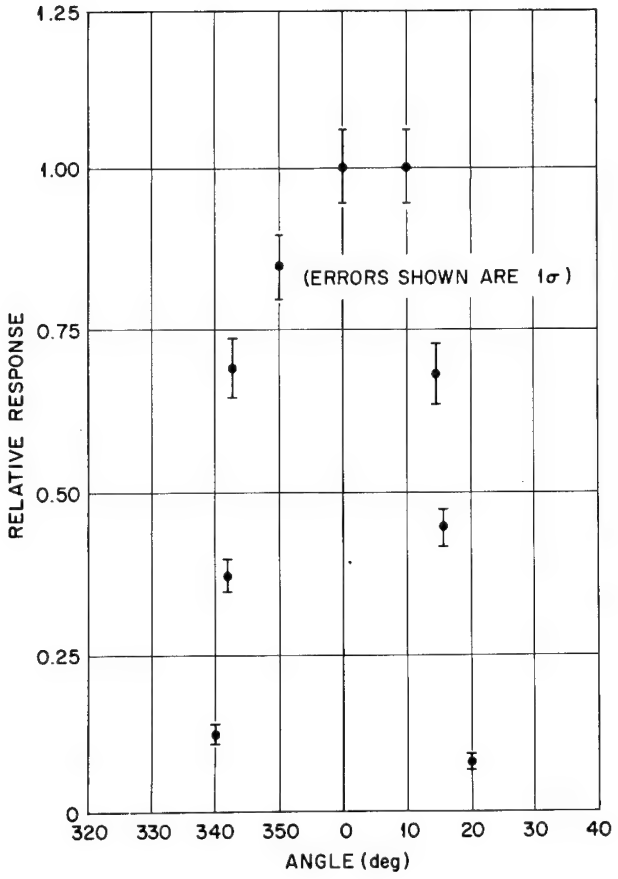

Fig. 2.7—Relative response vs. angle for the collimator used to measure neutron dose during HENRE with a 30° insert.

one collimator was required at 500 yds, an unmodified collimator was placed in one side of the turret to provide ballast. This arrangement is shown in Fig. 2.11.

2.2.3 Inclinometer

Collimators were aimed using a sight similar in operation to an artillery or mortar sight.[6] This inclinometer has two protractors mounted orthogonally in the vertical and horizontal directions. The vertical protractor was referenced to a spirit level while a telescopic sight on the horizontal protractor used the tower as a reference. A second spirit level located on the base of the inclinometer and orthogonal to both protractors served as a reference in placing the sight on the collimators.

A new sighting was required each time the collimator holding the gamma spectrometer at 500 yds was moved. The second turret needed to be resighted only when a change was made in the horizontal angle as the vertical angle on it was adjustable directly in fractions of a degree.

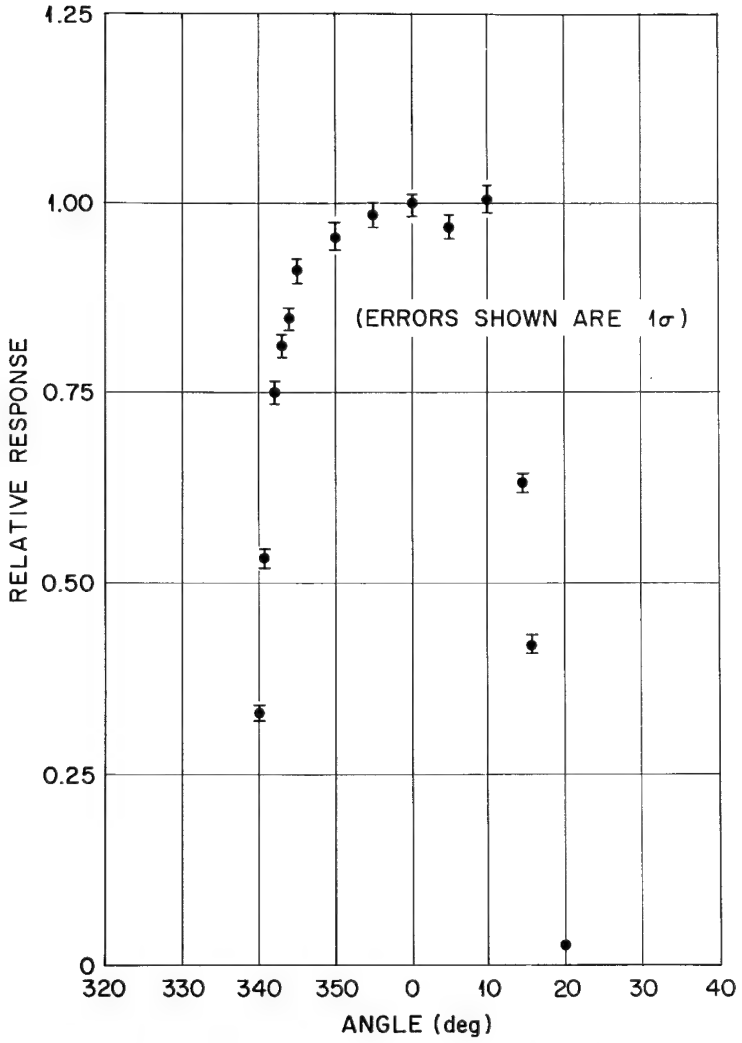

Fig. 2.8—Relative response vs. angle for the collimator used to measure gamma-ray dose during HENRE with a 30° insert.

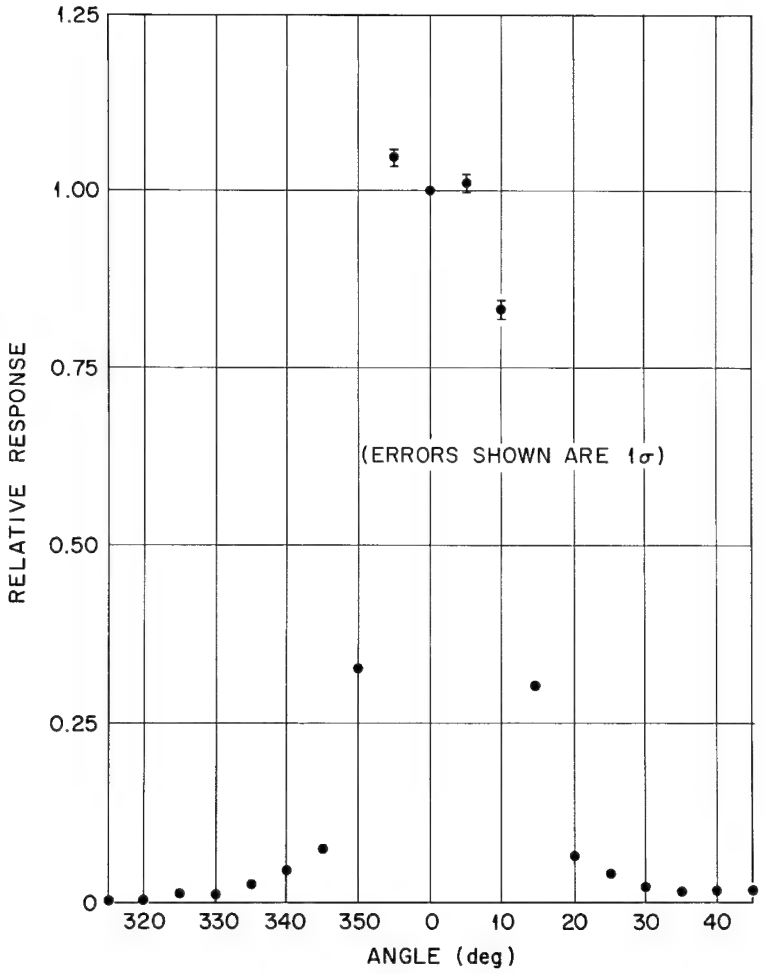

Fig. 2.9—Relative response vs. angle for the collimator used to measure gamma-ray spectrum during HENRE with a 30° insert.

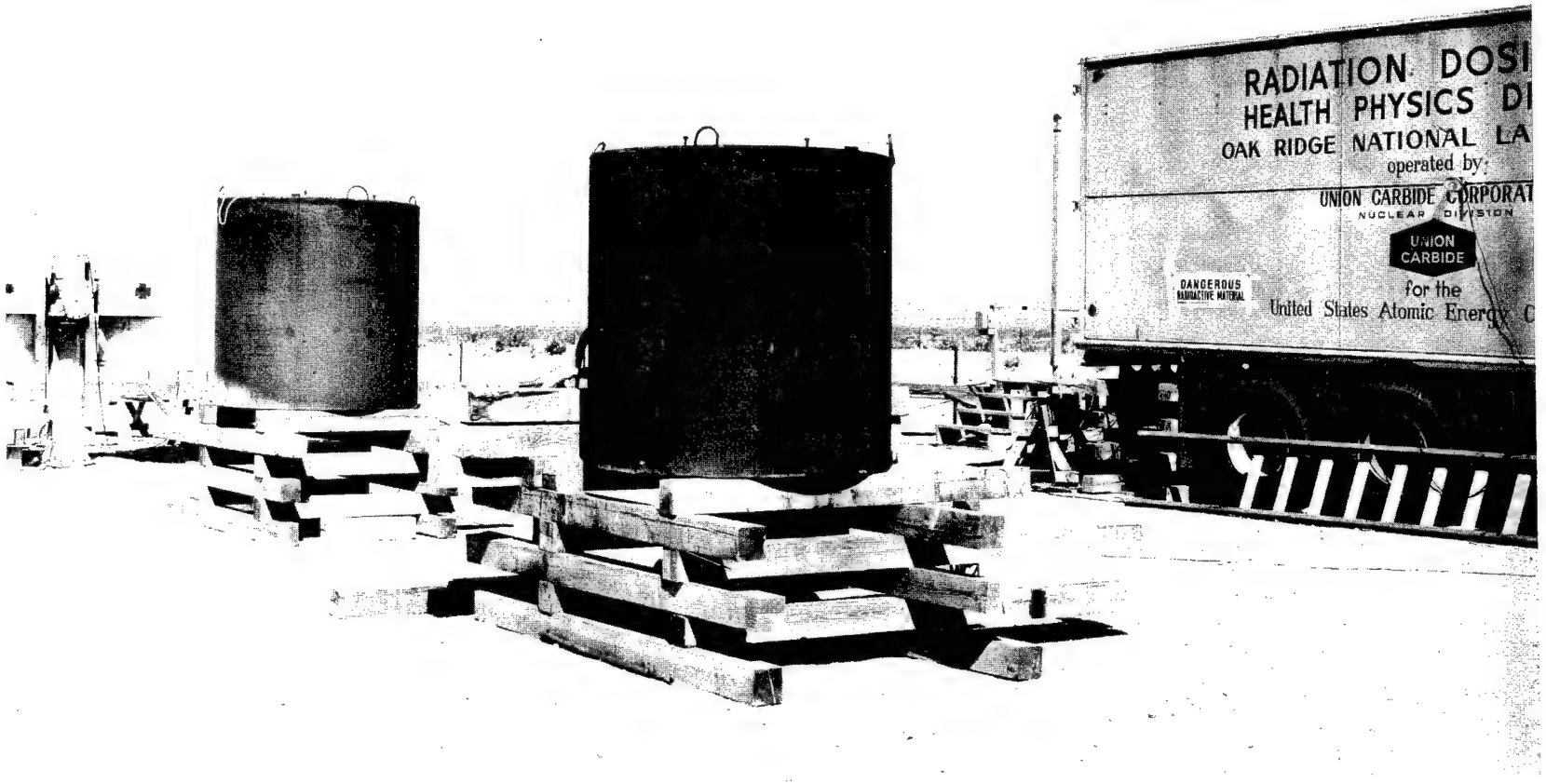

Fig. 2.10—Setup for experiment to compare collimating capabilities of weapon's test and HENRE configurations.

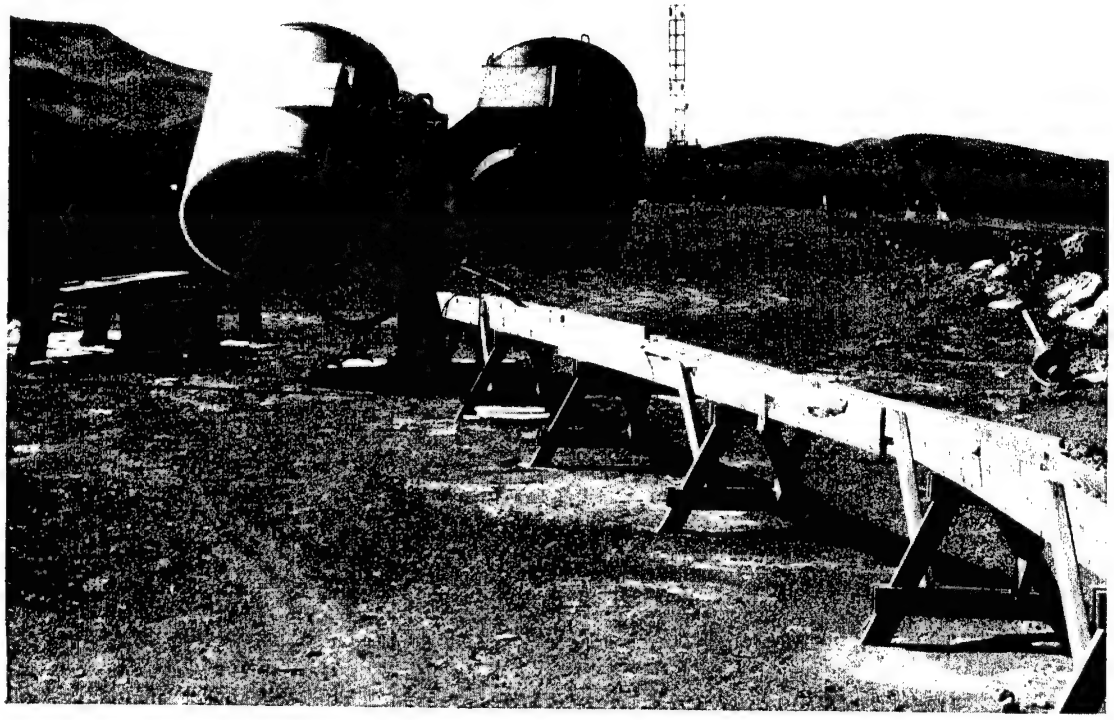

Fig. 2.11—Gamma spectrometer collimator mounted on turret at 500 yards from the base of the tower showing unmodified collimator used for ballast and troughs used to hold cables.

2.3 NEUTRON DOSIMETRY

The fast neutron dosimeter developed by Hurst and Wagner[7] was used for the measurements of dose as a function polar angle. This system used a polyethylene-lined, cyclopropane-filled proportional counter as the neutron detector. For gain calibration, the counter had an internal alpha source with a solenoid-operated shutter. A preamplifier using a field effect transistor input stage was designed for use in the field which, when operated from a battery supply, provided adequate low noise operation.[8] Detector output pulses were proportional to the energy absorbed within the sensitive volume and were integrated on a Radson binary integrator.[9] Signals were transmitted from the detector to the integrator over a 150-ft low capacitance coaxial cable (RG 62/U), and detector anode potential was supplied by the integrator via a 150-ft-high voltage cable (RG 59/U). An unshielded pair of wires was used to transmit the solenoid control current to the counter from a suitable low voltage supply. To reduce noise, the cables were kept off the desert floor in special cable troughs of the type shown in Fig. 2.11.

Operation of the Hurst proportional counter in conjunction with the Radsan pulse-height integrator required an elaborate set-up procedure. The condition of the proportional counter was determined regularly by using a multichannel pulse height analyzer to measure how well the counter resolved the pulse-height peak produced by the internal alpha source. If the measured alpha resolution was poorer than 10%, the counter was replaced. Resolution generally decreased with time due to contaminant gases leaking into the counter or outgassing from the polyethylene walls.

If the counter was satisfactory, setup proceeded to the checkout of the discriminators in the pulse-height integrator. When the discriminators were set properly, the solenoid was energized to expose the alpha source, and the fine gain control of the amplifier was adjusted. Adjustment of counter electron multiplication by varying high voltage sometimes was necessary. For neutrons measurements, the solenoid was deenergized to cover the alpha source, and the amplifier gain increased by a factor of 32 which resulted in a low energy cutoff of 160 kev for the neutron measurements. The system was calibrated by placing a neutron source of known yield at a fixed distance and measuring the count rate it produced.

Background runs were made before and after all operations. Noise picked up by the electronic system was the largest contributor to the measured background, so all possible precautions were taken to reduce it. Noise was monitored on an oscilloscope connected to the linear amplifier output. Output pulses produced by noise generally were shaped differently from acceptable pulses, so when a noise pulse occurred, the measurement was rejected.

A special holder was required to match the diameter of the neutron dosimeter to the 5-in. inner diameter of the collimator and to hold the detector so that the apex of the collimator entrance cone was at the center of the detector. Zero angle was defined as the direction from the collimator site to the source. With a collimator opening of 30° and the source at 1125 ft, measurements were made in the tower-collimator plane at angles from 0 to 90°. In order to provide more detailed data, measurements were made at angles of 15°, 45°, and 75° using the 30° cone. Zero, 30°, and 60° measurements were made with the 30°-cone with the source at 300 ft and at 500 ft. Using a 15° cone, measurements were made at 0°, 10°, and 20° when the source was at 1125 ft, and at 0°, 10°, 20°, 30°, 40°, and 50° with the source at 500 ft. The maximum angle at which values could be obtained was limited by the low dose rates available.

To obtain more information on the effect of the air-ground interface, two sets of measurements were made: one in the tower-detector plane and the other in a plane perpendicular to the source-detector line. A 30° acceptance angle was used with three values obtained in each position: (1) collimator just above the horizon; (2) collimator aimed at the horizon; and (3) collimator just below the horizon.

2.4 GAMMA-RAY DOSIMETER

The "Phil" dosimeter was used to measure gamma-ray dose as a function of angle during Operation BREN.[11,12] For Operation HENRE, the Phil was replaced with a more sensitive gamma-ray dosimeter.[13] It was found that when it was properly shielded for low energy photon and thermal neutron response, the RCL 10-60 G.M. tube had nearly the same low neutron sensitivity and photon energy response as the Phil, but with approximately 40 times more sensitivity. Additional measurements of the response of this detector as a function of energy and the response to neutrons were made, using an x-ray source and the Health Physics Research Reactor.

The output of the G.M. tube went to the input of a transistorized decade scaler in the instrument trailer via an emitter follower preamplifier and RG coaxial cable. Resolving time of the scaler was about 100 times less than the dead time of the detector so that it did not enter into counting corrections. Anode potential was supplied by a transistorized high voltage supply, the output of which was held at a voltage consistent with the counter plateau by a corona regulator tube.

For measurements of gamma-ray dose rate as a function of angle, the dosimeter was mounted in collimators and positioned so that the apex of the conical collimator opening was at the center of the sensitive volume of the detector. Measurement angles were generally identical with those used for neutron dose-rate studies. For more detailed measurements, a 20°angular acceptance was used. Higher sensitivity permitted measurements of gamma dose with the 20° collimator opening at polar angles up to 30° for a source height of 1125 ft.

2.5 NEUTRON SPECTROMETER

Even with the high neutron yield planned for the HENRE accelerator, the neutron flux available for dose and spectrum measurements at distances of several hundred yards from the tower was low. Thus a sensitive spectrometer was required in order to make measurements at large distances. It was concluded that the choice for such an application was a ^{6}LiI(Eu) spectrometer as described by Murray in 1958.[14] The advantages were: (1) high efficiency, 10^{-2} - 10^{-3} counts/neutron/cm^2; (2) acceptable neutron energy resolution at energies >3 Mev when cooled to less than 150° K; and (3) simplicity of electronics. The main disadvantage was the competing reactions which become significant when a considerable fraction of the neutrons have energies >7 Mev. The primary competing reaction expected in ^{6}LiI is ^{6}Li(n,dn')α which has a Q value of -1.47 Mev.

The pulses produced by the competing reactions can be stripped from the data if a shape is assumed for the background pulse height distribution produced by a monoenergetic neutron. Stripping is aided by the large difference between the Q of the foreground and background reactions, because response above a certain pulse height can be assumed to have been caused only by the foreground reaction and can be reduced to a number of incident neutrons. Knowing this number of neutrons, it is possible to calculate the response they would

produce due to the competing reaction which may be subtracted from the total measured response and the next lower pulse height region considered. Corrections must be made for differences in the light output versus particle energy and for differences in cross sections. Data reduction is simplified by the rather poor resolution of the detector so that a limited number of energy intervals are considered.

The 2-mm-thick, 2-in.-dia. ^{6}LiI scintillators were attached to 6-in.-long quartz light pipes equipped with copper bellows to permit thermal contraction during cooling operations. Quartz was selected in preference to lucite to reduce neutron scattering from the light pipe; the 6-in. length was chosen because the difference in pulse height resolution is not a sensitive function of light pipe length between 3 to 6 in., and six inches eliminated the necessity of considering the temperature at the photocathode of the photomultiplier (P.M.) tube used. The P.M. tubes were attached to the light pipes with silicone grease and centered firmly in place with a length of bicycle inner tube. Aluminum foil was used as a reflector for the 3 in. of exposed quartz and a magnetic shield enclosed the tube and the first 1/2 in. of the light pipe. An emitter follower preamplifier housed in the P.M. socket transmitted signals to a double differentiating linear amplifier with 4 μsec delay lines, the output of which was connected to a 256-channel analyzer. The cooling apparatus consisted of a stainless steel cooling jacket. A self-pressurized, 200-liter, liquid nitrogen dewar was used to cool the crystals. This setup is shown in Fig. 2.12. An insulated tube went from the output of the dewar to the cooling apparatus. Since considerable care must be taken during the cooling process to prevent thermal shocks from damaging the crystals, the first cooling was done with the gas escaping from the dewar. After this, the dewar valve was opened slowly to allow liquid nitrogen to enter the cooling apparatus. Liquid nitrogen flow was regulated so that only a fine stream of the liquid was emitted through the vent tube of the cooling jacket, which insured that the crystal itself was covered by liquid nitrogen. A full dewar held enough liquid nitrogen to last through the prerun cooling, spectrometer setup, and run. Figure 2.12 also shows the sheet of cadmium used to enclose the ^{6}LiI crystal to reduce the thermal neutron response.

After the spectrometer was set up, a thermal neutron calibration was performed to establish operating high voltage and gain settings. Detector pulses were biased at the input to the multichannel analyzer so those from the thermal neutron response of the ^{6}LiI detector fell in channel 16-18. Normally the gain setting used resulted in the 15 Mev peak falling in the region of channels 200-230. The ^{6}LiI data were generally taken for 2-hr periods and were normalized with a BF_3 normalization counter to allow comparisons of measurements made with different accelerator targets and at different ranges.

Measurements were made in an underground civil defense shelter located at 400 feet from the base of the tower to determine the effect of the amount of dirt covering the shelter. Dirt thicknesses were varied in one-foot increments from zero to three feet. For these measurements, the source was located at an elevation of 300 feet. A diagram of this arrangement is given in Fig. 2.13.

In-air measurements were made at distances of 500 ft and 2250 ft from the base of the tower when the source elevation was 500 ft and at 1500 ft and 2250 ft from the base of the tower when the source was at 1125 ft.

2.6 GAMMA-RAY SPECTROMETER

Selection criteria for a gamma-ray spectrometer for use during Operation HENRE were: (1) suitable energy range; (2) sufficient sensitivity:

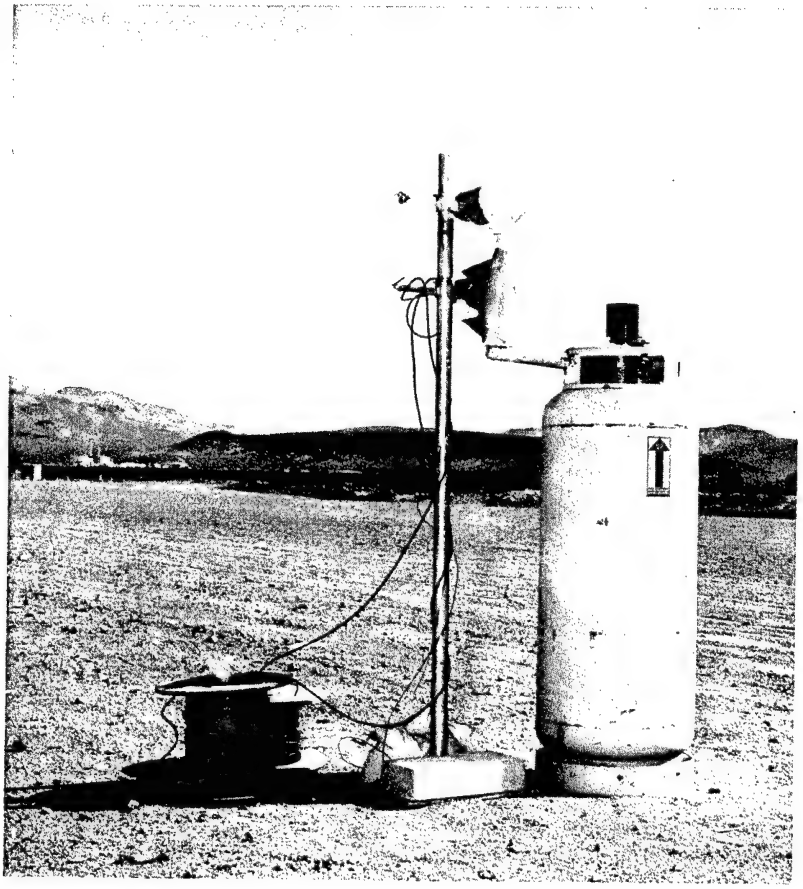

Fig. 2.12—Neutron spectrometer as operated during HENRE using liquid nitrogen from a 200 liter self-pressurized dewar to cool the crystal.

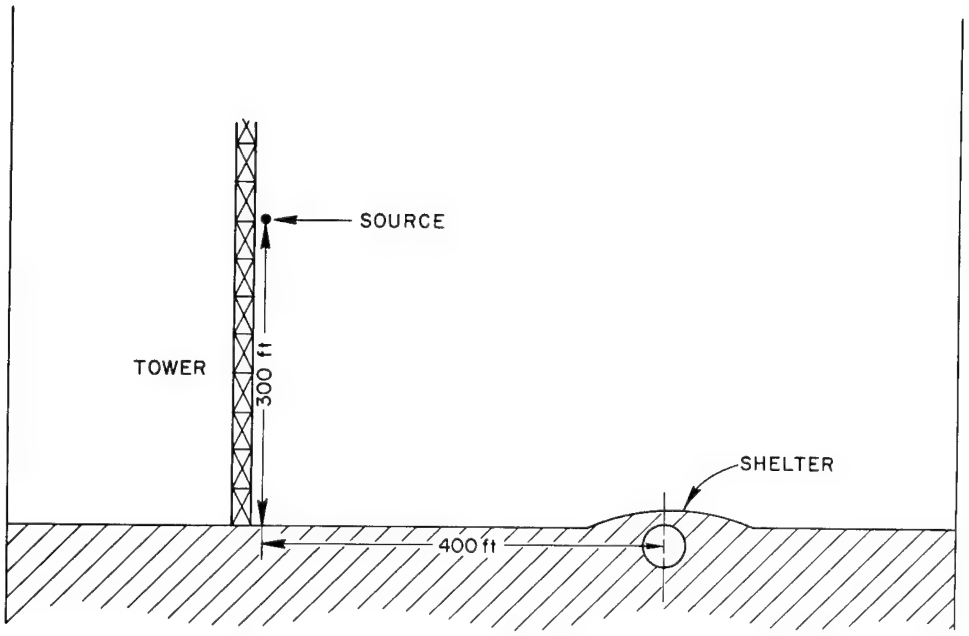

Fig. 2.13—Diagram of the location of the source and detector for measurements made in the civil defense shelter.

(3) ease of data reduction; and (4) low neutron response. A scintillation pair spectrometer was chosen because it coupled useful efficiency with the low neutron response, although it has no response below 1.02 Mev and a useful lower energy limit of 1.5 Mev.[15] As the photons of greatest interest during HENRE were expected to be above 1.5 Mev, this was the optimum choice.

The central detector was a NaI(Tl) crystal 1 in. in diameter by 2 in. long. To insure optimum and stable performance, this crystal was purchased as an integral unit with a magnetic shield and a selected photomultiplier tube. It was operated in the center of a crystal 9 in. long that had an axial hole 1 3/4 in. in diameter. Although the gamma rays were collimated to strike only the central crystal, the large crystal was divided into quadrants which were optically separated to decrease the "singles" counting rate. Each photomultiplier socket held a transistor preamplifier with unit gain that transmitted signals over low capacitance (RG 62/U) coaxial cables 1000 ± 1 ft in length. A double differentiating linear amplifier further amplified each signal and supplied power via the signal cable to operate the preamplifier.

Linear amplifier output signals were attenuated to operate transistorized discriminators that produced output pulses when the doubly differentiated pulses crossed through zero. This point was stable within 10 nsec with respect to the start of the pulse and, therefore, could be used for coincidence timing to minimize timing problems. The delay lines in each amplifier were adjusted to the same length. Signals produced by the annular crystals were selected so that only interactions depositing between 0.44 and 0.58 Mev produced a discriminator output pulse. This covered, within the resolution of the crystals, the total absorption of the 0.51 Mev annihilation gamma rays. The discriminator operated by the signal from the center detector was set to produce an output pulse for any input above noise. Discriminator output pulses went to pulse shapers that produced 25 nsec wide output pulses to operate a coincidence circuit that produced an output whenever a pulse produced by the center crystal occurred in the same 25 nsec interval as 0.51 Mev pulses in two or more of the outer crystals. An output pulse from the coincidence circuit operated a univibrator which produced a 2 μsec long pulse suitable for operating the linear gate of a multichannel analyzer. The signal from the central detector provided the analog input for the analyzer.

The gain of the double differentiating amplifier used to amplify signals from the center crystal was set using the gamma rays produced by a PuBe neutron source, so that full scale deflection on the multichannel analyzer would result from an 11 Mev gamma ray. At the operating gain setting, the amplifier was adjusted so output pulses produced by ^{137}Cs in the center crystal were correctly shaped. Any adjustment of the pulse shape or fine gain affected the time between the start of the pulse and the crossover, which was a problem because coincidence timing was based on the pulse crossover.

The four amplifiers used on the outer crystals were aligned using a ^{137}Cs source so that input pulses from 1 Mev photons produced full amplifier outputs. Good overload properties allowed the desired pulses to be amplified with good fidelity in the presence of larger pulses. With the detector exposed to 4.43 Mev gamma rays, the pulse shape controls on the amplifiers associated with the annulus crystal were adjusted for correct coincidence timing. With the amplifiers set for proper coincidence timing, the overall gains were adjusted by controlling the photomultiplier tube high voltages. A single high voltage supply was used with a voltage divider that provided five independent outputs. Gains for the outer crystals were set by adjusting the discriminator PHS to 0.59 Mev with a ΔE of 0.14 Mev and adjusting the high voltage to put the photopeak produced by a ^{137}Cs source in the center of this interval. Amplifier output pulses were transmitted to the discriminators over cables carefully cut to the same length. The multichannel analyzer was in-

stalled so that its input was approximately halfway along the cable from the center detector amplifier to the associated discriminator.

Coincidence gate bias levels were set by connecting the four pulse shapers assocated with the outer crystals to a single discriminator and adjusting the biases so no coincidence circuit output pulses were observed. Next, all combinations of the center plus two outer detectors were connected to a single discriminator to ensure that the gates were all operating properly.

The detector was operated in a modified collimator mounted in a turret located 500 yds from the base of the tower. Measurements were made of the gamma-ray energy spectrum above 1.5 Mev at angles of 0, 45, and 90 degrees with a 30° conical opening in the collimator for a source elevation of 1125 ft. With the source at 500 ft, a measurement was made at an angle of 0°. All measurements were normalized to a gamma detector located at 750 yds.

2.7 NORMALIZATION CHANNELS

2.7.1 Boron-10 Trifluoride

The principal means for normalizing neutron data between different runs or data taken at different times during a run was a $^{10}BF_3$ proportional counter enclosed in an aluminum-encased paraffin cylinder 37 cm long by 22.5 cm in diameter with a 3.8-cm-dia. axial hole to hold the counter. Except at the ends, this enclosed the counter in 9 cm of paraffin. The cylindrical assembly was positioned with its axis perpendicular to the plane containing the detector and tower. Two identical counters were installed at 750 yards from the base of the tower with one used as a backup.[3] Figure 2.14 is a picture of these two detectors.

Detector and shield were placed on a permanent stand approximately 4 ft above the ground. A preamplifier with a gain of ∿20 used an RG62 signal cable to transmit both the amplified detector signal and preamplifier power. High voltage coaxial cable (RG59) was used to transmit the detector anode potential. During the winter operations, both cables terminated in a small van truck used to house the following normalizing channel electronics: (1) a well-regulated high voltage supply for the anode potential; (2) an RC clipped linear pulse amplifier which supplied preamplifier power and further amplified the detector signal; (3) a decade scaler to count the output pulses of the linear amplifier pulse-height discriminator; and (4) a linear count rate meter and strip chart recorder to provide an analog record of the discriminator pulse rate as a function of time. Low capacitance coaxial cables were used to transmit the pulses from the van to other experimental trailers for use in normalizing individual instruments.

During summer operations, the neutron normalizing channels were modified. While the same neutron moderators were used with the same type of neutron detectors and similar preamplifiers, the power to operate the preamplifiers and subsequent amplification was provided by amplifiers using double delay line pulse shaping. As before, two channels were operated to provide continuous neutron monitoring in the event of the failure of the primary channel, but only the main channel was monitored with a count rate meter and strip chart recorder. This equipment was operated from the main instrument trailer. Careful measurements coupled with air density corrections established that the primary neutron monitor varied little between the winter and summer runs.

Proper operating parameters were determined by placing an AmB neutron souce in a reproducible position and measuring the count rate vs. anode potential and count rate vs. amplifier PHS setting. A test with a ^{60}Co source as-

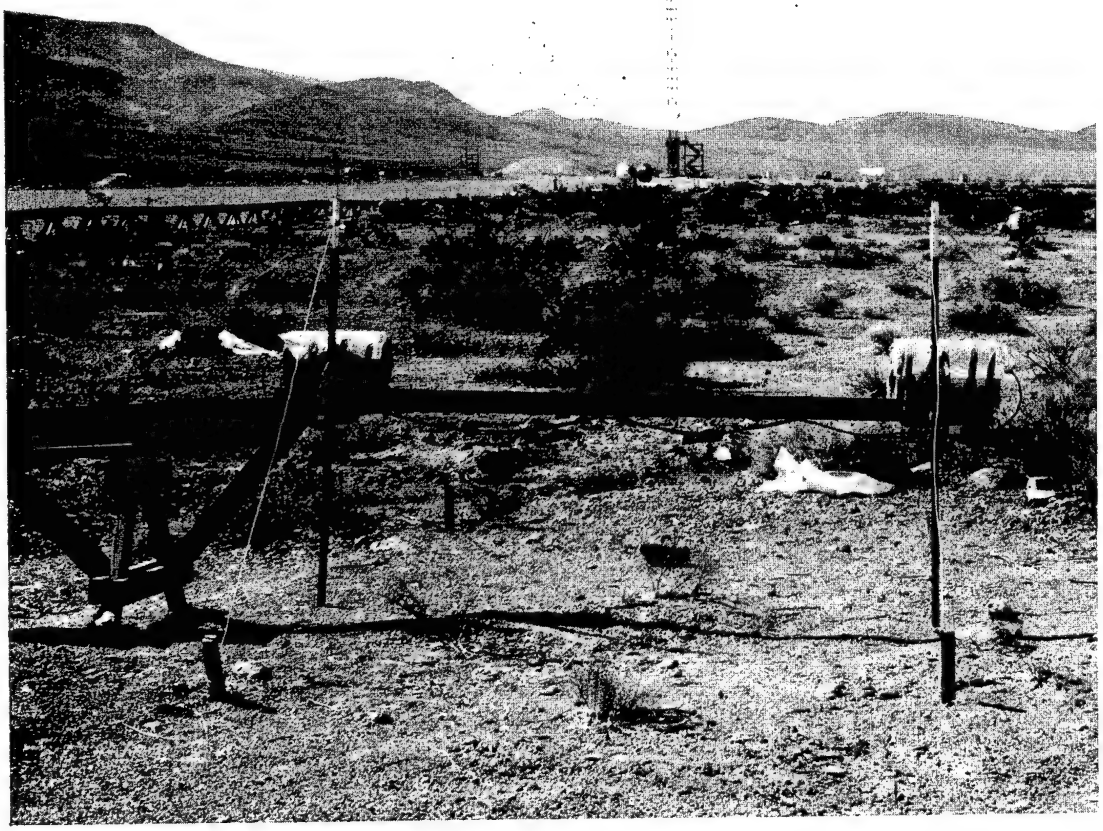

Fig. 2.14—Detectors used for neutron normalization by program 1 during Operation HENRE.

sured that the gamma-ray sensitivity was low. The same neutron source was used in the same position before and after each accelerator operation to standardize the counters.

2.7.2 GM Tube

To simplify the normalization of gamma-ray data, a gamma-ray normalization system was developed which utilized the same high sensitivity GM counter described in Section 2.4. Two of the detectors were mounted at 750 yds on a stand about 4 ft above the ground. They were positioned far away from the neutron normalization channels to eliminate the detection of hydrogen capture gamma rays produced in the neutron moderators. This setup is shown in Fig. 2.15, which also includes a general view of some of the Program 1 experimental area.

Emitter follower preamplifiers and transistorized high voltage supplies located and powered at the detector site were used to transmit the detector signals to the trailer 150 to 200 ft away where the signals went to several readout scalers. The relative sensitivities of the two systems were determined. Normally the two systems were operated together so that in the event of catastrophic failure of the main channel normalization could be quickly transferred to the second channel.

Setup procedure consisted of placing a ^{60}Co source in a reproducible position 2 m from the center of the detector and determining the response as a function of anode potential to choose a good operating point on the counter plateau. The same source was used before and after each accelerator run to standardize the detectors.

2.7.3 Fission Counter

Several means of monitoring accelerator operations were used. The primary means was a ^{238}U fission counter located in a fixed position in the source hoist car.[9] A cadmium can enclosed the detector to minimize thermal neutron response from residual ^{235}U. Care was taken to isolate the detector from a tower ground. Detector and preamplifier were mounted in such a way that they made no electrical connection with the box, and a single coaxial cable to the underground control bunker was used to transmit the preamplifier output pulse, detector anode potential and preamplifier power. Power was supplied by a low noise regulated power supply, but additional filtering was found necessary to reduce ripple to an acceptable level for the preamplifier power. In the bunker, the signal was amplified by a double delay line amplifier chosen for stability at high counting rate. The output of the amplifier pulse-height selector operated a 100 MHz scaler and a linear count rate meter that in turn operated a strip chart recorder.

2.7.4 Sulfur Foils

A second method used to normalize one run to another utilized sulfur pellets placed in a reproducible position on the source hoist car. The pellets were removed after each run and counted to determine the neutron fluence above 2.5 Mev. This energy threshold was low enough to measure the contaminant 3 Mev (D,D) neutrons as well as the primary 14 Mev (D,T) neutrons. Radioactive ^{31}Si from the n,α reaction (E_{th} = 6 Mev) was allowed to decay at least 24 hrs before the foils were counted.

2.7.5 Aluminum Foils

High purity aluminum foils were also placed in a fixed position on the source hoist car. The (n,α) reaction in ^{27}Al produces ^{24}Na which was counted

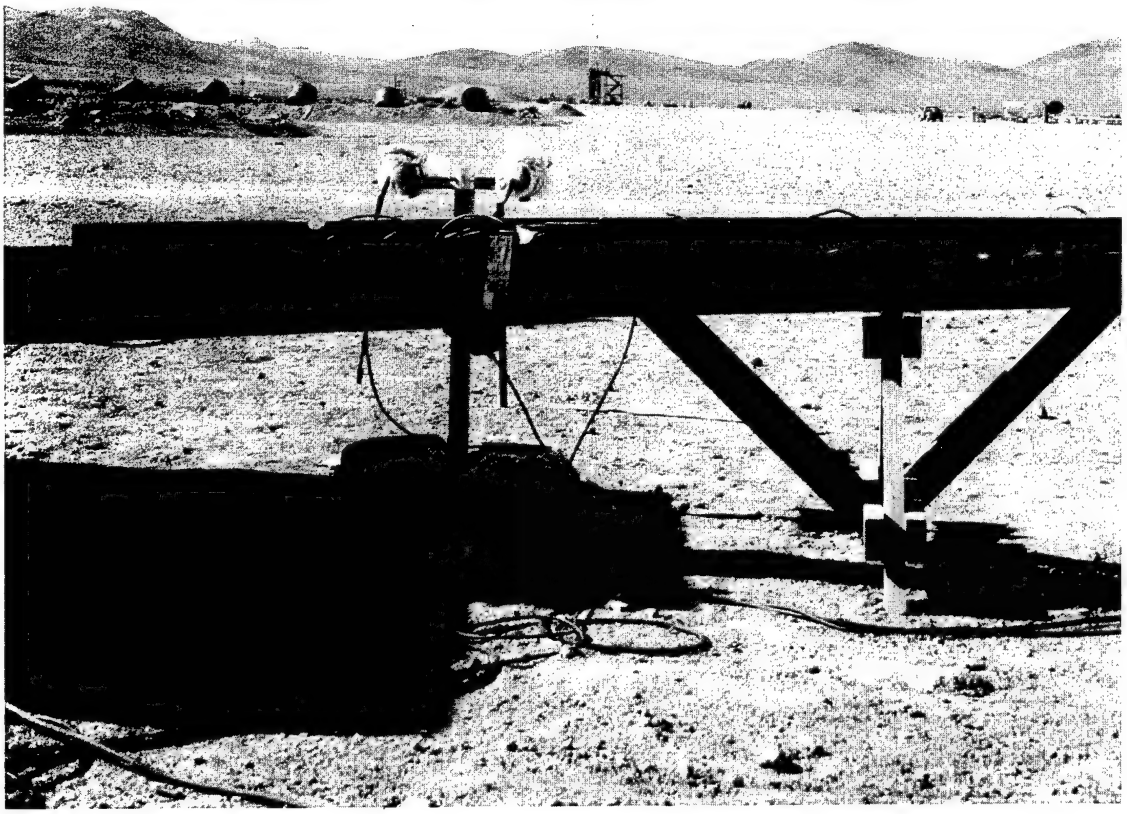

Fig. 2.15—Gamma-ray normalizing channels used by program 1 during Operation HENRE.

to determine the neutron flux above the reaction threshold of about 8 Mev. This threshold excluded the (D,D) neutrons. Magnesium-27 formed by the (n,p) reaction was allowed to decay before the foils were counted.

2.7.6 Weather Data

While the neutron and gamma-ray normalization systems described provided direct means of normalizing data taken at 750 yds, they were not sufficient for detectors located at some other distance. For these cases, the normalization data had to be coupled with distance and air density corrections. Distance corrections were straightforward, but air density corrections involved a knowledge of the air temperature and pressure coupled with the value of relaxation length for this spectrum of neutrons and gamma rays. Careful records of the air temperature and pressure were kept from data recorded by a weather station at the tower site. Relaxation lengths were measured during the course of another experiment.[16]

REFERENCES

1. F. F. Haywood and J. A. Auxier, *Technical Concept - Operation HENRE*, USAEC Report CEX 62.02, March 1965.

2. J. L. Fowler and J. E. Brolley, Jr., Monoenergetic Neutron Techniques in the 10 to 30 Mev Range, *Rev. Mod. Phys., 28, No. 2:* 103-134 (1956).

3. J. A. Auxier, F. F. Haywood, and L. W. Gilley, *General Correlative Studies-Operation BREN*, USAEC Report CEX 62.03, September, 1963.

4. R. H. Ritchie and G. S. Hurst, Penetration of Weapons Radiation: Application to the Hiroshima-Nagasaki Studies, *Health Phys., 1:* 390-404 (1959).

5. J. H. Thorngate, J. A. Auxier, F. F. Haywood, and S. Helf, *Energy and Angular Distribution of Neutrons and Gamma Rays - Operation BREN*, USAEC Report CEX 62.12, February, 1967.

6. *ibid.*, p. 24.

7. G. S. Hurst, An Absolute Dosimeter for Fast Neutrons, *Brit. J. Radiol., 27:* 353-357 (1954).

8. J. H. Thorngate, D. R. Johnson, and P. T. Perdue, *Neutron and Gamma-Ray Leakage from the Ichiban Critical Assembly*, USAEC Report CEX 64.7, June, 1966.

9. E. B. Wagner and G. S. Hurst, Advances in the Standard Proportional Counter Method of Fast Neutron Dosimetry, *Rev. Sci. Instr., 29:* 153-158 (1958).

10. D. R. Johnson, *Radsan Correction Factor Studies*, Health Physics Annual Progress Report for Period Ending July 31, 1966, ORNL-4007, 203, October, 1966.

11. E. B. Wagner and G. S. Hurst, A G-M Tube Gamma-Ray Dosimeter with Low Neutron Sensitivity, *Health Phys., 5:* 20-26 (1961).

12. J. H. Thorngate and D. R. Johnson, The Response of a Neutron Insensitive Gamma-Ray Dosimeter as a Function of Photon Energy, *Health Phys.*, *11*: 133-136 (1965).

13. E. B. Wagner, *Energy Response of G-M Tubes*, Health Physics Division Annual Progress Report for Period Ending July 31, 1962, ORNL-3347, 85, October, 1962.

14. R. B. Murray, Use of ^{6}LiI(Eu) as a Scintillation Detector and Spectrometer for Fast Neutrons, *Nucl. Instr.*, *2:* 237-248 (1958).

15. J. H. Thorngate, *Radiation Spectrometry*, Health Physics Division Annual Progress Report for Period Ending July 31, 1965, ORNL-3849, 161, October, 1965.

16. Z. Burson, *The Spatial Distribution of Dose in an Air-Over-Ground Geometry*, USAEC Report CEX 65.14, to be published.

Chapter 3

RESULTS

3.1 SPECTROMETRY

The results of the neutron and gamma spectral measurements made during HENRE are summarized in this section and compared with the available calculations. Difficulties involved in the data reduction are also summarized as well as the statistical problems which result from the reduction techniques that were necessary. For comparison with other HENRE experiments, the neutron spectra are presented as dose as a function of distance after weighting by the proper kerma factor and as a function of distance.

3.1.1 Neutron Spectral Data

Due to the large positive Q of the $^{6}Li(n,\alpha)$ reaction, a suppressed zero was used on the multichannel analyzer to eliminate the response of the analyzer to pulses produced by gamma interactions and recoil particles. The first correction required during data reduction was due to this suppressed zero. This was a simple additive correction to the data.

Next, the data were corrected for the nonlinear light output of the crystal as a function of the energy of the charged particles being stopped in the crystal. Two problems were encountered that hampered these corrections. The first resulted from the disparity among the published values for light as a function of neutron energy for the n,α reaction. This confusion was further compounded by the disagreement of preliminary measured values with any of the published values. A calculation using published values of dL/dE vs. dE/dX produced still another result.[1] The second problem encountered was a result of the nonlinear light output being a different function of energy for the competing reactions, specifically the n,n'd reaction. Due to the lower average dE/dX of the particles produced by this reaction, it produces light more efficiently than the foreground reaction, thus overcoming some of the foreground-to-background advantage obtained from the large difference in Q values. No published values of light output as a function of energy were available for this interaction, and a calculation was felt undesirable due to the uncertain results obtained for the calculated light output from the foreground reaction. These problems were resolved by making careful measurements of the response of the two available ^{6}LiI crystals to monoenergetic neutrons generated with a Van de Graaff accelerator using the P,T, D,D, and D,T reactions. The maximum energy of the accelerator used, coupled with the relatively poor resolution of the spectrometer, limited these measurements to 1, 4, 5, 16, 17, and 18 Mev. Pulse height data were normalized to the pulse height of the thermal neutron peak obtained in each case. It was assumed that the light output versus the total energy imparted by the charged particles was a power function, and the necessary parameters were obtained to allow interpolations to other energies.

An example of the response of this detector to monoenergetic neutrons of 16 Mev is shown in Fig. 3.1; a suppressed zero was not used for these measurements. The obvious features of the recorded pulse height spectrum are the foreground peak at the highest pulse heights, the background continuum below it, and the thermal neutron response. Maximum pulse height events from the background fall just below the foreground peak, although there is a 6.25 Mev difference in the Q values of the reactions; a good example of the differences in dL/dE for the two reactions. Two effects combine to produce an increasing response at low pulse heights: (1) the nonlinear L vs. E response decreases the number of channels per Mev and (2) the response to gamma-rays. To obtain an L vs. E curve for the background, an arbitrary point on the high energy edge of the measured distribution was chosen. Such a selection was consistent with the data reduction scheme, which will be described later.

Once the light output versus particle energy was obtained, it was related to neutron energy, and the channels corresponding to each Mev interval were integrated. A 1-Mev interval was felt to be consistent with the resolution of the spectrometer and the amount of data obtained. Decreased statistical uncertainty was the major benefit of such integration of the data. Background response as a function of neutron energy was also obtained in 1-Mev intervals. In general, the background intervals overlapped foreground intervals, further complicating the data reduction process.

To subtract the background from the recorded data, three assumptions were made. First, perfect resolution was assumed for which the pulse height distribution produced in the crystal by monoenergetic neutrons would look like that shown in Fig. 3.2. The data were not good enough to include a resolution function in the reduction routine without adverse statistical effects. The second assumption was that the data recorded at the highest pulse heights was due solely to the foreground reaction. Some possible limitations on such an assumption will be presented later. Third, the number of background pulses produced at any energy was assumed to be proportional to the total cross section for the background reaction with an equal number of pulses produced per Mev up to the maximum energy.[2]

To strip the data, once these assumptions were made, the counts in the highest energy interval were divided by the efficiency to obtain the number of neutrons required to produce such a response. Then the amount of background per Mev that would be produced by this many neutrons was calculated and subtracted from the recorded data. This process was repeated for the next lower energy and so on until the data were completely reduced. Error propagations made were consistent with the mathematical processes involved in each step with the assumption that each cross section used had an error of ±10%, a reasonable assumption.[3]

Another component of background which might contribute to the measured pulse height spectrum would be the $^{6}Li(n,P)$ reaction. To determine the effect of this reaction, the light output as a function of proton energy was calculated. The effects of a difference of 7.518 Mev in the Q values for the foreground reaction and this reaction were completely overcome by the much higher light production efficiency of the protons. In this case, it was no longer possible to assume that the highest pulse height values were produced by the foreground reaction. In order to reduce the data, a system of 32 equations in 16 unknowns, was derived. The redundancy allowed the determinant for the solution of the equations to be diagonalized. Solution of the resulting system of 16 equations in 16 unknowns was not difficult, but did not lead to results significantly different from those obtained from the less elaborate stripping procedure. It did result in the generation of large statistical uncertainties in the reduced data. As a result, the n,P reaction was not considered important.

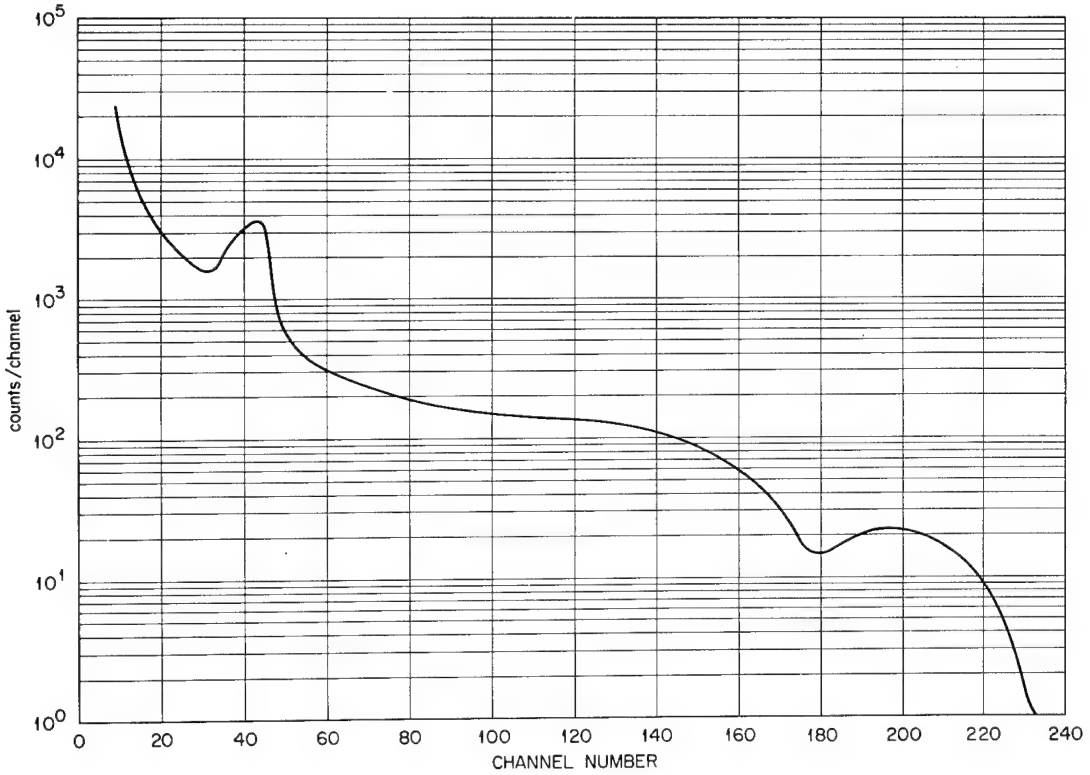

Fig. 3.1—Measured response of ^{6}LiI scintillator to 16 Mev neutrons with the detector cooled to the temperature of liquid nitrogen.

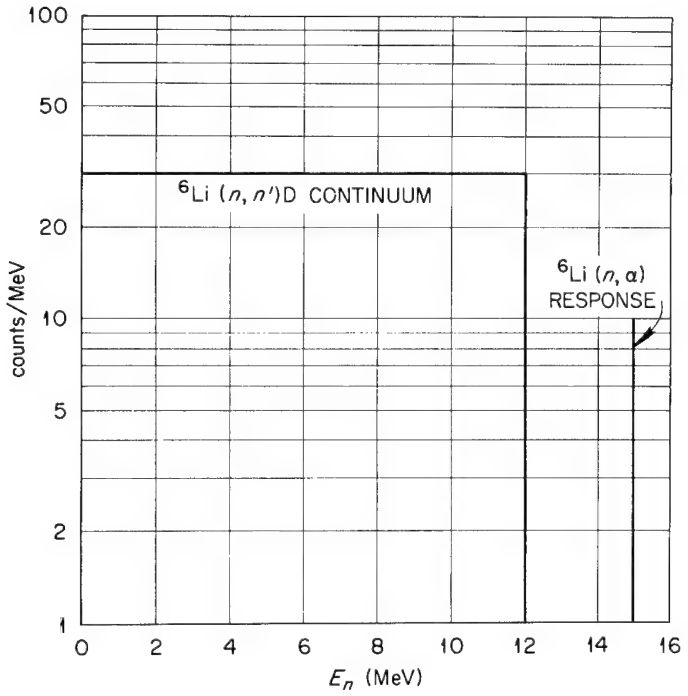

Fig. 3.2—Idealized response of ^{6}LiI scintillator to monoenergetic neutrons. Energy scale related to n,α reaction.

The efficiency of the spectrometer as a function of energy was calculated using cross sections and the known physical and geometrical parameters of the detector. In general, such calculations would be expected to overestimate the efficiency as they do not include losses due to edge effects, but the agreement between such a calculation and measured response to 15 Mev neutrons was good, so no further corrections were applied. For direct comparison with the calculations, the recorded values were multiplied by $4\pi r^2$ where r was the source-detector distance in centimeters. This assumes the response of the spectrometer is isotropic, which it is not due to the necessary mounting hardware and photomultiplier tube assembly. These effects were not large, so no correction was made for them.

During the field experiment, data were normalized to a modified long counter located at 750 yds from the base of the tower. In order to make direct comparisons with calculated spectra, the ratio of total neutrons produced by the source to total long counter counts was obtained for each run, then this was multiplied by the long counter value obtained for each spectrometer run to allow normalization to the number of source neutrons.

Spectra were measured in a civil defense shelter located at 400 ft from the base of the tower with the source at an elevation of 300 ft; earth coverings of zero, one, two, and three feet were used over the shelter. These data are presented in Figs. 3.3, 3.4, 3.5, and 3.6.

Figure 3.7 shows the neutron fluence as a function of earth covering. Data were integrated in 3 Mev steps to simplify presentation and decrease statistical variations. Relaxation lengths calculated from the one, two, and three-feet data give 1.07 ft for neutrons of 1-3 Mev, 0.63 ft for neutrons of 4-6 Mev, 0.79 ft for neutrons of 7-9 Mev, 1.03 ft for neutrons of 13-15 Mev. The long relaxation length for the lowest energy group is probably an effect of the uncertainties in the measurement for that group. In general, the relaxation length increases with increasing neutron energy until inelastic reactions become important.

When the measured spectra are weighted with the values of kerma per neutron per cm^2 calculated by Jones,[4] the results in Fig. 3.8 are obtained. The rather unusual units obtained result from the manner in which the spectral data are presented. Two sets of data are shown, one integrated from 0.5 Mev and the other from 1.5 Mev. For the first, the relaxation length for the 1, 2, and 3-feet depths is 0.90 ft. With the lowest energy neutrons omitted, it is 0.74 ft. Again, the differences reflect the uncertainties in the 0.5 to 1.5 Mev data caused by decreasing spectrometer resolution, the large thermal cross section, and noise generated by the atmosphere. The latter is a constant problem in field experiments like HENRE. Relaxation length determinations are also affected by the change in geometry incurred.

Spectral measurements in air were made at 500 ft and 2250 ft from the base of the tower for a source height of 500 ft and at 1500 ft and 2250 ft for a source height of 1125 ft. These results are shown, compared with calculations by Straker in Figs. 3.9, 3.10, 3.11, and 3.12.[5,6,7] Suitable calculations did not exist for direct comparison with the data, so interpolations were made based on an exponential fit of the calculations vs. range for each energy group. The error bars shown on the data are one sigma, and the calculations are estimated to have a deviation of ±20%, so the comparison between measurement and calculation are rather good for the larger distances. Data points fall above the calculations for the 1125 ft source height runs which may be attributed to the assumptions made in the efficiency and solid angle corrections. Obviously neither error can be too large. The data points for the large distance 500 ft source height run fall below the calculations due

(Text continued on page 46.)

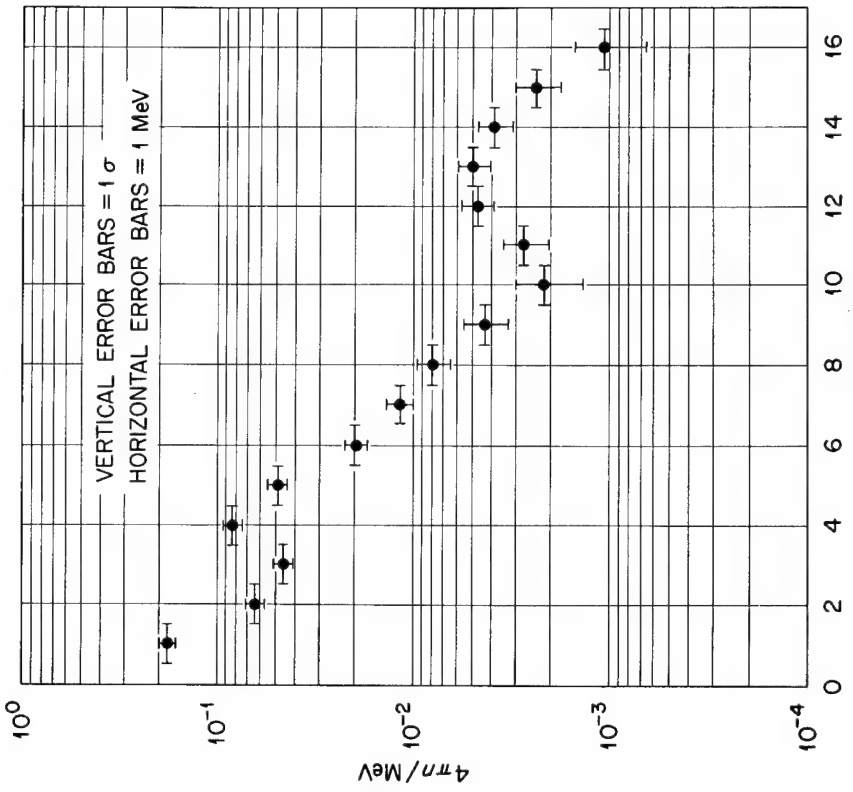

Fig. 3.4—Neutron spectrum measured in the civil defense shelter covered with 1 ft of earth. Data normalized to 4π neutrons per Mev per source neutron.

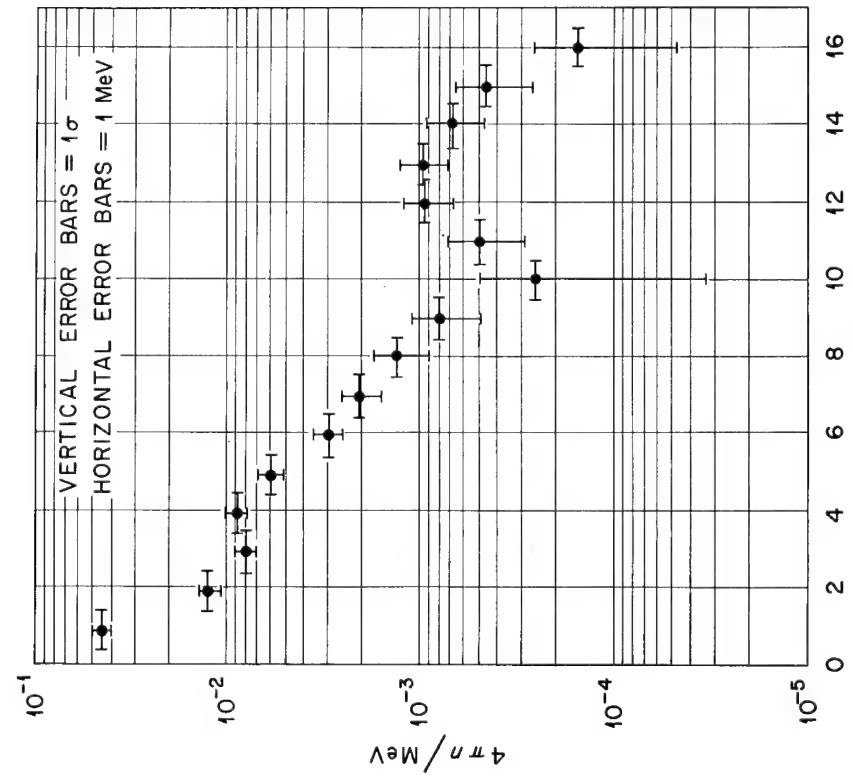

Fig. 3.3—Neutron spectrum measured in the civil defense shelter with no earth covering. Data normalized to 4π neutrons per Mev per source neutron.

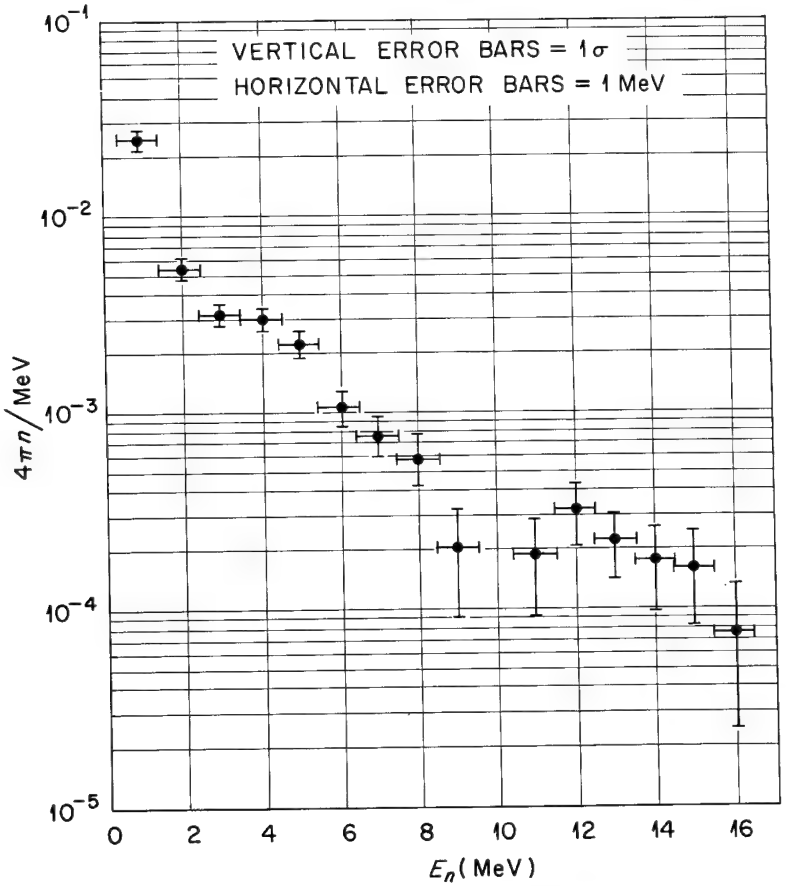

Fig. 3.5 — Neutron spectrum measured in the civil defense shelter covered with 2 ft of earth. Data normalized to 4π neutrons per Mev per source neutron.

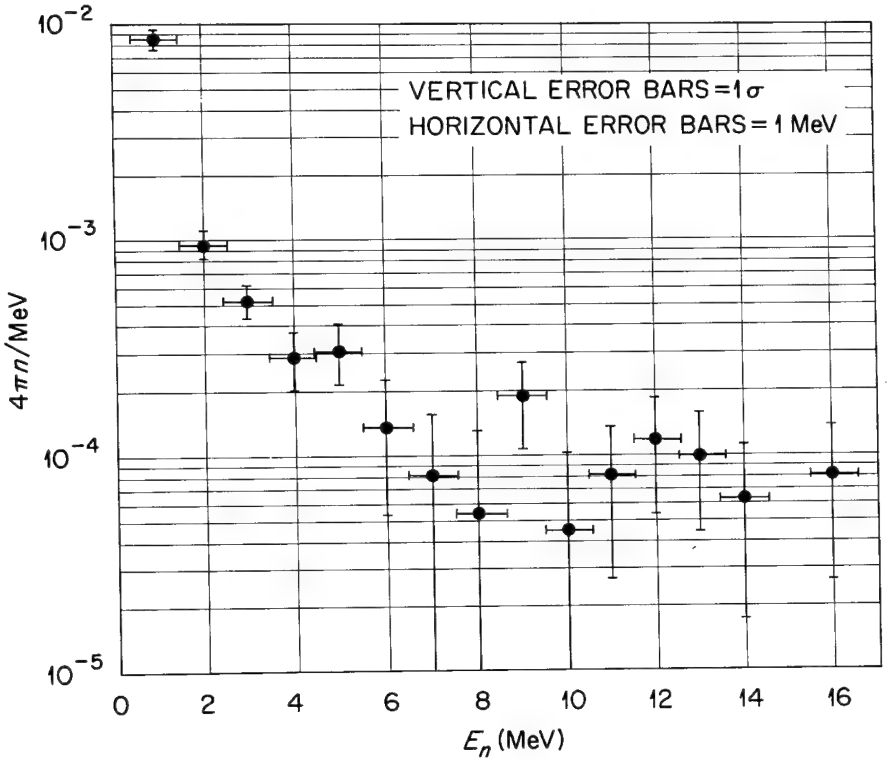

Fig. 3.6 — Neutron spectrum measured in the civil defense shelter covered with 3 ft of earth. Data normalized to 4π neutrons per Mev per source neutron.

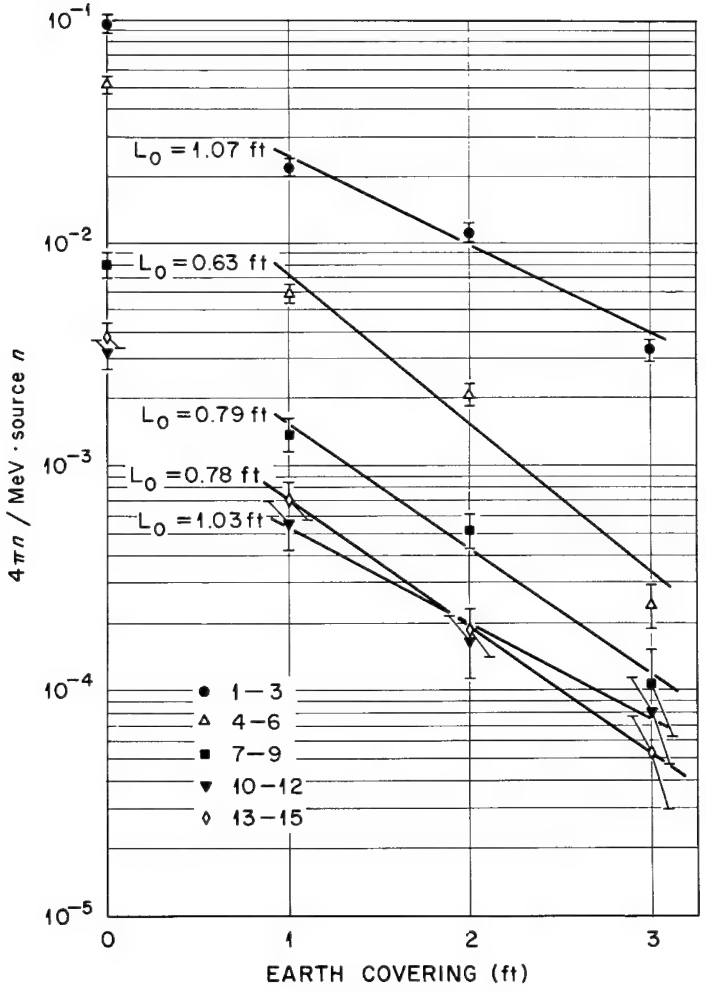

Fig. 3.7 — Neutron spectrum in the shelter vs. earth covering shown in 3-Mev intervals. Normalized to 4π neutrons per Mev per source neutron.

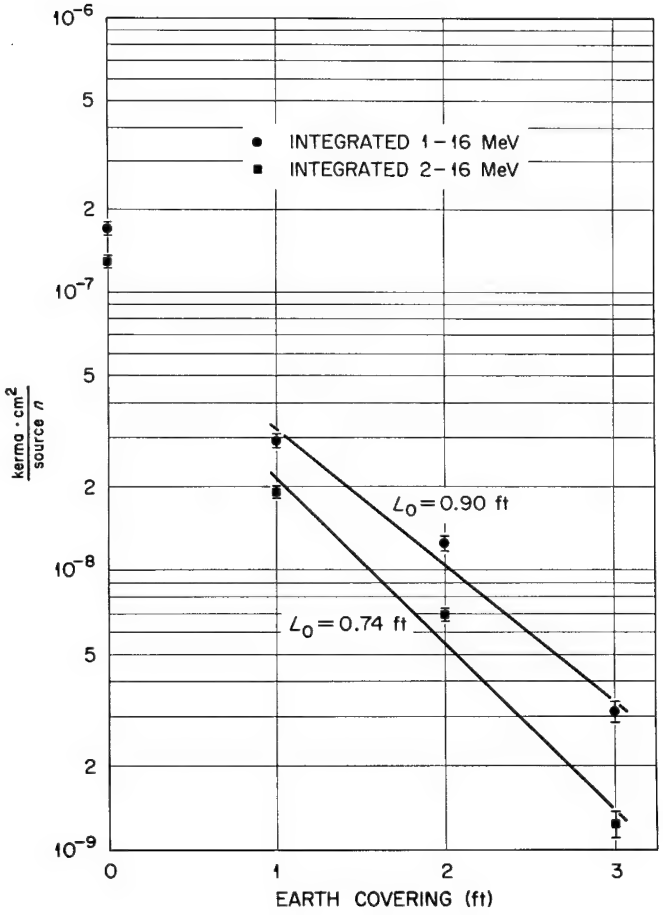

Fig. 3.8 — Kerma per source neutron in the shelter as a function of earth covering. Integrated over 0.5 to 16.5 Mev and 1.5 to 16.5 Mev.

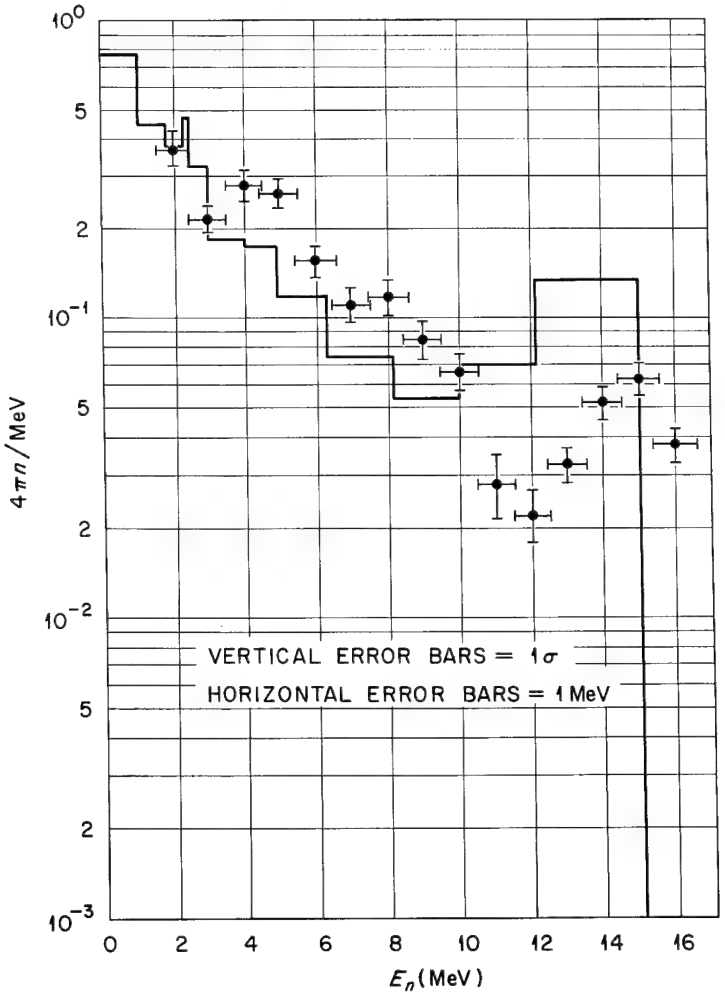

Fig. 3.9 — Neutron spectrum in air at a range of 215 meters. (Source height, 500 ft; lateral distance, 500 ft.) Data normalized to 4π neutrons per Mev per source neutron. Compared with calculations at the same range. (Source height, 1125 ft.)

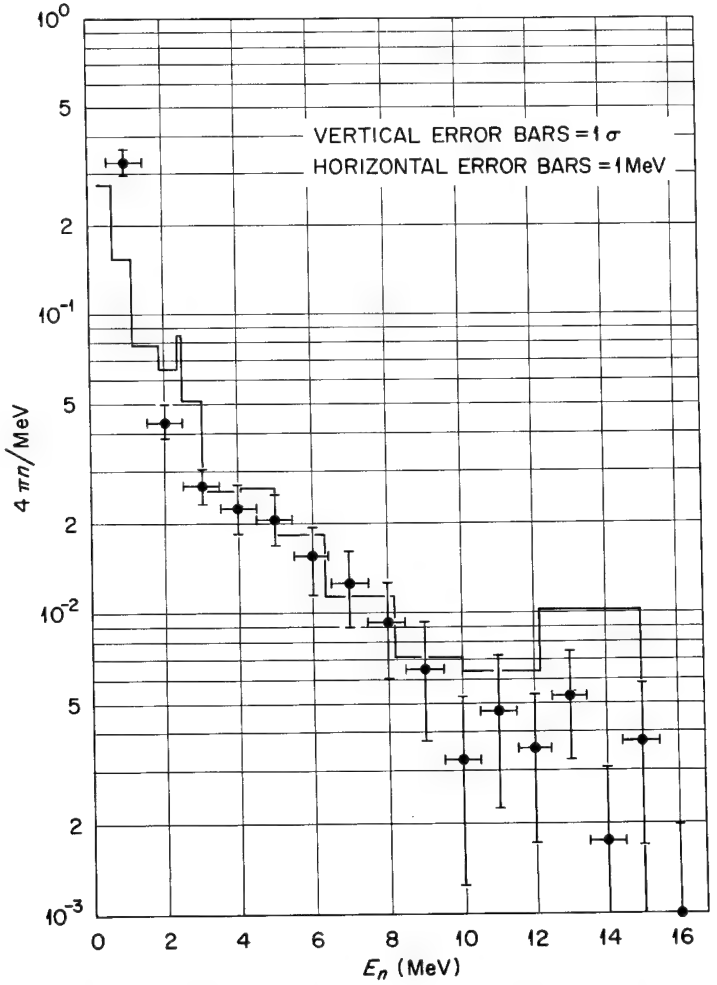

Fig. 3.10 — Neutron spectrum in air at a range of 702 meters. (Source height, 500 ft; lateral distance, 2250 ft.) Data normalized to 4π neutrons per Mev per source neutron. Compared with calculation for the same range. (Source height, 1125 ft.)

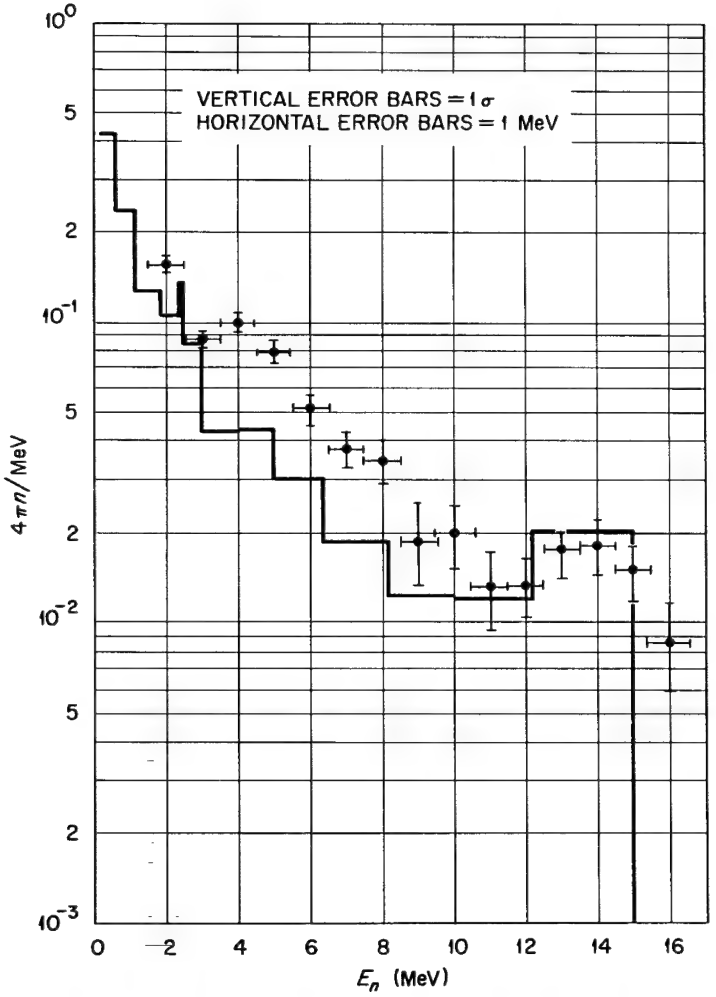

Fig. 3.11—Neutron spectrum in air at a range of 571 meters. (Source height, 1125 ft; lateral distance, 1500 ft.) Data normalized to 4π neutrons per Mev per source neutron. Compared with calculations for the same conditions.

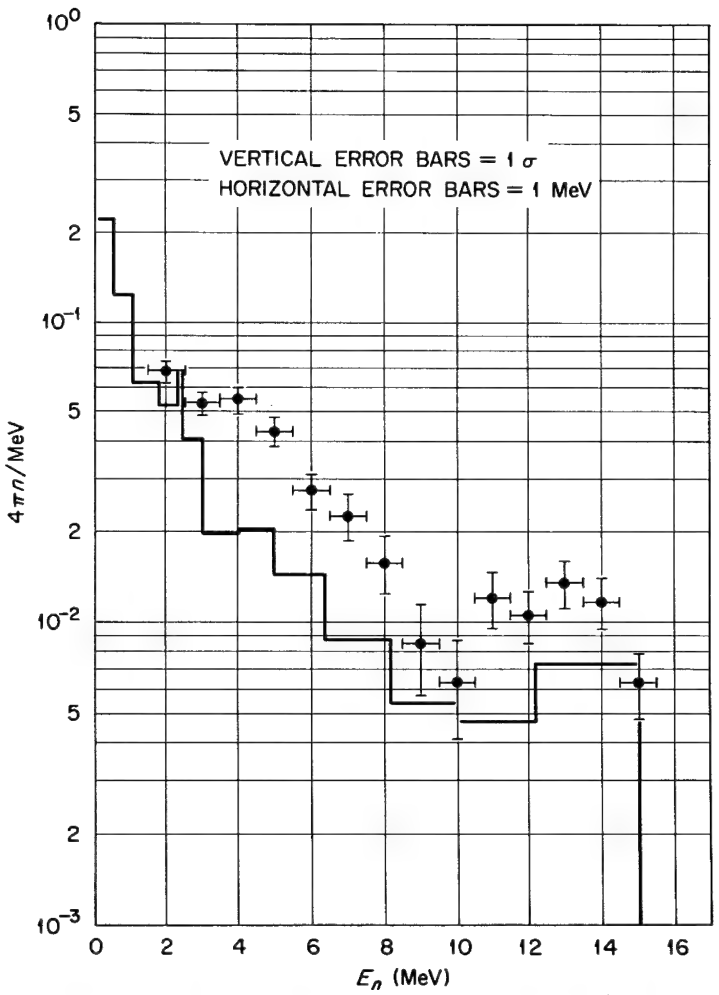

Fig. 3.12—Neutron spectrum in air at a range of 766 meters. (Source height, 1125 ft; lateral distance, 2250 ft.) Data normalized to 4π neutrons per Mev per source neutron. Compared with calculations for the same conditions.

to the effect of the air ground interface upon the measurements, a factor not included in the calculations for which a source height of 1125 ft was assumed. The peak occurring near 4 Mev is unexplained but appears in the calculations as well, and is probably due to the effects of inelastic neutron cross sections above 12 Mev. Both the calculations and the measurements indicate the spectrum has not reached equilibrium for the ranges involved. This is discussed in more detail in Section 3.1.3.

When the spectra measured in air are integrated in three Mev steps and plotted as a function of source detector distance, as in Fig. 3.13, the effects of the air ground interface on the one set of data is quite apparent. The close data were also recorded for a source height of 500 ft, but the small range minimized the interface effect. The remaining points fall on good exponential curves from which the relaxation lengths as a function of energy may be obtained. They are 323 M for the 1-3 Mev neutrons, 322 M for the 4-6 Mev neutrons, 292 M for the 7-9 Mev neutrons, 398 M for the 10-12 Mev neutrons, and 356 M for the 13-15 Mev neutrons.

The spread in the lowest energy data is undoubtedly due to the problems already mentioned in the 1 Mev data. For the higher energy intervals, the data show the relaxation length increases as a function of energy, up to 398 meters for the 10-12 Mev neutrons. The decrease for the 13-15 Mev neutrons is due to the increasing nonelastic cross sections for neutrons in this energy range. These highest data represent a number more like the mean free path than a relaxation length, since the energy requirements make these measurements a good geometry experiment as neutrons generally leave this energy interval after one interaction with the air.

When the in-air data are weighted to kerma, the results shown in Fig. 3.14 are obtained.[4] Once again two curves are shown, one integrated from 0.5 Mev, the other from 1.5 Mev. This is due to the previously mentioned errors possible in the 1 Mev data. The interface effect shows on these data for the points at $\sim$700 meters. For the data from 1.5 Mev up, the relaxation length obtained is 329 M for an air density of 1 gm/liter. This exceeds values obtained from dose measurements as would be expected due to the rather high low-energy cutoff, but it is not inconsistent with other measurements.

3.1.2 Gamma Ray Spectral Data

The theoretical response of a gamma spectrometer utilizing the pair production process is a single line limited only by spectrometer resolution. In the scintillation device used during HENRE, the response was limited further by edge effects, since the detector was made small enough to insure the escape of both annihilation quanta. Typical response of the HENRE spectrometer to a 4.43 Mev gamma ray is given in Fig. 3.15. It shows a resolution of about 4% for the double escape peak. A low energy tail occurs in the measured pulse height distribution that is caused by three factors: (1) the electron leaves the detector without giving up its entire kinetic energy in the sensitive region; (2) the positron leaves the sensitive region and annihilates in the light reflecting material or case surrounding the detector; and (3) a pulse is measured when an accidental coincidence occurs. During HENRE, the last contributed far less than the first two, since the occurrence of accidental coincidences is a function of the count rate in each channel of the coincidence system, which was low, and the resolving time of the coincidence circuit which was short (25 nsec). Chance coincidences would fall not only on the low energy side of a particular pulse height, but over the entire range of γ energies present.

Measurements made of the response of the detector to gamma rays of 6.14 Mev and 7.48 Mev gave substantially the same results as those shown for

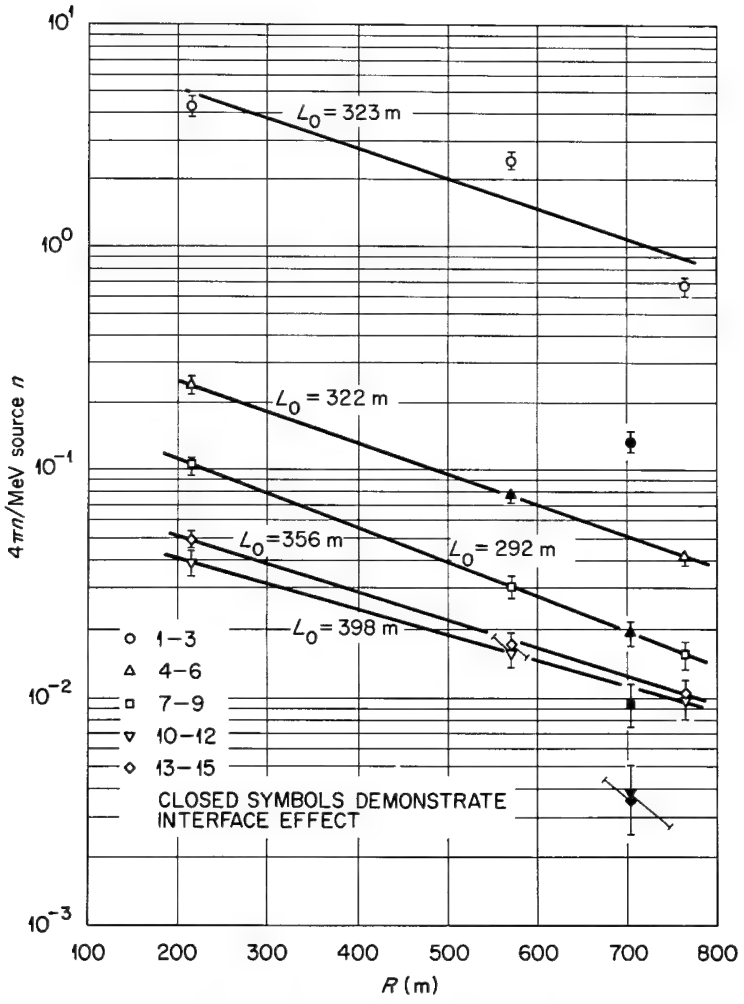

Fig. 3.13—Neutron spectrum as a function of range integrated in 3-Mev intervals. Data normalized to 4π neutrons per Mev per source neutron. Data at 702 meters illustrate effect of air–ground interface.

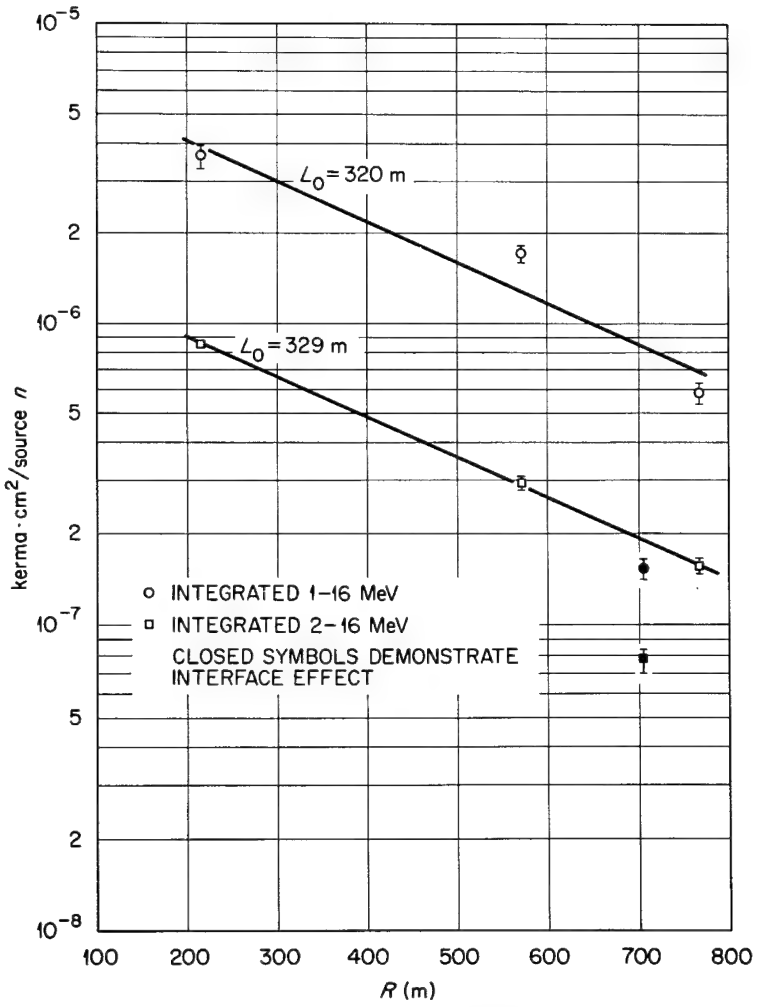

Fig. 3.14—Kerma per source neutron vs. range. Integrated over 0.5 to 16.5 Mev and 1.5 to 16.5 Mev.

a 4.43 Mev gamma ray.[8] Because the shape of the measured response varied little in the energy range of interest, a simplified response was assumed to facilitate data reduction. It is shown in Fig. 3.16. Basically, this is the same as the response shown in Fig. 3.15 but with perfect resolution. In the following discussion, the features of this response will be referred to as the peak and the continuum. It was not thought that the amount and quality of the data obtained warranted the inclusion of a resolution parameter in the data reduction. Using this idealized response, data were stripped by assuming the counts recorded in the highest channel were due to a double escape peak and subtracting the appropriate continuum from the data in the lower channels. In order to determine what fraction the continuum was of the peak height, the gain standardization data for each run was stripped with the requirement that the results of this operation should not yield negative values. To determine what ratio of peak to continuum would produce this desired result, a mathematical model of the stripping program was evolved which could be solved as an nth degree polynomial in the required fraction. Errors generated by this method of data reduction were assumed to be related to the error of the energy peak. These errors were propagated using standard techniques for the mathematical processes involved.[3] No errors were assumed for the cross section values used.[9]

Many other corrections were also required. Zero corrections were made to correct for a slight zero error in the multichannel analyzer used. Linearity-zero measurements using a pulser were the basis for these corrections with a straight line fitted to the resulting data using least squares techniques to find the proper zero intercept. To decrease the statistical fluctuations, the data were reduced in steps of 0.1 Mev by integrating several channels for each point.

The efficiency of the spectrometer was measured at 4.43 Mev using a PuBe source of known neutron output and a recently published ratio for the yield of 4.43 Mev gamma rays per neutron.[10] Efficiency vs. energy was calculated for all other energies by assuming it varied with the cross section and with that volume of the center detector in which the pair could be formed and deposit all of its kinetic energy. In order to do this, a function was required to relate the average angle of the electron and positron with the initial gamma ray energy. First, the average electron or positron energy was assumed to be one-half the available kinetic energy,

$$\bar{T} = \frac{h\nu - 2\, m_0 C}{2}$$

This value was then used in a formula derived by M. Stearns,

$$\Theta = q \frac{m_0 C^2}{\bar{T}} \ln \frac{\bar{T}}{m_0 C^2} .$$

where q is a slowly varying function of energy near one.[11] Stearns estimated this relation was within 10% for angles up to $\Theta = 20°$ which corresponds to an $h\nu$ of about 1.5 Mev for the approximations used. Once $\bar{T}$ and Θ were calculated, the electron or positron range along the crystal axis and perpendicular to the crystal axis could be determined as a function of energy. Values for the range of the electrons and positrons in sodium iodide were obtained from the tables of Berger and Seltzer.[12] The ranges calculated represent that section at the back and outer circumference of the detector in which an electron or positron could not deposit its entire kinetic energy before striking the detector walls. A macroscopic cross section may be calculated from these data, which can be normalized by the efficiency measured at 4.43 Mev. Such a

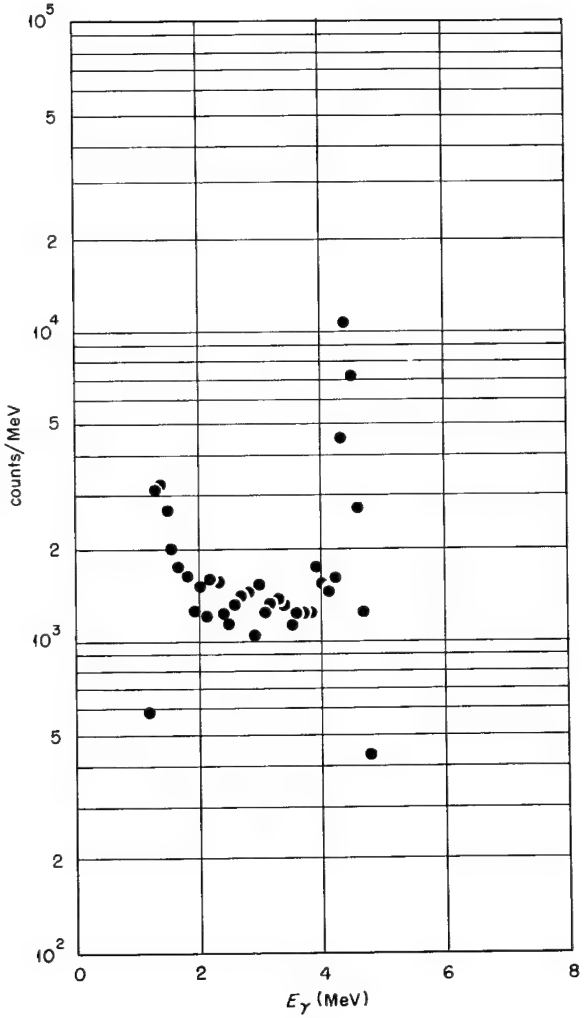

Fig. 3.15—Typical uncorrected response of the pair spectrometer as a function of gamma energy to 4.43-Mev gamma rays.

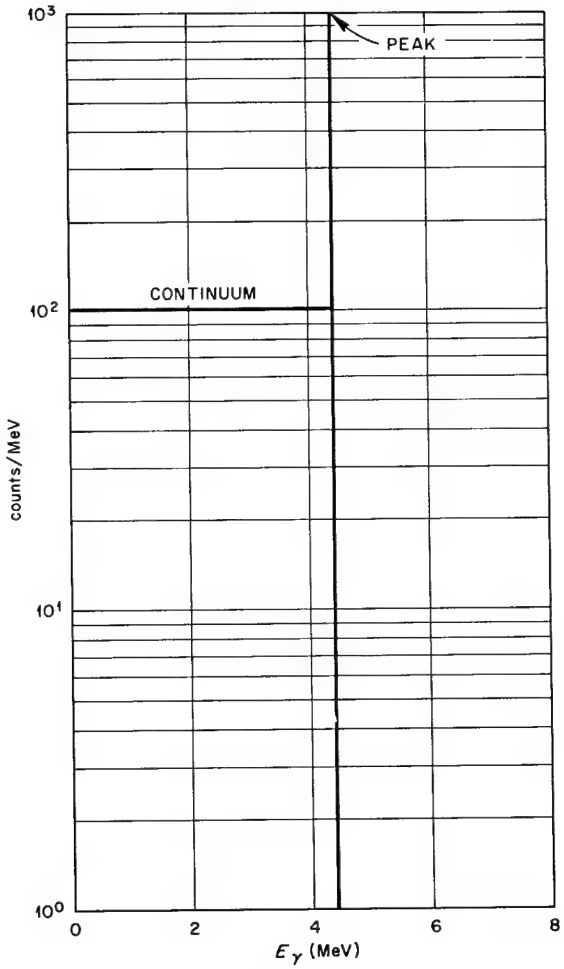

Fig. 3.16—Idealized spectrometer response showing assumed peak and the continuum resulting from edge effects.

normalization is required to correct for the energy insensitive losses in the efficiency due to the geometry of detection of the annihilation quanta.

Once the efficiency had been determined, data could be reduced to gamma rays cm^{-2} Mev^{-1}. The available calculations of the gamma-ray spectra were expressed in terms of gamma rays integrated over all space per Mev per source neutron. Thus, the data were multiplied by 4π times the range squared and normalized to total source neutrons.

Figures 3.17, 3.18, 3.19, and 3.20 show the results for a polar angle of 0° with the source at 500 ft elevation and at 0°, 45°, and 90° for the source at 1125 ft. For these data, the solid angle subtended by the collimator opening was 0.214 steradians.

When the 0°-500 ft data is studied, a number of peaks are observed. Table 3.1 summarizes the distinct gamma-ray lines obtained along with the possible source of these gamma rays from neutron interactions in ^{16}O or ^{14}N. Also indicated are the Q values for the reactions considered and an approximate cross section value. An interesting point is that none of the gamma rays appear to be associated with the $^{14}N(n,\gamma)^{15}N$ reaction which accounts for the majority of the gamma rays produced in air by a source of fission neutrons. Of particular interest is the prominent peak at 4.4 Mev. Several reactions can result in a gamma ray near this energy, so that the total cross section for its production is almost as large as that for the well-known 6 Mev line. Since this peak decreases with respect to the higher energy peak as a function of angle, it appears its production depends on high energy neutrons, although part of the apparent decrease must be due to increasing statistical uncertainties.

Atmospheric electrical noise increased the recorded data at the lowest energies for several of the measurements. No attempt was made to subtract this response from the data.

To further facilitate the comparison of the recorded data with the calculations, the data for the two 0° runs were integrated over the energy intervals used in the calculations and then multiplied by the ratio of total solid angle to the solid angle subtended at the collimator. The results are shown in Figs. 3.21 and 3.22. Such a procedure would be expected to produce measured spectra larger in general than the calculations because it assumes that the spectrum is the same per unit solid at all polar angles. The 45° and 90° measurements show this is definitely not so, but sufficient data do not exist for a more realistic integration. The agreement between calculations and measurements is good. Variations as large as a factor of 2 could be expected due to cross section errors.[10] The biggest differences occur in the 3 to 5 Mev region and may be due to insufficient or incorrect cross section data in the calculations. This conclusion is consistent with the measured spectra being lower than the calculations at the higher energies although instrumentation difficulties also reduce the response of the spectrometer at high energy. To simplify comparison of the gamma spectra as a function of polar angle, the data measured with a 1125-ft source height was integrated over the energy ranges used for the calculations. The results, shown in Fig. 3.23, indicate no significant change in the gamma spectra.

3.1.3 Calculated Values of the Neutron and Gamma-Ray Spectra as a Function of Range

Because the information presented will be important in the discussion of the results obtained for the neutron and gamma-ray dose as a function of polar angle discussed in the next section, this topic will briefly present some of the neutron and gamma-ray spectra calculated for the HENRE experiment.[5,6,7]

(Text continued on page 55.)

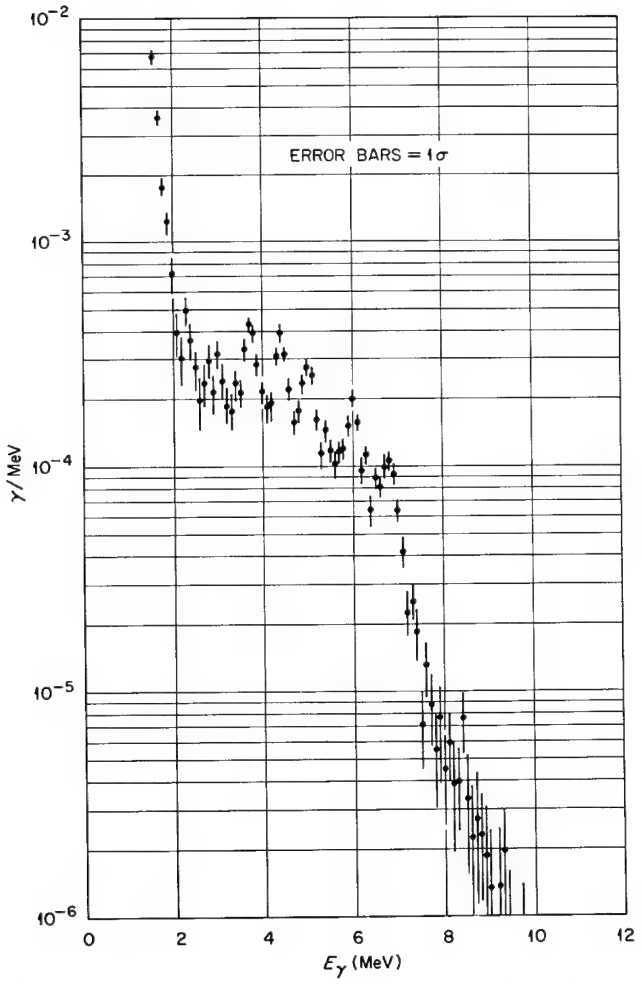

Fig. 3.17—Gamma-ray spectrum from a 0° polar angle, 30° collimator acceptance angle, source height of 500 ft, and a slant range of 527 yards (482 meters). Data normalized to 4π gamma rays per Mev per source neutron.

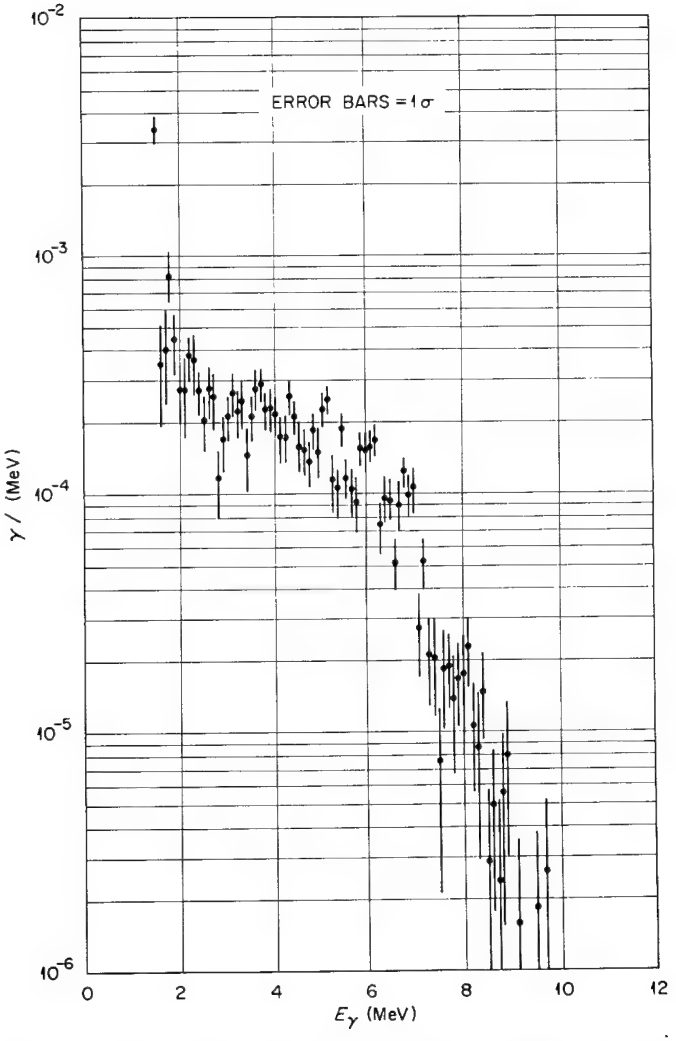

Fig. 3.18—Gamma-ray spectrum for a 0° polar angle, 30° collimator acceptance angle, source height of 1125 ft, and a slant range of 624 yards (571 meters). Data normalized to 4π gamma rays per Mev per source neutron.

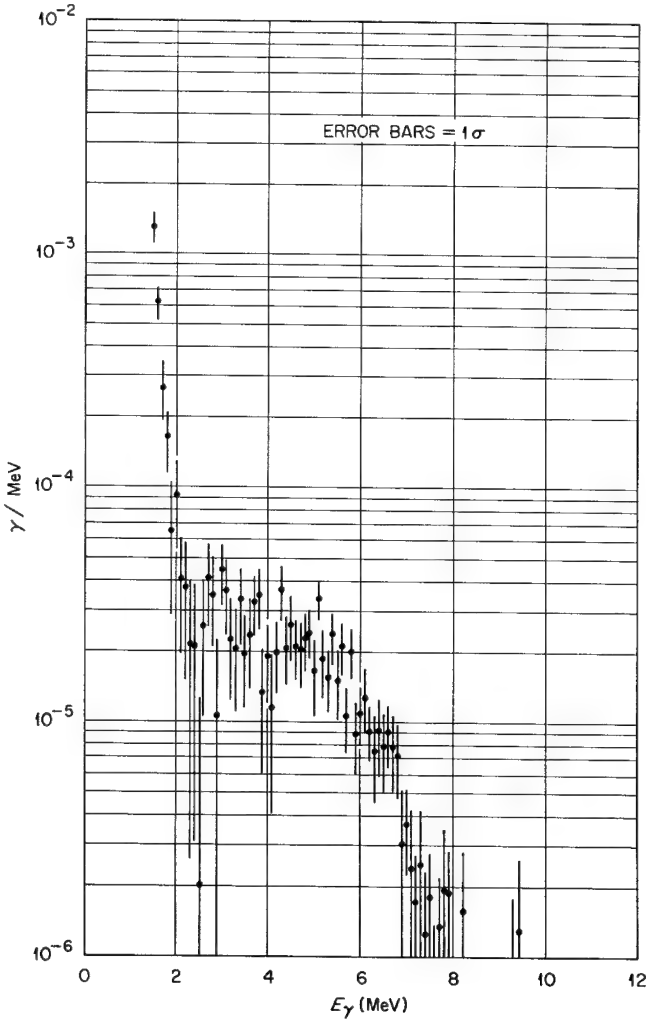

Fig. 3.19—Gamma-ray spectrum for a 45° polar angle, 30° collimator acceptance angle, source height of 1125 ft, and a slant range of 624 yards (571 meters). Data normalized to 4π gamma rays per Mev per source neutron.

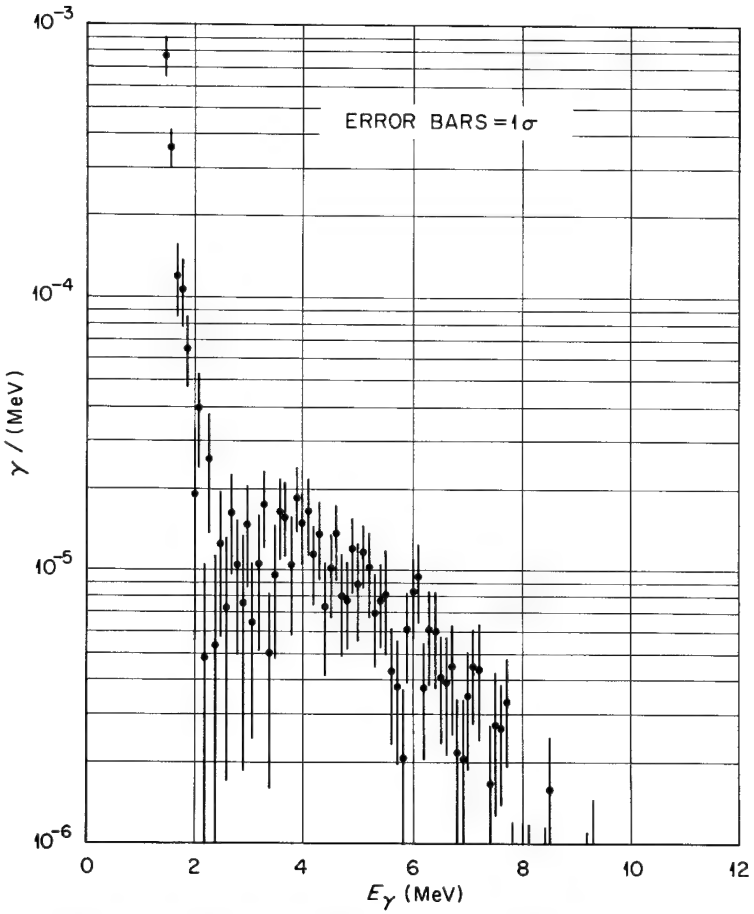

Fig. 3.20—Gamma-ray spectrum for a 90° polar angle, 30° collimator acceptance angle, a source height of 1125 ft, and a slant range of 624 yards (571 meters). Data normalized to 4π gamma rays per Mev per source neutron.

Table 3.1

CORRELATION OF OBSERVED GAMMA RAYS WITH POSSIBLE SOURCES

Observed E_γ(MeV)	Possible γ(MeV)	Source	Q MeV	Cross Section
2.3	2.312	$^{14}N(n,n'\gamma)$	-	> 5 MeV 50 mb
3.0	3.085	$^{16}O(n,\alpha)$	-2.214	> 5 MeV 75 mb and up to 200 around 14 MeV
3.7	3.680	$^{16}O(n,\alpha\gamma)$	-2.214	10 mb max
4.4	4.459	$^{14}N(n,\alpha\gamma)$	-0.157	> 5.5 MeV 30 mb
	4.433	$^{14}N(n,T\gamma)$	-4.014	> 5.5 MeV 20 mb
	4.433	$^{16}O(n,\alpha n)$ $^{12}C^* + \gamma$	∿-12	>12 ∿10 mb
5.0 - 5.1	5.035	$^{14}N(n,\alpha\gamma)$	-0.157	> 6 50 mb
	5.104	$^{14}N(n,n'\gamma)$	-	
6.0	6.091	$^{14}N(n,p)$	0.626	- 40 mb
	6.135	$^{16}O(n,p)$ $\rightarrow\beta^- + ^{16}O^*$	-9.626	
6.8	6.758	$^{14}N(n,\alpha\gamma)$	-0.157	
	6.808			
	6.923	$^{16}O(n,p)$ $\rightarrow\beta^- + ^{10}O^*$	-9.626	>12 30 mb

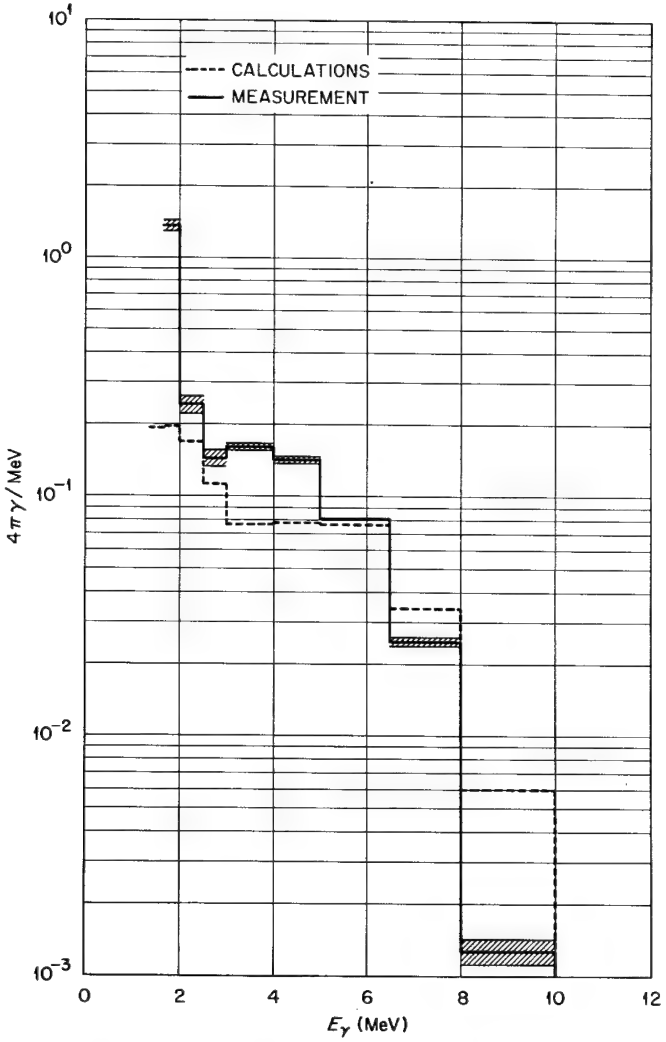

Fig. 3.21—Comparison of measured 0°, 500-ft gamma spectrum with calculations.

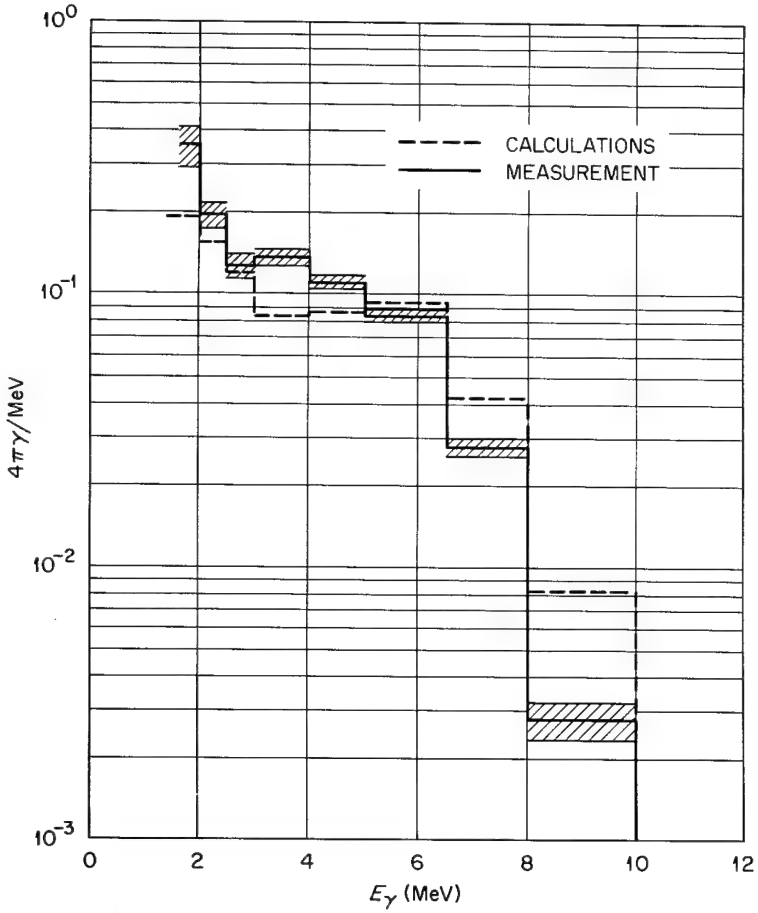

Fig. 3.22—Comparison of measured 0°, 1125-ft gamma spectrum with calculations.

It would be more desirable to use the measured spectra, but the calculations are available at ranges for which measurements were impractical, and it has been shown that the agreement is good when the calculations are interpolated to distances consistent with the measurements.

Figure 3.24 shows the calculated neutron spectra for ranges of 343, 519, 770, 1104, and 1539 meters. All of the measurements were made at ranges similar to the first three shown. A similar set of calculations for the gamma-ray spectra are shown in Fig. 3.25. The most important point to be noted about these data is that the neutron and gamma-ray spectra are changing as a function of distance, even at distances considerably greater than those at which measurements were made. While such a variation may not be surprising,it is contrary to the results obtained with fission sources for which the spectra reach equilibrium at distances greater than two or three relaxation lengths from the source.[13] Results of calculations of the mean energy of the neutron and gamma-ray spectra as a function of distance are shown in Table 3.2. Mean energy is

Table 3.2

AVERAGE ENERGY OF CALCULATED NEUTRON AND GAMMA-RAY SPECTRA AS A FUNCTION OF RANGE

Range (Meters)	Average Energy of Neutrons > 0.1 Mev (Mev)	Average Energy of Gamma Ray > 1.33 Mev (Mev)
344	3.96	3.87
519	3.41	3.92
770	2.80	3.87
1104	2.47	4.10
1539	2.31	4.68

one indication of the shape of a spectrum, although it is not too sensitive. The neutron mean energy is shown to decrease monotonically with range while the mean energy of the gamma-rays is quite uniform for ranges up to 1100 meters. The sharp increase in the mean gamma-ray energy at 1500 meters is probably due to an increasing number of high energy gamma rays from the $^{14}N(n,\gamma)^{15}N$ reaction as proportionately more low energy neutrons become available. A greater percentage of the gamma-rays are in the 8-10 Mev region at 1500 meters as well, further substantiating the assumption. Although the mean energy is stable with distance, considerable variation in the spectra are evident in Fig. 3.25, thus indicating the low sensitivity of the mean energy as an indicator of spectrum shape.

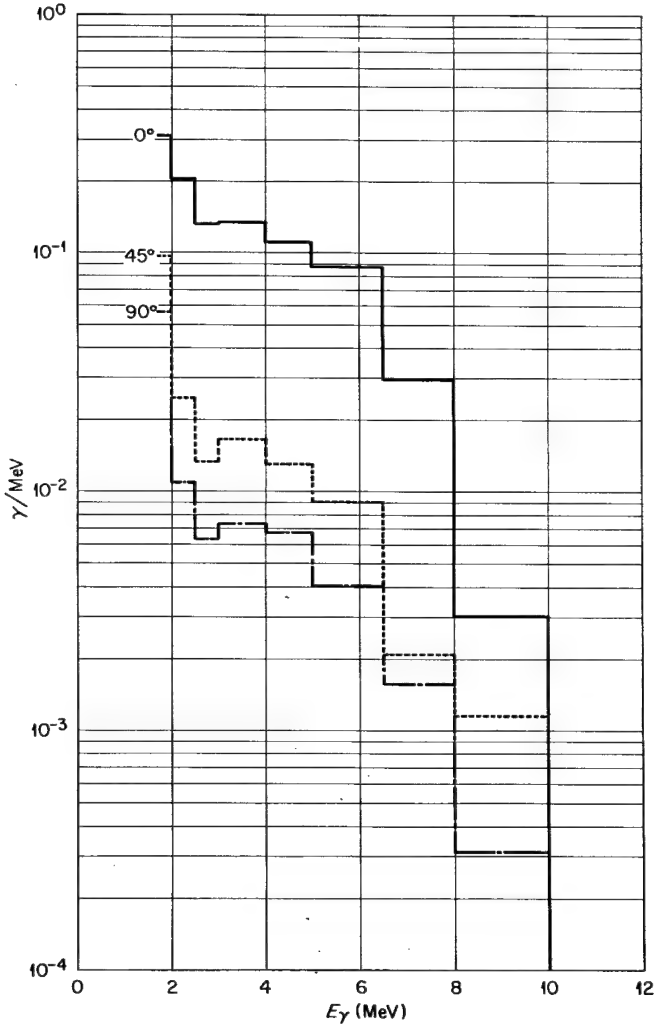

Fig. 3.23—Gamma-ray spectra as a function of polar angle for a source height of 1125 ft. Data integrated over the energy intervals used for the calculations.

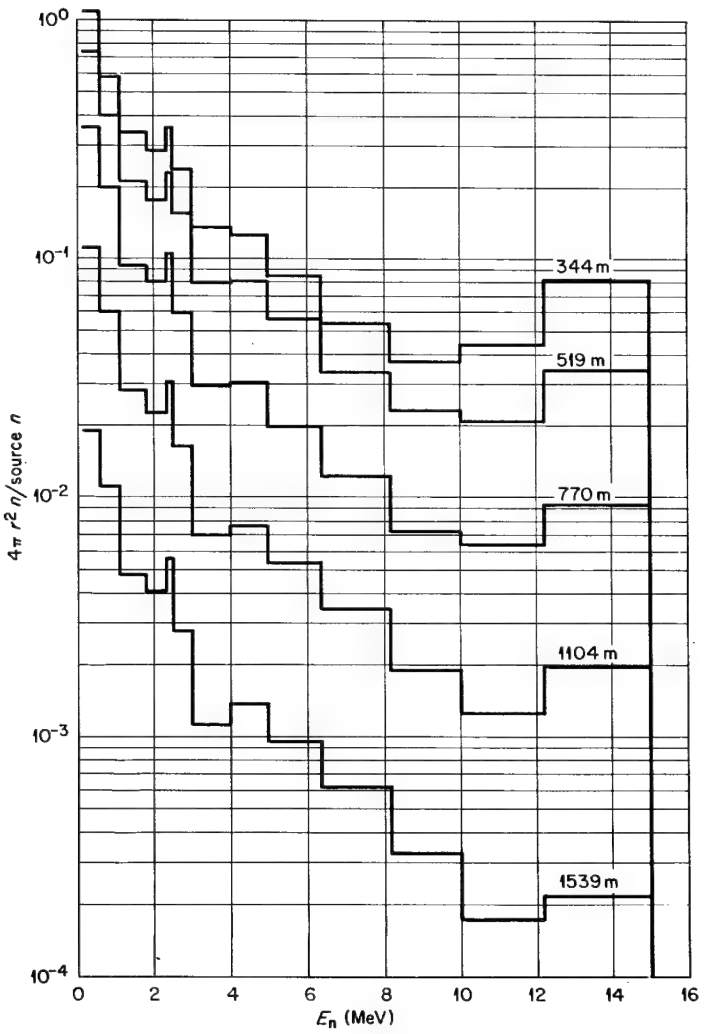

Fig. 3.24—Calculated HENRE neutron spectra as a function of range.

The importance of these spectrum variations will become more evident in the following section and in the results for other HENRE measurements. Measurements of neutron dose as a function of range should be particularly sensitive.[14,15]

3.2 DOSIMETRY

This section summarizes the measurements made at 750 yds from the base of the tower of dose as a function of polar angle. Low source yields coupled with the low sensitivity of the detector increased the statistical uncertainties associated with the neutron measurements. No attempts were made to estimate the dose loss below the bias of about 160 kev imposed by the neutron dosimeter readout system because the relative nature of the angular dose measurements limited the effects of such a loss. Data were recorded which would make such corrections possible if necessary. Greater detector sensitivity allowed somewhat more precise measurements of the gamma-ray dose as a function of angle. No corrections were made for the approximately 100 kev lower limit of the gamma dosimeter. The statistical variations indicated are in all cases one standard deviation as calculated from the average deviation. Widely varying data points were rejected through the application of Chauvenet's criterion.[16]

3.2.1 Neutron Angular Dose Distribution

Table 3.3 summarizes the neutron dose as a function of polar angle using a 30° acceptance cone. One angle, 300°, was measured with a 45° cone and is also given in this table. Data are given as integrator readout values per normalizing channel count. Detector readings were not corrected to kerma due to the relative nature of the angular measurements.

Figure 3.26 shows the neutron dose measured with the collimated detector with a source height of 300 ft. Vertical bars represent one standard deviation and horizontal bars represent the width of the collimator opening used. The next figure, 3.27, gives the data measured during January and February for a source height of 1125'. Data taken at 300° and 330° are affected by the air-ground interface which lay at 333° for this combination of detector position and source height. These data include several overlapping points taken at intermediate angles. The resulting curve is smooth and sharply peaked in the forward direction. Deviation of the 75° measurement was most probably the result of low neutron levels coupled with high noise levels. Similar data were taken during the July-August runs but at fewer angles. They are shown in Fig. 3.28. Small corrections were made to the summer data to account for the variation in normalizing channels between the winter and summer runs.

Because the neutron normalizing channel count was related to the total number of neutrons at 750 yards and was not sensitive to changes in neutron spectrum, the differences in air density between the winter and summer runs produced a significant effect on the normalized dose measurements. The average air density on the ground during the winter runs was 1.08 g/ℓ and was 1.00 g/ℓ during the summer. A smaller air density would produce the same effect as reducing the range, resulting in the neutron spectrum having a higher average energy. Increasing the average energy of the spectrum should increase the dose per neutron which is shown in Table 3.3 by the higher dose per normalizing count recorded during the summer. The total neutron dose recorded at 750 yds from the base of the tower also show the same effect with the values being 0.854 mrad/10^5 long counter counts in the winter and 0.960 in the summer.[14] Using the summer run as the standard, this amounts to a difference of 11%. The difference in the 0° polar angle measurements is 14%, which is consistent with the in-air value.

Table 3.3

NORMALIZED NEUTRON DOSE AS A FUNCTION OF
POLAR ANGLE FOR A 30° ACCEPTANCE ANGLE

Degrees Angle	Slant Range (yds) / Source Height (ft)	756 / 300 ($\times 10^{-5}$)	838 Winter / 1125 ($\times 10^{-5}$)	838 Summer / 1125 ($\times 10^{-5}$)	768 / 500 ($\times 10^{-5}$)
0		1.87 ± 0.52	1.78 ± 0.48	2.08 ± 0.53	1.80 ± 0.52
15			0.83 ± 0.36		
30		1.03 ± 0.21	0.73 ± 0.31	0.58 ± 0.21	0.77 ± 0.37
45			0.61 ± 0.28		
60		0.84 ± 0.16	0.43 ± 0.31	0.30 ± 0.16	0.52 ± 0.20
75			0.61 ± 0.32		
90			0.32 ± 0.20	0.28 ± 0.22	
300			0.14 ± 0.15*		
330			0.60 ± 0.36		

*45° acceptance angle

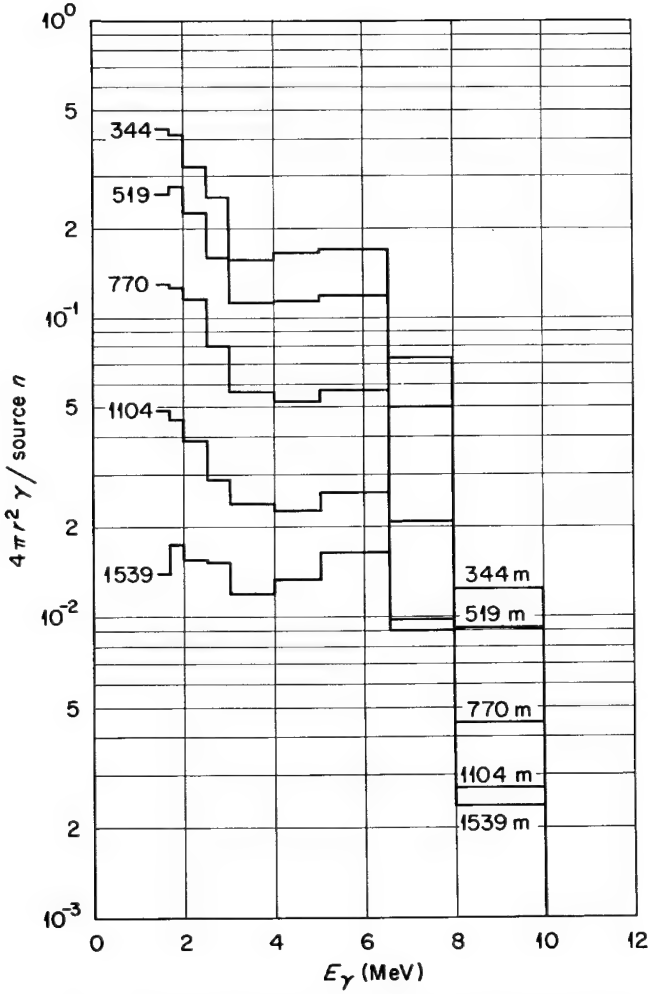

Fig. 3.25—Calculated HENRE gamma-ray spectra as a function of range.

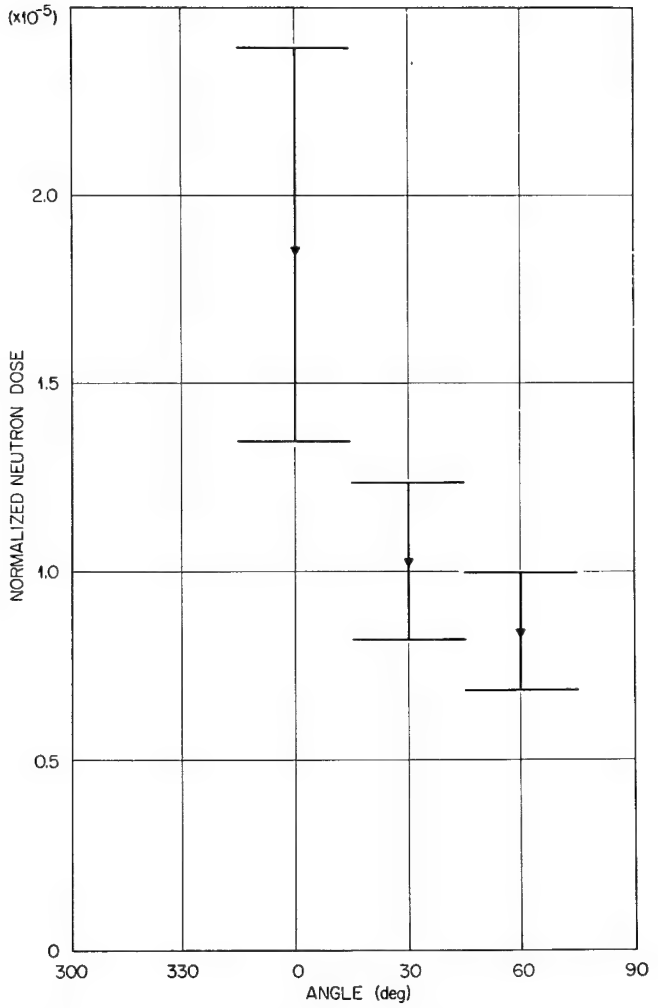

Fig. 3.26—Neutron dose as a function of polar angle for an acceptance angle of 30°, a source height of 300 ft, and a slant range of 756 yards. Data normalized to the number of neutrons at the detector site during each measurement. Vertical bar indicates one standard deviation; horizontal bar indicates the size of the collimator opening.

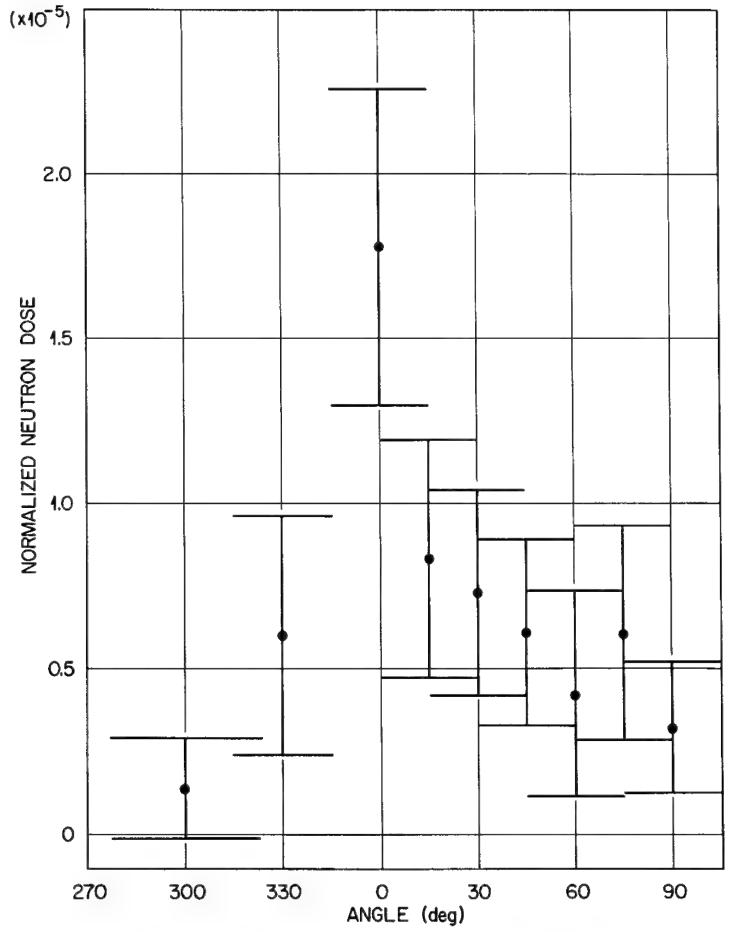

Fig. 3.27 — Neutron dose as a function of polar angle for an acceptance angle of 30°, a source height of 1125 ft, and a slant range of 838 yards. Data normalized to the number of neutrons at the detector site during each measurement. Value at 300° polar angle obtained with a 45° acceptance angle. Data from winter runs. Vertical bar indicates one standard deviation; horizontal bar indicates the size of the collimator opening.

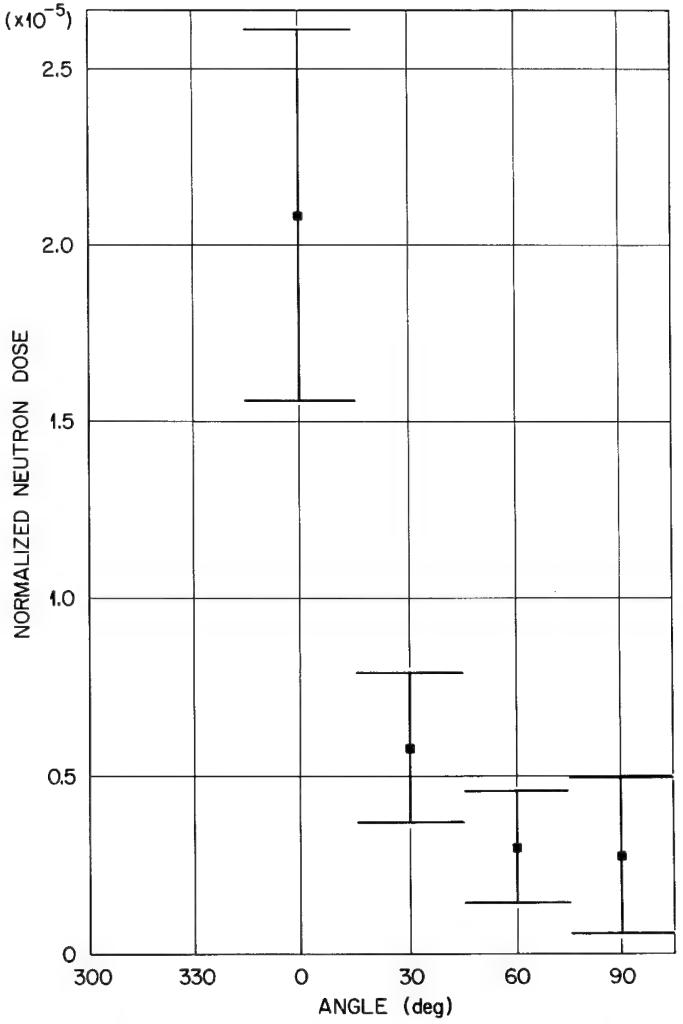

Fig. 3.28 — Neutron dose as a function of polar angle for an acceptance angle 30°, a source height of 1125 ft, and a slant range of 838 yards. Data normalized to the number of neutrons at the detector site during each measurement. Data from summer runs. Vertical bar indicates one standard deviation; horizontal bar indicates the size of the collimator opening.

Since more collisions could occur between the source and detector for the denser air, the neutron dose as a function of polar angle would be expected to be more diffuse, which is the case as shown by comparing Figs. 3.27 and 3.28. When the neutron spectrum is in equilibrium as a function of distance, such variations as those observed here would not occur. Further, the lower mean energy of the spectrum encountered at a fixed distance when the air is denser explains why the data recorded during the winter agrees with the data from BREN, which had an input spectrum with a lower average energy.[17]

Figure 3.29 gives the data recorded for a source height of 500 ft. Agreement with the data from 1125-ft runs and the 300-ft runs is good, since the range variation involved is small. That it is less peaked may be due to increased ground scatter.

In order to determine the neutron dose-distribution as a function of polar angle in greater detail, measurements were made for source heights of 1125 ft and 500 ft using a collimator acceptance angle of 15°. Runs were made at 10° intervals in the polar angle so that data points overlap somewhat. These results are summarized in Table 3.4. Figure 3.30 shows the data taken for a source height of 1125 ft, and Fig. 3.31 shows the data for a source height of 500 ft. Better data were obtained during the 500-ft run due to a better target yield coupled with the lower elevation. Agreement between the two elevations is not particularly good with the 1125-ft data apparently more sharply peaked in the forward direction. This is inconsistent with the data obtained with a larger collimator opening or with changes in the neutron spectrum. The difference may indicate the effect of increased ground scatter for the lower elevation, and measurement difficulties may account for some of the difference.

In order to determine the effects of the air-ground interface on the angular dose distribution, two sets of measurements were made in which the collimator was aimed just above and just below the interface. For neutrons, these measurements are summarized in Table 3.5. In the first set of numbers, the normalized doses at 11.5° and 348.5° should agree, and they do. The number at 333.5° is best compared with that at 30° for which a best value is $0.777 \pm 0.142 \times 10^{-5}$. This indicates the value just intersecting the interface is not much different from that for a similar polar angle above the interface. In this case, surface scattering may compensate for losses due to ground absorption. A good comparison for the 318.5° point is that at 45° for which the value is $0.611 \pm 0.280 \times 10^{-5}$. In this case, a significant reduction due to ground absorption is noted. A second series of measurements were made with the collimator aimed at a polar angle of 90° at all times, but with half of the measurements above the interface and half below. Low doses are present at this angle; the results are not statistically different from one another.

3.2.2 Gamma-Ray Angular Dose Distribution

The same angles were used for gamma-ray dose measurements as indicated for the neutron measurements. Gamma-ray dose as a function of angle is summarized for a 30° acceptance angle in Table 3.6. Like the neutron runs, the 300° measurement made during the January-February period at 1125 ft used a 45° acceptance angle. These data are shown as gamma detector counts per normalizing channel count. No attempt was made to reduce the data to exposure due to the relative nature of the measurements. The difference that occurs between the winter and summer measurements can be explained on the basis of the variation in the air density during the two periods. There is a significant difference between the normalized neutron and gamma-ray data. Whereas the neutron normalizing channel responded to total neutrons without much sensitivity for differences in neutron energy, the gamma-ray normalization detector measured exposure and as such was sensitive to variations in the gamma-ray spec-

(Text continued on page 66.)

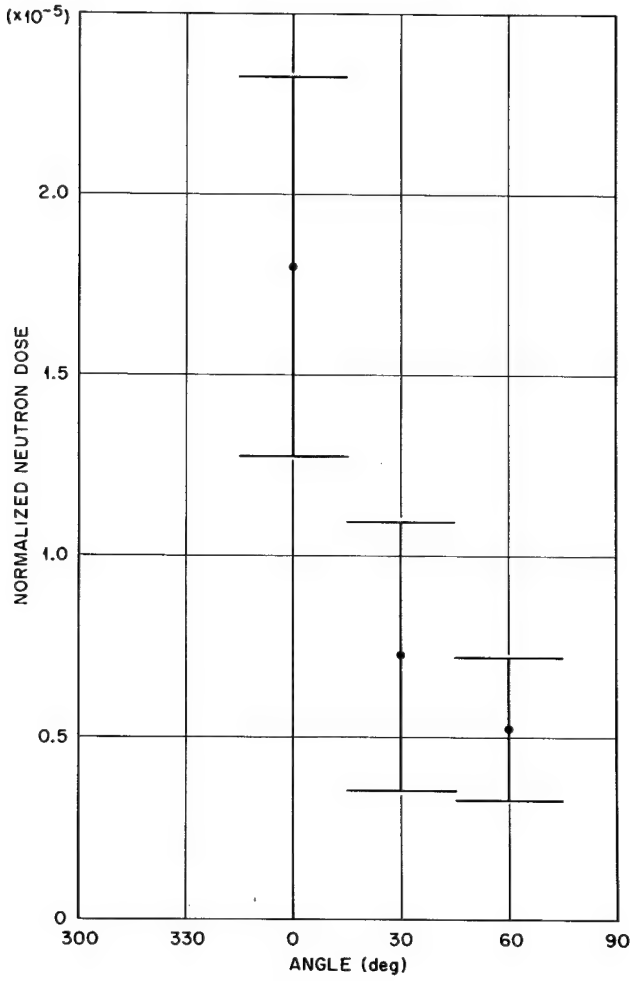

Fig. 3.29 — Neutron dose as a function of polar angle for an acceptance angle of 30°, a source height of 500 ft, and a slant range of 768 yards. Data normalized to the number of neutrons at the detector site during each measurement. Vertical bar indicates one standard deviation; horizontal bar indicates the size of the collimator opening.

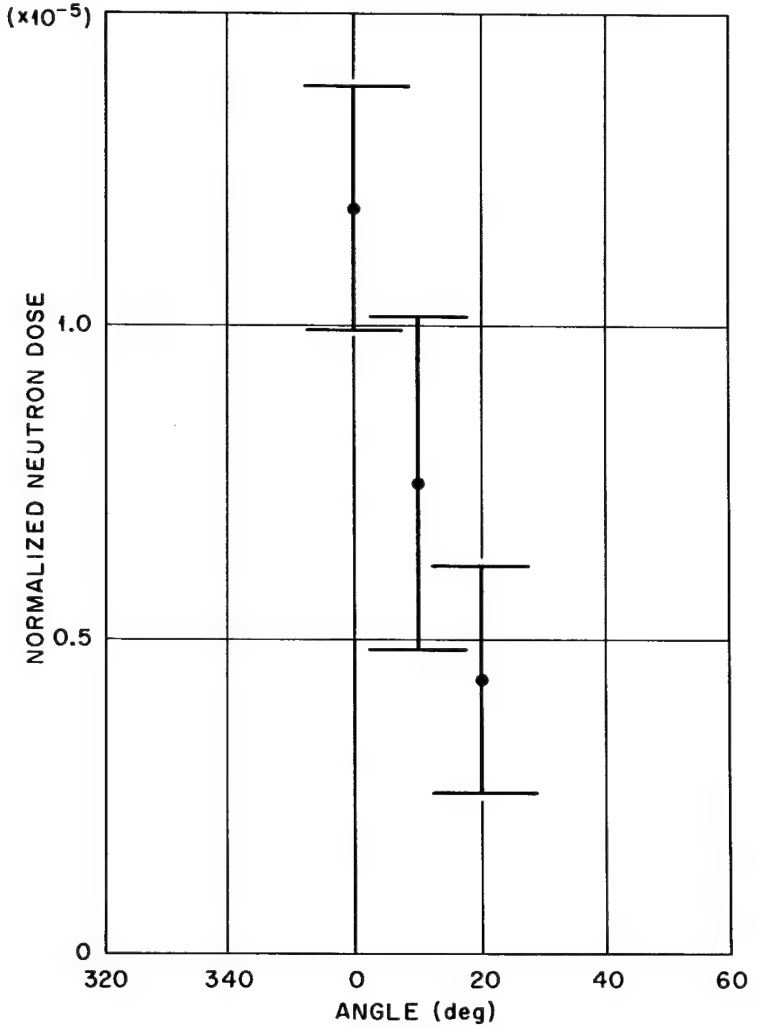

Fig. 3.30 — Neutron dose as a function of polar angle for an acceptance angle of 15°, a source height of 1125 ft, and a slant range of 838 yards. Data normalized to the number of neutrons at the detector site during each measurement. Vertical bar indicates one standard deviation; horizontal bar indicates the size of the collimator opening.

Table 3.4

NORMALIZED NEUTRON DOSE AS A FUNCTION OF POLAR ANGLE
FOR A 15° ACCEPTANCE ANGLE

Degrees Angle	Slant Range (yds) / Source Elevation (ft)	838 / 1125 ($\times 10^{-5}$)	768 / 500 ($\times 10^{-5}$)
0		1.19 ± 0.19	1.48 ± 0.35
10		0.75 ± 0.27	1.18 ± 0.20
20		0.44 ± 0.18	0.47 ± 0.12
30			0.26 ± 0.07
40			0.30 ± 0.19
50			0.13 ± 0.19

Table 3.5

NORMALIZED NEUTRON DOSE AS A FUNCTION OF POLAR ANGLE
AROUND THE AIR-GROUND INTERFACE
Acceptance Angle, 30°

Angle	Position with Respect to the Interface	1125 ft
11.5	above	1.70 ± 0.12 x 10^{-5}
318.5	below	0.47 ± 0.23 x 10^{-5}
333.5	intersecting	0.71 ± 0.24 x 10^{-5}
348.5	above	1.53 ± 0.22 x 10^{-5}
90	above	0.27 ± 0.14 x 10^{-5}
90	below	0.31 ± 0.31 x 10^{-5}

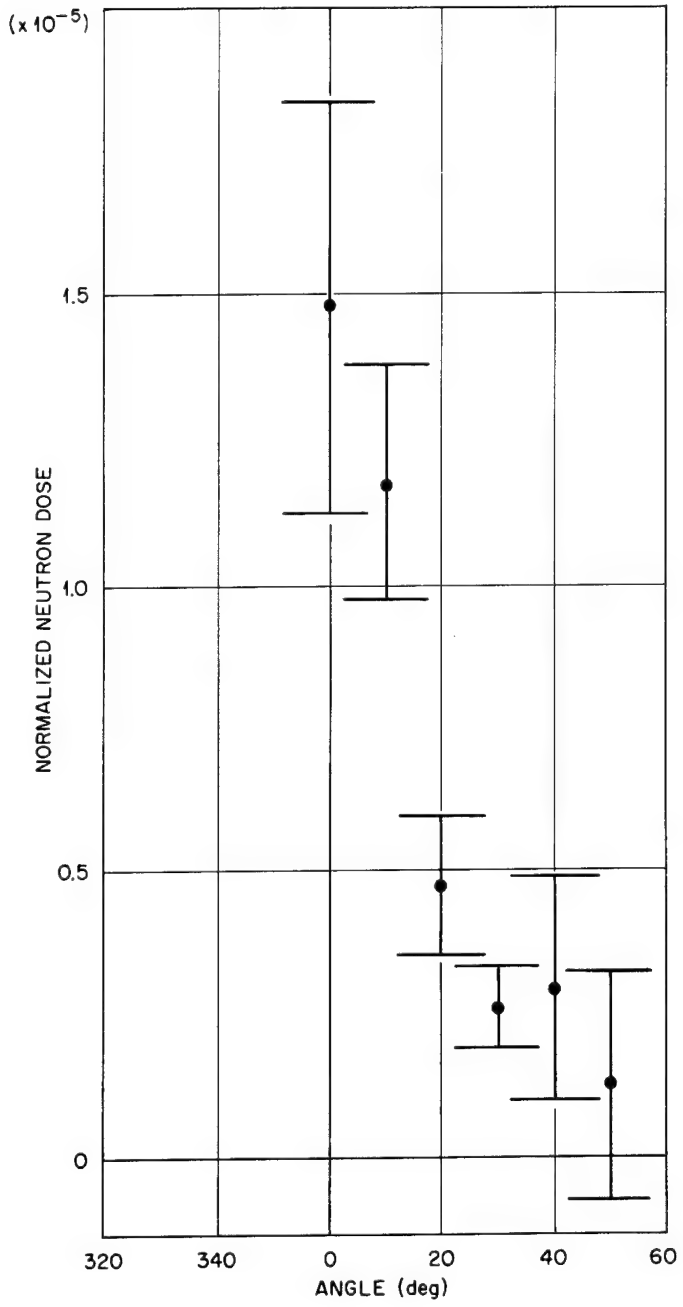

Fig. 3.31—Neutron dose as a function of polar angle for an acceptance angle of 15°, a source height of 500 ft, and a slant range of 768 yards. Data normalized to the number of neutrons at the detector site during each measurement. Vertical bar indicates one standard deviation; horizontal bar indicates the size of the collimator opening.

Table 3.6

NORMALIZED GAMMA-RAY DOSE AS A FUNCTION OF POLAR ANGLE
FOR AN ACCEPTANCE ANGLE OF 30°

Degrees Angle	Slant Range (yds) / Source Elevation (ft)	756 / 300	838 Winter / 1125	838 Summer / 1125	768 / 500
0		0.461 ± 0.038	0.388 ± 0.033	0.315 ± 0.026	0.379 ± 0.024
15			0.332 ± 0.024		
30		0.186 ± 0.011	0.124 ± 0.015	0.075 ± 0.011	0.080 ± 0.012
45			0.050 ± 0.008		
60		0.052 ± 0.003	0.030 ± 0.008	0.023 ± 0.010	0.030 ± 0.015
75			0.025 ± 0.004		
90		0.034 ± 0.006	0.015 ± 0.007	0.016 ± 0.011	
300*			0.063 ± 0.008		
330			0.109 ± 0.004		

*α = 45°

trum. This is illustrated by the similarity of the normalized dose values measured in air in the summer to those measured in the winter.[14] However, differences do exist between the winter and summer values obtained for dose as a function of polar angle that are due to the variation in the neutron spectrum as a function of range.

When the gamma-rays measured result from neutron reactions, data taken when the air was denser should be more peaked in the forward direction when compared with the total dose, since a greater percentage of the total reactions would occur in the volume of air between the source and the detector. For air with less density, the value obtained for a 0° polar angle should be less than that obtained for denser air because the dose integrated over all angles normalized to the total dose should remain constant. The results shown in Table 3.6 are consistent with these hypotheses, although the effects are smaller than those observed for the neutrons due to the slower variation of gamma-ray spectrum with range and the different normalization technique used. The effect of actually changing the range without changing the air density may be somewhat different, since the primary result of such a change is to move the detector closer to the source and thus towards the region where the most gamma rays are produced per cubic centimeter of air. Results of the measurements made at a source height of 300 ft are given in Fig. 3.32. Figures 3.33 and 3.34 show the results for a source height of 1125 ft for the January-February runs and the July-August runs, respectively. The measurements for a source height of 500 ft are given in Fig. 3.35. Reasonable agreement was obtained for the July-August 1125-ft data and this 500-ft data. Few points could be obtained due to the low radiation levels measured.

For more detailed measurements of the gamma-ray angular dose distribution, a 20° collimator was used with measurements made at 10° intervals. Table 3.7 gives a summary of these data for the runs at 1125 ft and 500 ft source height. The differences probably result from changing the range without changing the air density. Figures 3.36 and 3.37 give these results graphically: The large deviation for the 30° angle, 1125-ft source elevation data is an example of the problems encountered in accumulating this data.

Table 3.7

NORMALIZED GAMMA-RAY DOSE AS A FUNCTION OF POLAR ANGLE
FOR AN ACCEPTANCE ANGLE OF 20°

Degrees Angle	Slant Range (yds)	838	768
	Source Elevation (ft)	1125	500
0		0.198 ± 0.002	0.253 ± 0.028
10		0.158 ± 0.046	0.190 ± 0.006
20		0.062 ± 0.004	0.064 ± 0.010
30		0.025 ± 0.011	0.044 ± 0.013
40			0.026 ± 0.012
50			0.013 ± 0.006

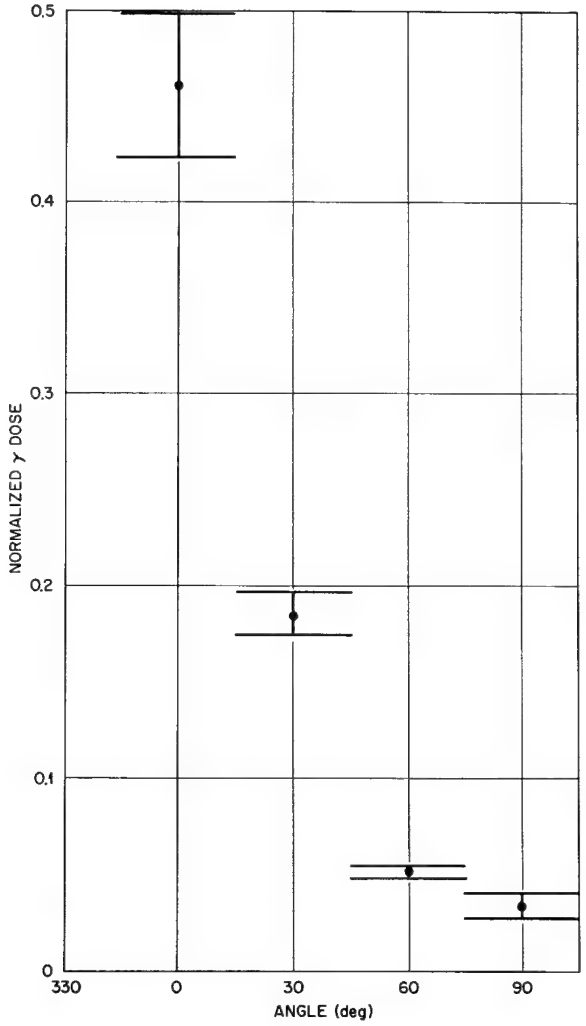

Fig. 3.32—Gamma-ray dose as a function of polar angle for an acceptance angle of 30°, a source height of 300 ft, and a slant range of 756 yards. Data normalized to the total gamma-ray dose at the detector site during each measurement. Vertical bar indicates one standard deviation; horizontal bar indicates the size of the collimator opening.

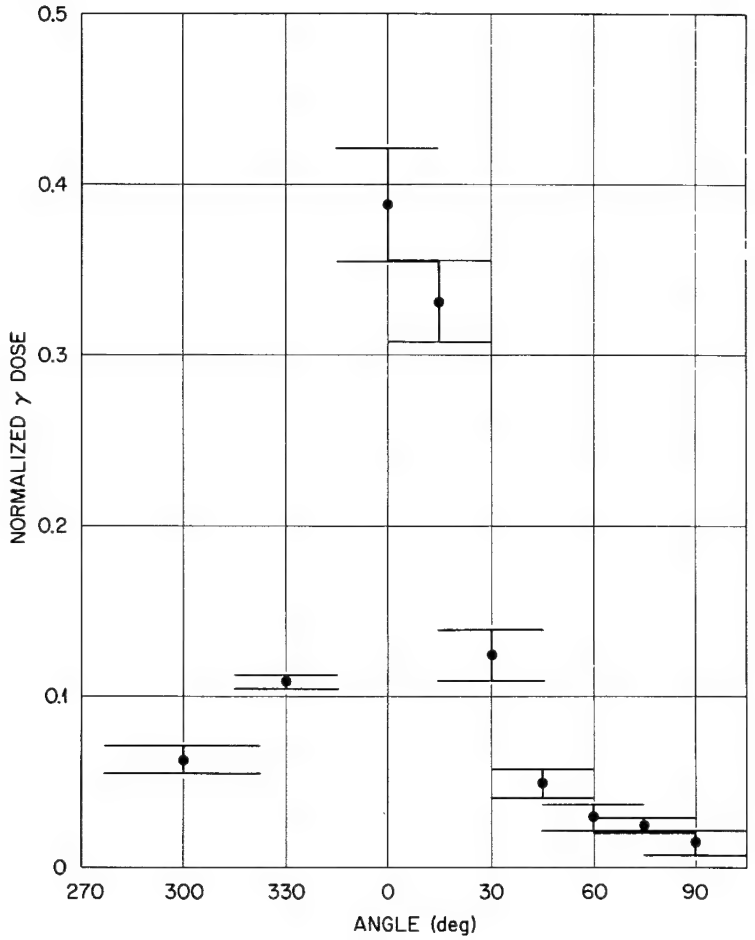

Fig. 3.33—Gamma-ray dose as a function of polar angle for an acceptance angle of 30°, a source height of 1125 ft, and a slant range of 838 yards. Data normalized to the total gamma-ray dose at the detector site during each measurement. Value at 300° polar angle obtained with a 45° acceptance angle. Data from winter runs. Vertical bar indicates one standard deviation; horizontal bar indicates the size of the collimator opening.

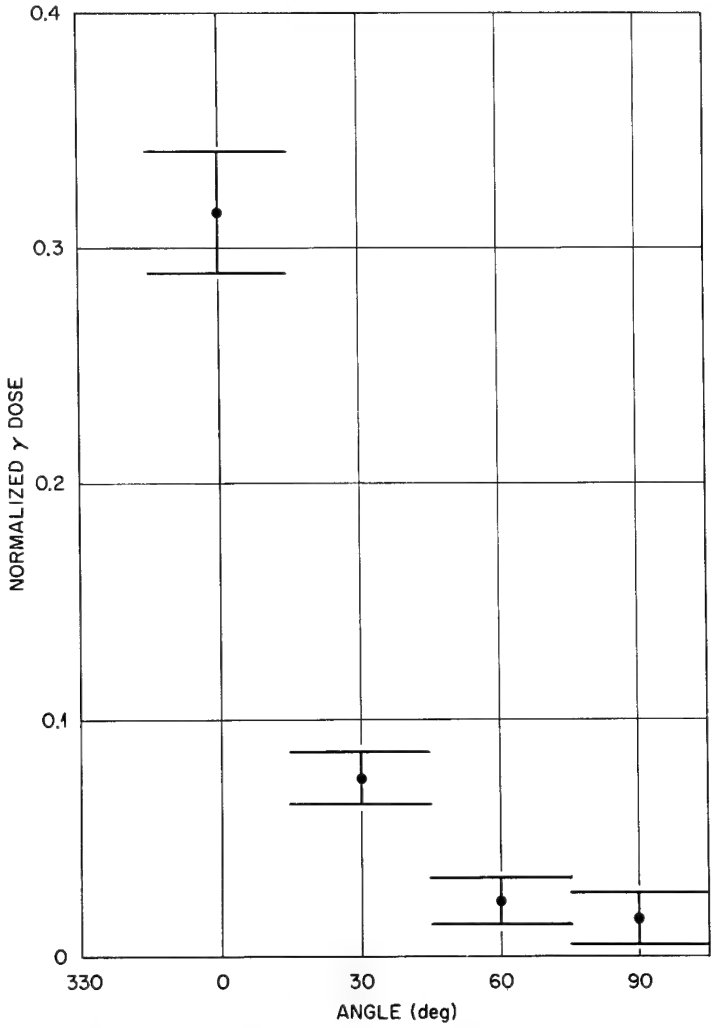

Fig. 3.34—Gamma-ray dose as a function of polar angle for an acceptance angle of 30°, a source height of 1125 ft, and a slant range of 838 yards. Data normalized to the total gamma-ray dose at the detector site during each measurement. Data from summer runs. Vertical bar indicates one standard deviation; horizontal bar indicates the size of the collimator opening.

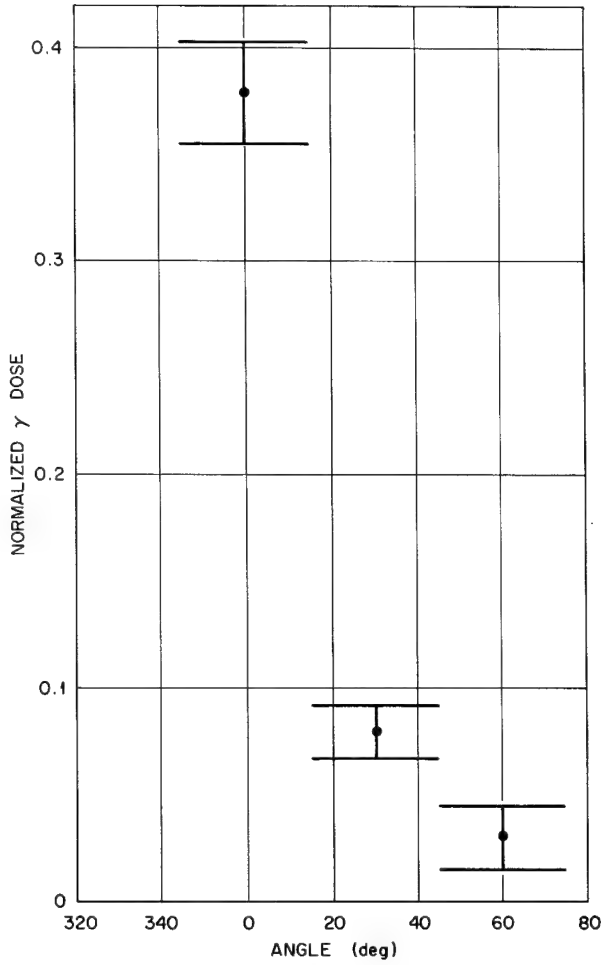

Fig. 3.35—Gamma-ray dose as a function of polar angle for an acceptance angle of 30°, a source height of 500 ft, and a slant range of 768 yards. Data normalized to the total gamma-ray dose at the detector site during each measurement. Vertical bar indicates one standard deviation; horizontal bar indicates the size of the collimator opening.

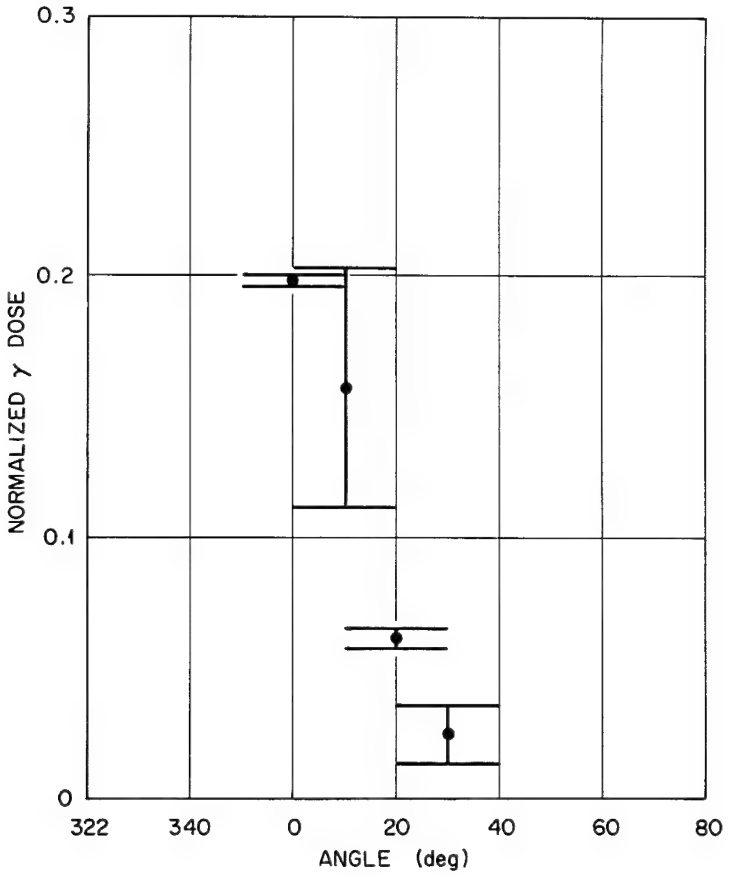

Fig. 3.36—Gamma-ray dose as a function of polar angle for an acceptance angle of 20°, a source height of 1125 ft, and a slant range of 838 yards. Data normalized to the total gamma-ray dose at the detector site during each measurement. Vertical bar indicates one standard deviation; horizontal bar indicates the size of the collimator opening.

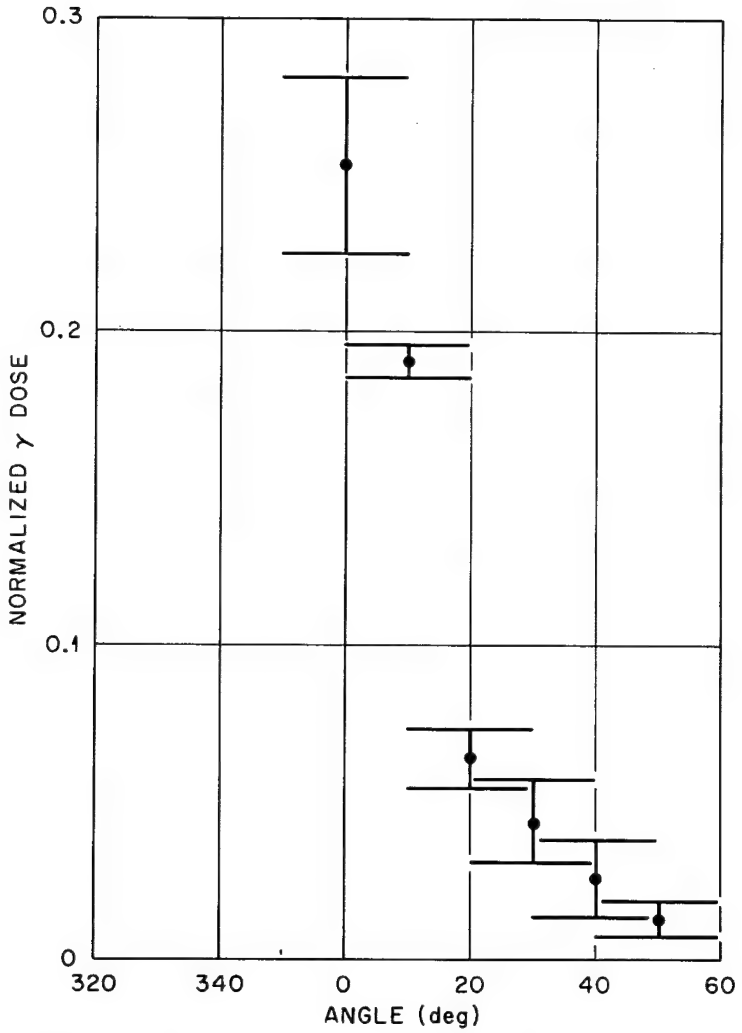

Fig. 3.37—Gamma-ray dose as a function of polar angle for an acceptance angle of 20°, a source height of 500 ft, and a slant range of 768 yards. Data normalized to the total gamma-ray dose at the detector site during each measurement. Vertical bar indicates the size of the collimator opening.

Measurements to determine the effects of the air-ground interface were made with the gamma-ray dosimeter at the same angles used for the similar neutron measurements. The results are summarized in Table 3.8. Agreement between the 11.5° and 348.5° data is reasonable. Data at 333.5° should be compared with the value 0.116 ± 0.006 obtained at 30° and is found to be less. However, the data at 318.5°, below the interface, is greater than at 45°, the most suitable comparison point above the interface for which a value of 0.050 ± 0.008 was obtained.

Table 3.8

NORMALIZED GAMMA-RAY DOSE AS A FUNCTION OF POLAR ANGLE AROUND AIR-GROUND INTERFACE FOR AN ACCEPTANCE ANGLE OF 30°

Angle	Position with Respect to the Interface	1125 ft
11.5	above	0.300 ± 0.021
318.5	below	0.052 ± 0.032
333.5	intersecting	0.091 ± 0.005
348.5	above	0.328 ± 0.060
90	above	0.041 ± 0.021
90	below	0.032 ± 0.019

Data taken during weapon tests gave a decrease in the gamma-ray dose for similar polar angles. Such may be the case when a significant portion of the total gamma-rays come from fission products in the fireball, but for cases like HENRE or BREN, where almost all of the gamma-rays come from neutron interactions in the air and ground, results such as those given are reasonable. The BREN data also shows an increase in the normalized gamma-ray dose for polar angle just below the air-ground interface.[17] A diffuse source results in a greater solid angle for scattering of radiation from the earth into the collimator. This effect would be more important when the collimator was aimed towards the tower than when it was turned away, which seems to be consistent with the data obtained at a polar angle of 90°, although the uncertainties of these data are large.

Table 3.9 gives a comparison between the HENRE angular distribution data, the BREN data, weapons data, and calculations for HENRE by Straker.[5-7,13,17] Agreement in the neutron angular distribution for HENRE, BREN, and the weapons test is good. A more sharply peaked gamma-dose distribution was obtained during HENRE than during BREN. In this respect, the HENRE data is more like the weapons test data. It is thought that most of the difference is due to the differ-

ent neutron spectra, but a part of the difference may be due to uncertainties resulting from the lower sensitivity of the gamma-ray detectors used during BREN and to an incompletely corrected contribution from the collimators during BREN. In both HENRE and BREN, almost all of the gamma-rays measured were produced in the air, but the available reactions differ for the two neutron spec-

Table 3.9

NEUTRON AND GAMMA-RAY DOSE AS A FUNCTION OF POLAR ANGLE FOR A 30° ACCEPTANCE ANGLE NORMALIZED TO THE VALUE AT 0° AND COMPARED WITH DATA FROM BREN, WEAPON'S TEST, AND CALCULATIONS FOR HENRE

Angle	HENRE n	BREN n	Weapon's Test n	Calculated n
0	1.00 ± 0.14	1.00 ± 0.22	1.00	1.00
30	0.41 ± 0.09	0.45 ± 0.12	0.53	0.48
60	0.28 ± 0.07	0.29 ± 0.10	0.28	0.18
90	0.16 ± 0.08	0.15 ± 0.08	0.17	0.08
	γ	γ	γ	γ
0	1.00 ± 0.04	1.00 ± 0.03	1.00	1.00
30	0.30 ± 0.02	0.48 ± 0.03	0.20	0.29
60	0.09 ± 0.01	0.32 ± 0.04	0.05	0.05
90	0.06 ± 0.01	0.22 ± 0.05	0.03	0.02

tra; for example, more gamma rays would be expected during BREN from the thermal n,γ reaction in ^{14}N. However, the BREN neutron spectrum and the instantaneous weapon spectrum should be quite similar, which may be an indication of the relative contributions of the different gamma rays. The comparison between the various neutron dose results is shown in Fig. 3.38 while the gamma-ray results are compared in Fig. 3.39.

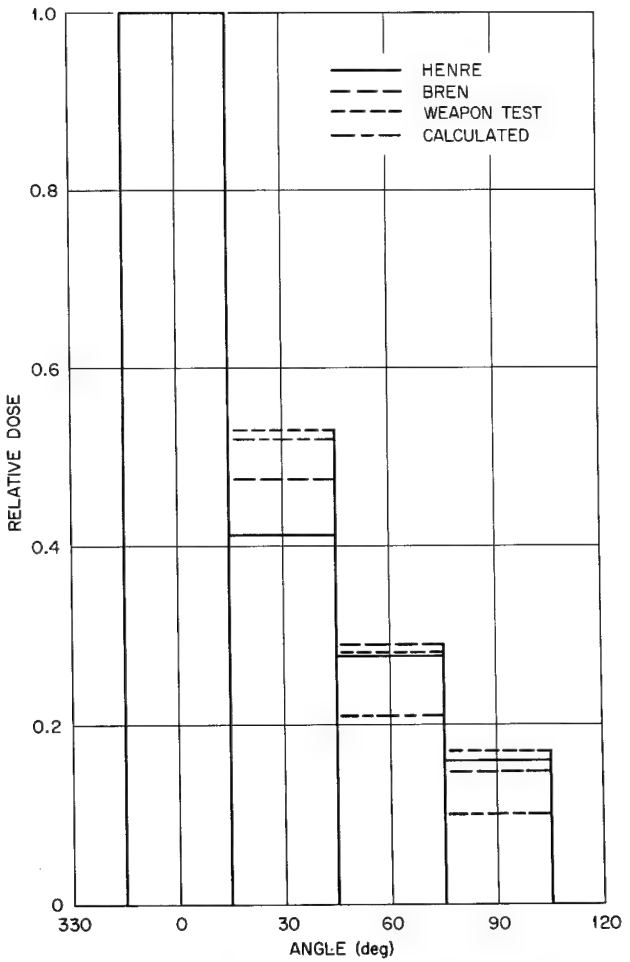

Fig. 3.38 — Comparison of neutron dose as a function of polar angle for a 30° acceptance angle. Data from HENRE, BREN, weapons test, and calculations for HENRE. Normalized to one for a 0° polar angle.

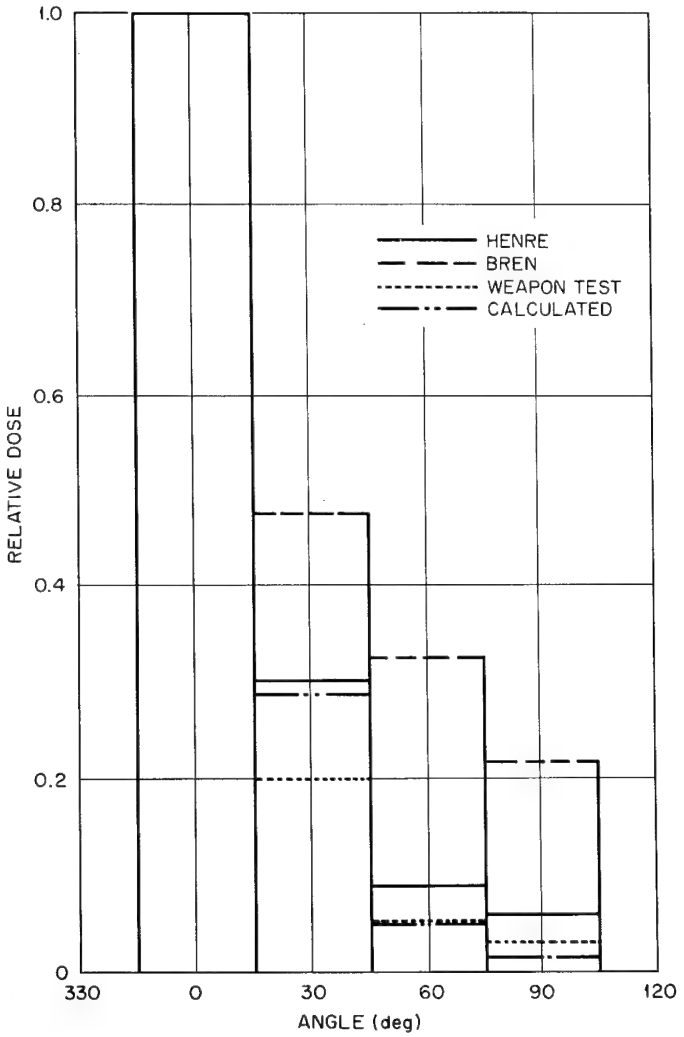

Fig. 3.39 — Comparison of gamma-ray dose as a function of polar angle for a 30° acceptance angle. Data from HENRE, BREN, weapons test, and calculations for HENRE. Normalized to one for 0° polar angle.

REFERENCES

1. J.R.P. Eaton and J. Walker, The Response of $^{6}Li(Eu)$ to Neutrons as a Function of Temperature, *Proc. Phys. Soc., 83:* 301-309 (1964).

2. J. R. Stehn, M. D. Goldberg, B. A. Magurno, and R. Wiener-Chasman, *Neutron Cross Sections,* BNL-325, second edition, Supplement No. 2, May, 1964.

3. Y. Beers, *Introduction to the Theory of Error,* Addison-Wesley, Reading, Massachusetts, 1957.

4. J. A. Auxier, W. S. Snyder, and T. D. Jones, *Neutron Interactions and Penetration in Tissue,* in *Radiation Dosimetry,* edited by F. H. Attix and W. C. Roesch, Academic Press, New York, 1968.

5. E. A. Straker, private communication.

6. E. A. Straker, *Calculations of the Transport of Neutrons from Fission and 14 Mev Point Sources in an Infinite Medium of Air,* ORNL-TM-1547, August, 1966.

7. E. A. Straker, *Time-Dependent Neutron and Secondary Gamma-Ray Transport in an Air-Over-Ground Geometry. Vol. II. Tabulated Data,* ORNL-4289, Vol. II, September, 1968.

8. R. Nordhagen, Proton Resonances Suitable to Shape Calibrate a Scintillation γ-Ray Spectrometer, *Nucl. Instr. and Meth. 12,* 291-298 (1961).

9. E. Storm, E. Gilbert, and H. Israel, *Gamma-Ray Absorption Coefficients for Elements 1 through 100 Derived from the Theoretical Values of the National Bureau of Standards,* LASL Report LA-2237, November, 1958.

10. D. M. Drake, J. C. Hopkins, J. T. Martin, and H. Condé, The Use of Pu-α-Be as a Calibrated Gamma-Ray Source, *Nuc. Instr. and Meth. 62:* 349-350 (1968).

11. B. Rossi, *High-Energy Particles,* Prentice-Hall, Inc., New York (1952).

12. M. J. Berger and S. M. Seltzer, *Tables of Energy Losses and Ranges of Electrons and Positrons,* NASA SP-3012 (1964).

13. R. H. Ritchie and G. S. Hurst, Penetration of Weapon's Radiation Application to the Hiroshima-Nagasaki Studies, *Health Physics 1:* 390-404 (1959).

14. J. S. Cheka, *Distribution of Radiation from a 14 Mev Neutron Source In and Near Structures,* USAEC Report CEX 65.12 (to be published).

15. Z. Burson, *The Spatial Distribution of Dose in an Air-Over-Ground Geometry,* USAEC Report 65.14 (to be published).

16. A. G. Worthing and J. Geffner, *Treatment of Experimental Data,* John Wiley and Sons, Inc., New York (1943).

17. J. H. Thorngate, J. A. Auxier, F. F. Haywood, and S. Helf, *Energy and Angular Distribution of Neutrons and Gamma Rays - Operation BREN,* USAEC Report CEX 62.12, February, 1967.

Chapter 4

CONCLUSIONS

Data obtained during HENRE should be useful for many cases where the radiation fields produced in air by a source of 14 Mev neutrons need to be known. This report covered data taken at relatively large distances from the source for the neutron and gamma-ray spectra and the neutron and gamma ray dose as a function of polar angle. In that respect, it is similar to other reports concerned with weapon test measurements. What will be summarized in this final chapter are the results which depend upon the radiation source used during HENRE.

The most important conclusion is that an equilibrium condition in the neutron spectrum has not been reached even at ranges as great as 1500 meters from the source. That is, the mean energy of the fast neutron spectrum decreases monotonically for ranges between 350 to 1500 meters. In fact, between these ranges, the mean energy can be expressed by a power function of the range, $\bar{E}_n = 35.04\ R^{-0.375}$ with a correlation coefficient of -0.992. Because all of the data measured depend upon what happens to the neutrons from the source, most of the effects that will be discussed result from the variation of the neutron spectrum.

Conclusions reached from the measurement of the gamma-ray spectrum are: (1) that little of the observed gamma field is produced by the $^{14}N(n,\gamma)^{15}N$ reaction, (2) more gamma-rays were measured in the 3-5 Mev region than found in the calculations, and (3) less was observed above 8 Mev than in the calculations. The latter two could be correlated if the difference between measurement and calculation is assumed to be a result of the omission from the calculation of some possible reactions that produce 3-5 Mev gamma rays. The omitted reactions would otherwise use some of the neutrons that yielded gamma-rays in the energy region above 8 Mev. To produce gamma-rays from the $^{14}N(n,\gamma)^{15}N$ reaction requires low energy neutrons, so the measurements show, not unexpectedly, that for ranges near 500 meters there are few low energy neutrons. Calculations of the mean energy of the gamma spectra as a function of range show it is quite stable until the range nears 1500 meters where the neutron spectrum contains a greater percentage of low energy neutrons, so that more of the $^{14}N(n,\gamma)^{15}N$ reactions will occur. The neutron spectrum produced by a reactor, such as during Operation BREN, would result in the $^{14}N(n,\gamma)^{15}N$ reaction being the predominant source of gamma-rays and should result in a higher mean energy than the HENRE spectrum. In either case, the air is the primary source of gamma-rays with the earth being the source of the remainder.

The effects of the changing neutron spectrum are shown by comparing neutron dose as a function of polar angle measured at a given range for two different air densities. When the neutron spectrum is in equilibrium, little effect would be produced by changes of the air density in the ratio of dose to

total neutrons. For a neutron spectrum with a decreasing mean energy, the dose per neutron decreases with increasing air density and the distribution becomes less peaked at 0° polar angle.

Related changes are observed in the gamma ray dose as a function of polar angle. Most of the gamma-rays measured are produced by neutron interactions with the air so a greater air density produces more of the total reactions between the source and the detector. The distribution is more peaked towards 0° polar angle for a higher air density. These measurements were related to the total gamma-ray dose at the detector site rather than the total fluence; thus, changes in range at a given air density can overcome the effects of changes in air density. That is, the gamma measurements, as taken, were more sensitive to geometric effects than to changes in the gamma-ray spectrum.

Another observation made during the measurement of the gamma dose as a function of polar angle is of some importance. During BREN and HENRE, the gamma dose for a polar angle just below the air-ground interface was found to be higher than for a comparable polar angle above the interface. This is contrary to the results obtained during the weapon tests in Nevada. The variation is the result of the variation in the source of the gamma rays. From a weapon, an appreciable part of the total field originates in the fission products in the fireball; for HENRE and BREN neutron interactions with the air and ground were the principal source of gamma rays. The increase in dose below the interface, when the collimator is in the tower-detector plane, may be explained by the increased importance of the gamma rays produced in the ground and by the change in geometry caused by the diffuse source. These effects are apparently less for angles in a plane perpendicular to the source detector line.

With all of these effects in mind, it is hoped the data presented in this report will be of value in solving shielding problems encountered at these distances in air from sources of 14 Mev neutrons. One conclusion often reached after work of this type remains unchanged by the work described: considerably better and more complete cross section data is required for neutron interactions with the air.

CIVIL EFFECTS TEST OPERATIONS REPORT SERIES (CEX)

Through its Division of Biology and Medicine and Civil Effects Test Operations, the Atomic Energy Commission conducts certain technical tests, exercises, surveys, and research directed primarily toward practical applications of nuclear effects information and toward encouraging better technical, professional, and public understanding and utilization of the vast body of facts useful in the design of countermeasures against weapons effects. The activities carried out in these studies do not require nuclear detonations.

The following is a partial list of reports available from studies that have been completed. All reports listed are available, at $3.00 each, from the Clearinghouse for Federal Scientific and Technical Information, U. S. Department of Commerce, Springfield, Va. 22151.

CEX-58.1, Experimental Evaluation of the Radiation Protection Afforded by Residential Structures Against Distributed Sources, J. A. Auxier, J. O. Buchanan, C. Eisenhauer, and H. E. Menker, 1959.

CEX-58.7, AEC Group Shelter, AEC Facilities Division, Holmes & Narver, Inc., 1960.

CEX-58.8, Comparative Nuclear Effects of Biomedical Interest, C. S. White, I. G. Bowen, D. R. Richmond, and R. L. Corsbie, 1961.

CEX-58.9, A Model Designed to Predict the Motion of Objects Translated by Classical Blast Waves, I. G. Bowen, R. W. Albright, E. R. Fletcher, and C. S. White, 1961.

CEX-59.1, An Experimental Evaluation of the Radiation Protection Afforded by a Large Modern Concrete Office Building, J. F. Batter, Jr., A. L. Kaplan, and E. T. Clarke, 1960.

CEX-59.7B (Pt. I), Experimental Radiation Measurements in Conventional Structures. Part I. Radiation Measurements in Two Two-story and Three One-story Typical Residential Structures Before and After Modification, Z. G. Burson, 1966.

CEX-59.7B (Pt. II), Experimental Radiation Measurements in Conventional Structures. Part II. Comparison of Measurements in Above-ground and Below-ground Structures from Simulated and Actual Fallout Radiation, Z. G. Burson, 1964.

CEX-59.7B (Pt. III), Experimental Radiation Measurements in Conventional Structures. Part III. The Attenuation of Air-scattered Radiation in a Basement, Z. G. Burson, 1965.

CEX-59.13, Experimental Evaluation of the Radiation Protection Afforded by Typical Oak Ridge Homes Against Distributed Sources, T. D. Strickler and J. A. Auxier, 1960.

CEX-59.14, Determinations of Aerodynamic-drag Parameters of Small Irregular Objects by Means of Drop Tests, E. P. Fletcher, R. W. Albright, V. C. Goldizen, and I. G. Bowen, 1961.

CEX-60.1, Evaluation of the Fallout Protection Afforded by Brookhaven National Laboratory Medical Research Center, H. Borella, Z. Burson, and J. Jacovitch, 1961.

CEX-60.3, Extended- and Point-source Radiometric Program, F. J. Davis and P. W. Reinhardt, 1962.

CEX-60.5, Experimental Evaluation of the Fallout-radiation Protection Afforded by a Southwestern Residence, Z. Burson, D. Parry, and H. Borella, 1962.

CEX-60.6, Experimental Evaluation of the Radiation Protection Provided by an Earth-covered Shelter, Z. Burson and H. Borella, 1962.

CEX-61.1 (Prelim.), Gamma Radiation at the Air–Ground Interface, K. O'Brien and J. E. McLaughlin, Jr., 1963.

CEX-61.4, Experimental Evaluation of the Fallout-radiation Protection Provided by Selected Structures in the Los Angeles Area, Z. G. Burson, 1963.

CEX-62.01, Technical Concept—Operation BREN, J. A. Auxier, F. W. Sanders, F. F. Haywood, J. H. Thorngate, and J. S. Cheka, 1962.

CEX-62.2, Nuclear Bomb Effects Computer (Including Slide-rule Design and Curve Fits for Weapons Effects), E. R. Fletcher, R. W. Albright, R. F. D. Perret, Mary E. Franklin, I. G. Bowen, and C. S. White, 1963.

CEX-62.11, Distribution of Weapons Radiation in Japanese Residential Structures, J. S. Cheka, F. W. Sanders, T. D. Jones, and W. H. Shinpaugh, 1965.

CEX-62.12, Energy and Angular Distribution of Neutrons and Gamma Rays—Operation BREN, J. H. Thorngate, J. A. Auxier, F. F. Haywood, and S. Helf, 1967.

CEX-62.13, Post Pulse Gamma-radiation Spectrum—Operation BREN, J. H. Thorngate and E. T. Loy, 1966.

CEX-62.14, An Experimental Investigation of the Spatial Distribution of Dose in an Air-over-Ground Geometry, F. F. Haywood, J. A. Auxier, and E. T. Loy, 1964.

CEX-62.50, Neutron-field and Induced-activity Measurements—Operation BREN, F. M. Tomnovec and J. M. Ferguson, 1965.

CEX-62.80b, Small Boy Project 62.80b Aeroradioactivity Survey, Edgerton, Germeshausen & Grier, Inc., 1967.

CEX-62.80c, Sedan Project 62.80c Aeroradioactivity Survey, Edgerton, Germeshausen & Grier, Inc., 1967.

CEX-62.81 (Final), Ground Roughness Effects on the Energy and Angular Distribution of Gamma Radiation from Fallout, C. M. Huddleston, Z. G. Burson, R. M. Kinkaid, and Q. G. Klinger, 1964.

CEX-63.3, Barrier Attenuation of Air-scattered Gamma Radiation, Z. G. Burson and R. L. Summers, 1965.

CEX-63.7, A Comparative Analysis of Some of the Immediate Environmental Effects at Hiroshima and Nagasaki, C. S. White, I. G. Bowen, and D. R. Richmond, 1964.

CEX-63.10, Design of a Shielded Source for the Irradiation of Natural Animal Populations, A. C. Lucas, Z. G. Burson, and R. E. Lagerquist, 1966.

CEX-64.3, Ichiban: The Dosimetry Program for Nuclear Bomb Survivors of Hiroshima and Nagasaki—A Status Report as of April 1, 1964, J. A. Auxier, 1964.

CEX-64.7, Neutron and Gamma-ray Leakage from the Ichiban Critical Assembly, J. H. Thorngate, D. R. Johnson, and P. T. Perdue, 1966.

CEX-65.01, Feasibility Study: Intense 14-Mev Neutron Source for Operation HENRE, T. G. Provenzano, E. J. Story, F. F. Haywood, and H. T. Miller, 1966.

CEX-65.02, Technical Concept—Operation HENRE, F. F. Haywood and J. A. Auxier, 1965.

CEX-65.03, Operations Plan—Operation HENRE, Technical Director's Staff, 1965.

CEX-65.4, Biological Tolerance to Air Blast and Related Biomedical Criteria, C. S. White, I. Gerald Bowen, and D. R. Richmond, 1965.

CEX-65.13, Distribution of Radiation from a 14 Mev Neutron Source in and Near Structures, J. S. Cheka, 1969.

CEX-68.3, Nuclear Weapons Effects Tests of Blast Type Shelters, A Documentary Compendium of Test Reports, Christian Beck (Comp.), 1969.

CEX-68.4, Radiosensitivity of Certain Perennial Shrub Species Based on a Study of the Nuclear Excavation Experiment, Palanquin, with Other Observations of Effects on the Vegetation, W. A. Rhoads, Robert B. Platt, and Robert A. Harvey, 1969.